NOAA Technical Memorandum ERL ARL-156

METEOROLOGICAL AND AEROSOL MEASUREMENTS FROM THE NOAA WP-3D AIRCRAFT DURING WATOX-86, JANUARY 4-9, 1986

Howard Bridgman
Barbara Stunder
Richard Artz
Glenn Rolph
Russell Schnell
Barry Bodhaine
Samuel Oltmans

Air Resources Laboratory
Silver Spring, Maryland
July 1987

noaa NATIONAL OCEANIC AND ATMOSPHERIC ADMINISTRATION / Environmental Research Laboratories

NOAA Technical Memorandum ERL ARL-156

METEOROLOGICAL AND AEROSOL MEASUREMENTS FROM THE NOAA WP-3D AIRCRAFT DURING WATOX-86, JANUARY 4-9, 1986

Howard Bridgman*
Geophysical Monitoring for Climatic Change
Boulder, Colorado

Barbara Stunder
Richard Artz
Glenn Rolph
Air Resources Laboratory

Russell Schnell
Cooperative Institute for Research in Environmental Sciences
University of Colorado
Boulder, Colorado

Barry Bodhaine
Samuel Oltmans
Geophysical Monitoring for Climatic Change
Boulder, Colorado

Air Resources Laboratory
Silver Spring, Maryland
July 1987

*Permanent Address: Department of Geography, University of Newcastle, NSW 2308, Australia

UNITED STATES DEPARTMENT OF COMMERCE
Malcolm Baldrige, Secretary

NATIONAL OCEANIC AND ATMOSPHERIC ADMINISTRATION
Anthony J. Calio, Administrator

Environmental Research Laboratories
Vernon E. Derr, Director

NOTICE

Mention of a commercial company or product does not constitute an endorsement by NOAA Environmental Research Laboratories. Use for publicity or advertising purposes of information from this publication concerning proprietary products or the tests of such products is not authorized.

For sale by the National Technical Information Service, 5285 Port Royal Road
Springfield, VA 22161

FOREWORD

James N. Galloway, WATOX Director

(Dept. of Environmental Sciences, University of Virginia,
Charlottesville, VA 22903)

The Western Atlantic Ocean Experiment (WATOX), begun in 1980, is designed to determine the amount and fate of selected sulfur, nitrogen, metal, and organic compounds that are advected eastward from North America.

WATOX has two components: long-term and intensive. The long-term component includes three sites that collect and analyze precipitation on an event basis. Two of the sites, Harbor Radio Tower, Bermuda, and Lewes, Delaware, were started in 1980. Another site was added at Adrigole, Ireland, in 1984. In addition, between 1981 and 1985, during May-October, precipitation samples were collected on two ships cruising on a weekly basis between New York City, Bermuda, and Nassau.

As a supplement to the long-term program, intensive sampling programs are held on a regular basis to investigate the processes that control the transport, transformation, and deposition of materials to the western Atlantic Ocean. During intensives, which last 1-4 weeks, instrumentation to determine atmospheric concentration of gas and aerosol species is used at long-term sites and on mobile sampling platforms (ships, aircraft).

The first two intensives (WATOX-82, WATOX-83) occurred in October 1982 and February 1983. Their objectives were to investigate the changes that occurred in the composition of air parcels during transit from North America to Bermuda. In addition to the long-term measurments of wet deposition, measurments of the concentrations of trace gas and aerosol species were made at Lewes, Delaware, and at High Point, Bermuda. The third intensive (WATOX-84) used a ship (RV Knorr) to sample gases and aerosols between North America and Africa to determine the extent of transport across the North Atlantic.

The above three intensives sampled air in the marine boundary layer during transport over the Atlantic Ocean. An obvious limitation of this approach is that measurements at sea level give no information about upper-air transport. To overcome this deficiency, the fourth intensive (WATOX-85) included an aircraft component. The NOAA King Air research aircraft was used to sample atmospheric gases and aerosols as a function of altitude and latitude during frontal passage between North American and Bermuda.

The King Air platform provided unique information on the vertical distribution of a few parameters in the western Atlantic atmosphere. However, due to its limited payload and range, the data were limited. To compensate for this problem, WATOX-86 was designed to include two aircraft. A NOAA WP-3D was based at McGuire Air Force Base, New Jersey, and flew parallel to the coast between Newfoundland and Florida. The NOAA King Air was based at Hanscom Field near Boston, Massachusetts, and flew off Cape Cod, Massachusetts. Both aircraft had sampling and analytical equipment designed to determine the vertical and horizontal chemical structure of the atmosphere. This report contains a summary of the results of the NOAA WP-3D flights.

Contents

Figures

METEOROLOGICAL AND AEROSOL MEASUREMENTS FROM THE NOAA WP-3D AIRCRAFT DURING WATOX-86, JANUARY 4-9, 1986

Howard Bridgman, Barbara Stunder, Richard Artz, Glenn Rolph, Russell Schnell, Barry Bodhaine, and Samuel Oltmans

ABSTRACT. On January 4, 6, 8, and 9, 1986, a series of NOAA WP-3D research flights were conducted over the Western Atlantic Ocean, 2-300 km off the coast of North America. Flights were made perpendicular to NW airflow to establish the flux of gas and aerosol emissions from the east coast of North America. Air fluxes from the NW ranged from less than 5 kg $m^{-2}s^{-1}$ near the center of a high-pressure system to over 40 kg $m^{-2}s^{-1}$ in strong NW airflow in the free troposphere on January 4. Representative condensation nuclei (CN) concentrations averaged 150-250 cm^{-3} in the free troposphere in clean conditions, but in atmospheric layers containing CN transported from long distances, concentrations reached 6500 cm^{-3} (January 4). In the marine boundary layer, CN concentrations averaged 500 to 750 cm^{-3} under clean conditions, and 1500 to 3000 cm^{-3} in polluted air. Aerosol scattering extinction (b_{sp}) ranged from 70 × 10^{-6} m^{-1} in the marine boundary layer to 20 × 10^{-6} m^{-1} in the free troposphere. Aerosol b_{sp} was not as responsive to changes in atmospheric structure as CN. Aerosol size spectra in the marine boundary layer were an order of magnitude higher than those in the free troposphere. Consistent peaks in the volume spectra between 8 and 10 μm diameter established the importance of sea salt as the major aerosol component. Ozone profiles in the free troposphere normally in the 30-40 ppb range, exhibited laminae of enhanced concentrations (up to 70 ppb) at moisture boundaries, suggesting active ozone production was occurring at the levels. Ozone concentrations within the marine boundary layer were generally lower than in the free troposphere. The following details are presented for each flight: a horizontal projection of the flight track on a latitude-longitude grid; the relevant synoptic situation; air-parcel back-trajectories; a flight log; vertical cross sections of potential temperature, mixing ratio, and flight track; vertical cross sections of CN and b_{sp}; and representative aerosol size distributions. Vertical cross sections of potential temperature and mixing ratio normal to the coast are presented for two flights; vertical cross sections of potential temperature and mixing ratio along the coast are presented for one flight; examples of the horizontal and vertical variability of aerosols on the small scale are presented where appropriate.

INTRODUCTION

On January 4, 6, 8, and 9, 1986, the National Oceanic and Atmospheric Administration (NOAA) conducted a series of research flights over the western portion of the North Atlantic Ocean in support of the Western Atlantic Ocean Experiment (WATOX). This intensive study (WATOX-86) was designed to evaluate, in three dimensions, the fluxes of air and pollution emissions moving from the east coast of North America to the western Atlantic under NW airflow. Measurements of meteorological and aerosol air quality parameters were made aboard the NOAA WP-3D aircraft. The plane flew on a NE-SW flight path between 30 and 45°N at a distance of approximately 2-300 km from the coast.

This report presents results of the meteorological, aerosol, and ozone measurements, including detailed vertical cross sections for the portions of the flight track parallel to the North American coast. Vertical cross sections normal to the coast are presented where appropriate. Synoptic weather maps and discussions are presented for each day. Twice daily isobaric air-parcel back-trajectories for six positions off the coast between Nova Scotia and South Carolina at 850 and 700 mb were computed with the Gridded Atmospheric Multilevel Backward Isobaric Trajectories (GAMBIT) model (Harris, 1982). A latitude-longitude plot of each flight track is presented for geographical orientation. For each flight, a flight log is given describing the movements of the aircraft, and the observations of clouds and haze. Meteorological wind analyses were used to calculate the flux of air (standard temperature and pressure, 0°C, 1013 mb) from the continent arriving at 15-minute intervals along the flight track. Wind was divided into the U segment, representing the NW component perpendicular to the idealized flight track (negative U means SE winds), and the V segment, representing the SW component parallel to the idealized flight track (negative V means NE winds). The idealized flight track was defined as being 200-300 km east of the Atlantic coast of North America on a line running 45° east of north (see Appendix B, fig. B.1). The U component was then used to calculate 15-min. average air mass fluxes in units of either $m^3\ s^{-1}$ or $kg\ m^{-2}\ s^{-1}$ (Appendix B).

Aerosol data are presented as cross sections of condensation nuclei (CN) concentration and aerosol scattering extinction (b_{sp}), and as log dN/dlogD (number) and log dV/dlogD (volume) spectra of aerosol size distributions, where D is diameter. Condensation nuclei were measured with a General Electric CN Counter, aerosol scattering extinction,corrected for Rayleigh scattering, was measured by a Meteorology Research, Inc., Model 1591 nephelometer, and aerosol particle diameters were measured by a Particle Measuring Systems Active Scattering Aerosol Spectrometer Probe (ASASP) and a Forward Scattering Spectrometer Probe (FSSP). Aerosol particle diameters were measured in eight size ranges from 0.615 to 3.12 μm (ASASP) and in 15 ranges between 1 to 15 or 3 to 45 μm (FSSP). Aerosol spectra in the free troposphere and marine boundary layers were averaged over 10 to 50 minutes. Limited flight time in the cloud layer required averaging over periods of 2 to 5 minutes. The ASASP cannot measure aerosols accurately when relative humidities are greater than 80%, and thus FSSP data are presented for the cloud layer. Marine boundary layer ASASP data are presented only for air with humidities less than 80%. The overall gas sampling and aerosol systems were described by Schnell (1984 and Schnell et al, 1987). All times and dates are given in Greenwich Mean Time (GMT).

1. WATOX FLIGHT 1, JANUARY 4, 1986

1.1 Flight Track

The aircraft flew SE from McGuire Air Force Base (New Jersey) to latitude 37.5°N, longitude 71.5°W (fig. 1.1). The aircraft then flew NNE to east of Cape Cod, Massachusetts (42.3°N), and then turned ENE. Upon reaching the end of the flight track (44°N, 58°W), the aircraft reversed course, returning to base along the same flight track. During the flight, the aircraft crossed between the marine boundary layer and free troposphere five times, and reached a maximum altitude of 4566 m (43-44°N) while sampling in an elevated haze layer. Total flight time was 8 hours, 46 minutes.

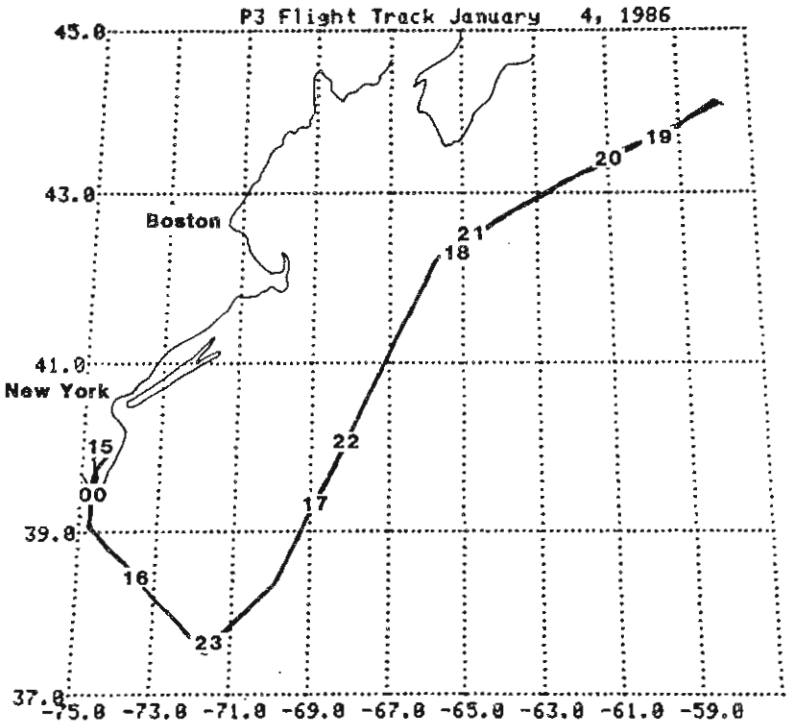

Figure 1.1.--Horizontal projection of the flight track on a latitude-longitude grid, on January 4, 1986. The numbers on the flight track are hours (GMT).

1.2 Synoptic Situation

At 0000 GMT on January 5, the closest synoptic summary to flight time, a weak low-pressure system (1008 mb) was centered over the southern Great Lakes area (fig. 1.2). From this low, a cold front extended south along the western flank of the Appalachian Mountains to southern Louisiana, and a warm front was moving north through Pennsylvania. A strong cyclonic flow extended through the Canadian Maritime Provinces from a second low near Nova Scotia. Between the low-pressure areas a weak ridge covered the New England and Northern Atlantic States, including a major portion of the aircraft flight track. Air flow at flight altitude was NW except at the southern limit of the track, where it became SE.

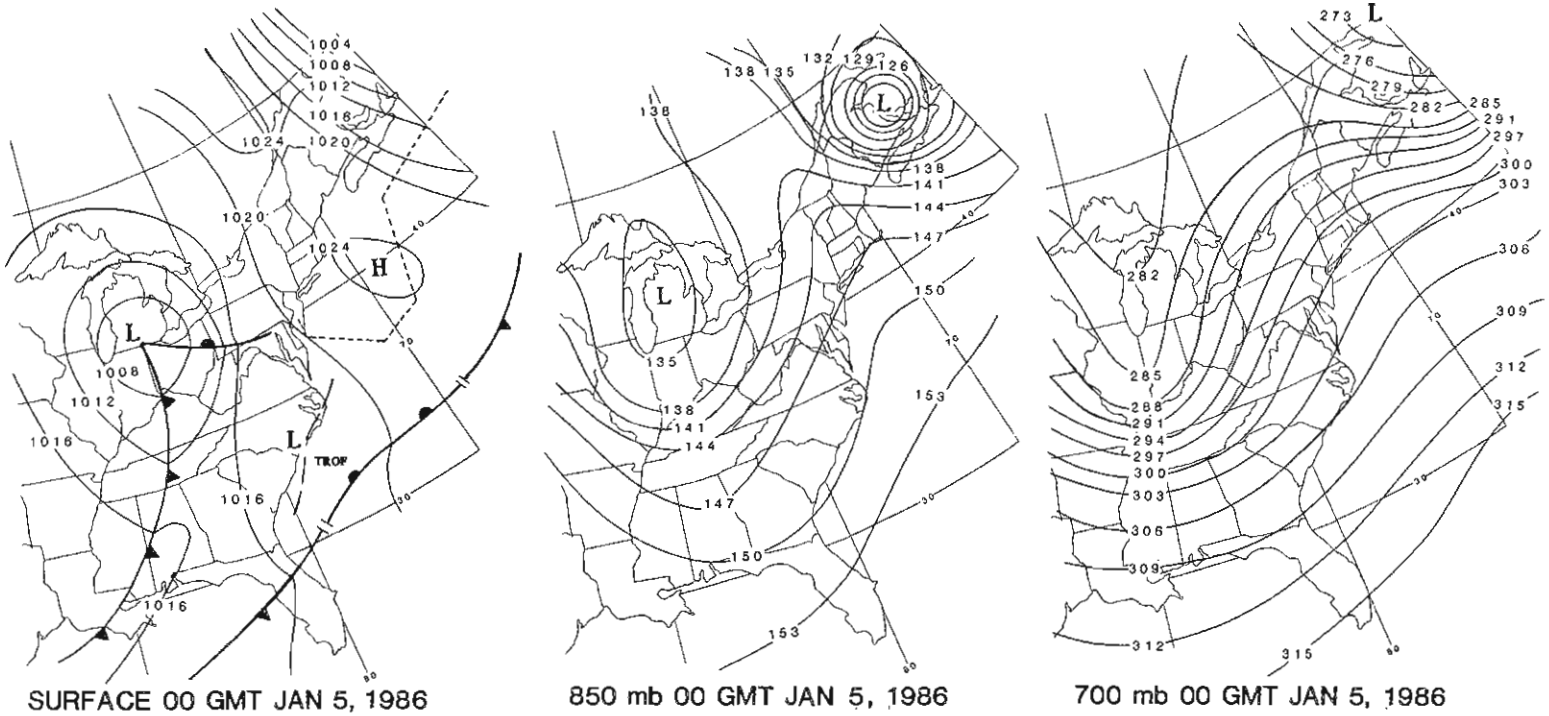

Figure 1.2--Surface (pressure, mb), and 850- and 700-mb (geopotential height, decameters) synoptic analyses, 0000 GMT, January 5, 1986. The flight track is shown by the dashed line on the surface analysis.

Low geopotential heights at 850 mb and 700 mb were present over the Nova Scotia area, and to a lesser extent, Michigan. Ridging was evident between these two systems; there was SW flow along the coast south of New York City and W flow along the New England coast.

1.3 Air-Parcel Back-Trajectories

Isobaric (850 mb) air-parcel back-trajectories arriving at 0000 GMT January 5 at six positions off the coast between Nova Scotia and South Carolina are given in fig. 1.3. Each successive 12-h interval is indicated on the trajectory. Trajectories A, B, and C clearly indicate the presence of low pressure near Nova Scotia. Air parcels at 850 mb followed a cyclonic path around the low for at least 24 hours before crossing the flight path. Farther south, air parcels traveled across the Ohio Valley from the NW for the 24- to 36-h period before arriving at points D and E. Trajectory F indicates flow across Florida. The 700-mb trajectories (fig. 1.4) show WNW transport winds. The northern two trajectories, closer to the center of the low, show NW transport across Canada and New England. Trajectory C crosses the Great Lakes and New York. Air parcels in southwestern Ohio and near the Tennessee/Georgia border reach points D and E, respectively, on a generally SE path. Trajectory F again indicates flow across Florida.

A comparison of three methods of calculating trajectories is included in Appendix A.

1.4 Flight Log, January 4, 1986

1525 GMT	Takeoff.
1526-1544	Climb SE to 4465 m, 579 mb, 37°N; air is cloud free and hazy
1610-1651	Encountering stratocumulus (Sc) cloud deck; descend to 897 mb, 1007 m, cirrus (Ci) high overhead.
1620	Turn to a NE flight track.
1648	Within haze layer above the Sc clouds, 897 mb, 1007 m, 39°N; CN > 2000 cm^{-3}.
1701-1727	Climb to 699 mb, 3025 m, 41°N; Sc more scattered, Ci gone; CN ~250 cm^{-3}.
1806	Have now descended through cloud layer into boundary layer, 990 mb, 180 m, 42.5°N; air is very clean; cloud base 550 m, wind speed 25 m s^{-1} at surface.
1815	Snow showers.
1820-1856	Climb to 709 mb, 2709 m, 43°N; cloud tops 1128 m.

1845	Haze layers clearly visible in free troposphere.
1910	Flying in well-defined haze layer, 727 mb, 2715 m, 43°N; shallow altocumulus (Ac) layer exists above the aircraft; CN > 5000 cm^{-3}.
1917-1930	Climb to 572 mb, 4566 m, 43.5°N; flew out of the top of haze.
1930-2014	Descend through haze layer and boundary layer clouds to 989 mb, 200 m, 43°N; entered clean air at 2001; cloud tops 1205 m.
2014-2044	Flying S, level in the boundary layer, 989-1000 m, 43-41°N; cloud base 610 m; CN ~ 1000 cm^{-3}.
2144-2156	Climb through cloud layer to 814 mb, 1806 m, 41-40°N; cloud tops 915 m.
2208-2218	Descend into boundary layer to 970 mb, 355 m, 39°N; CN 1500-1800 cm^{-3}.
2304	Turn W toward coast.
2349-2357	Climb to 850 mb, 1454 m.
0004-0011	Descend to surface and land.

1.5 Vertical Profiles Across the Marine Boundary Layer Inversion

The aircraft collected a wide range of meteorological, gas, and aerosol data on a continuous basis. Some of these parameters, when plotted against altitude, reveal much about the structure of the atmosphere affecting the distribution and transport of the gases and aerosols. One such profile is presented in fig. 1.5 for a day when the higher troposphere contained exceptionally large concentrations of CN. The changes in CN concentration, b_{sp}, ozone, and relative humidity parameters observed across the marine boundary layer inversion on this day were typical of all the flights. As shown in fig. 1.5, there is considerable variation in the fine structure of the parameters, particularly CN concentration, humidity, and ozone, but certain major features are apparent. For instance, the moist marine boundary layer with reduced ozone values is a regular feature on all flight profiles occurring beneath the marine boundary layer temperature inversion.

The zone of elevated CN concentrations in the free troposphere, between 600 and 700 mb, is distinctive, and is matched in part by a relative humidity increase above 700 mb. It is probable that moisture and CN were transported together in a relatively cohesive layer from a source region to the

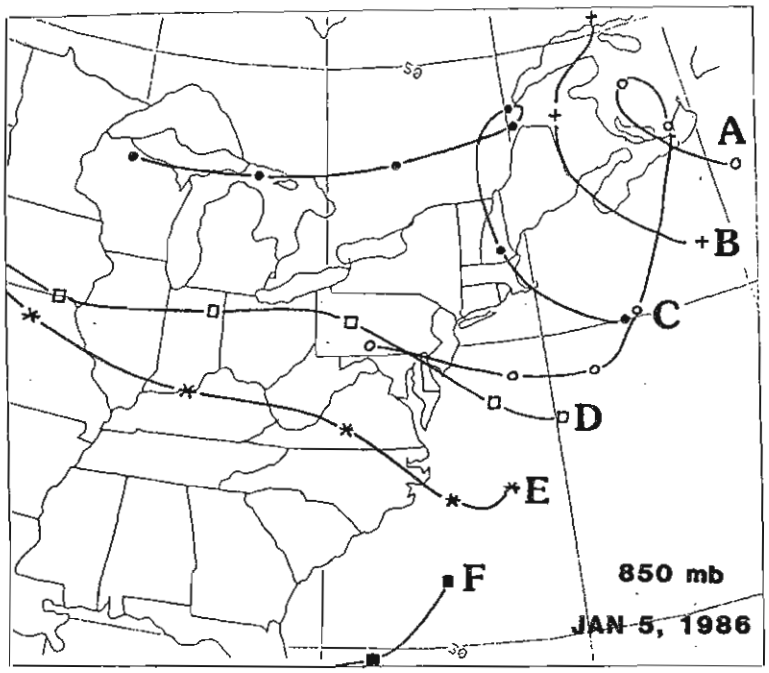

Figure 1.3--850-mb isobaric back-trajectories arriving at points A-F at 0000 GMT, January 5, 1986. Successive symbols indicate 12-h intervals.

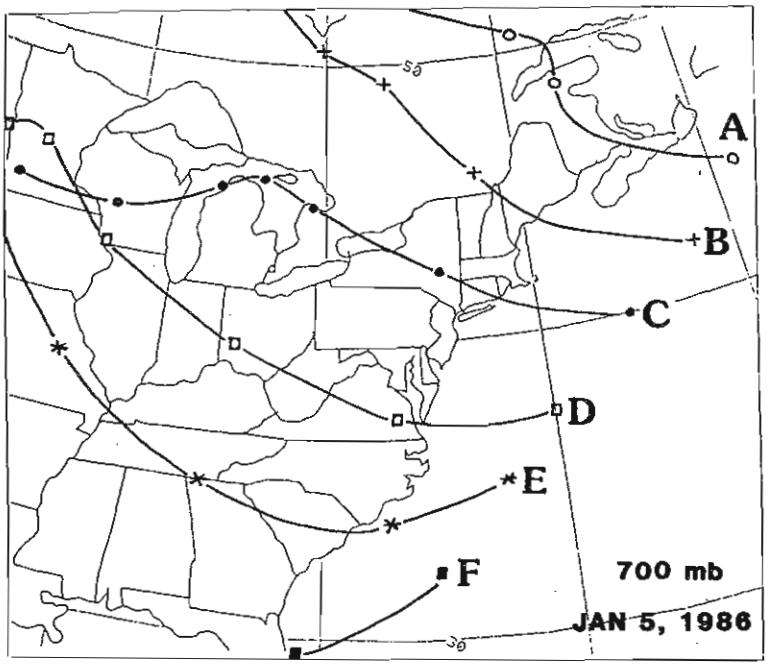

Figure 1.4--700-mb isobaric back-trajectories arriving at points A-F at 0000 GMT, January 5, 1986. Successive symbols indicate 12-h intervals.

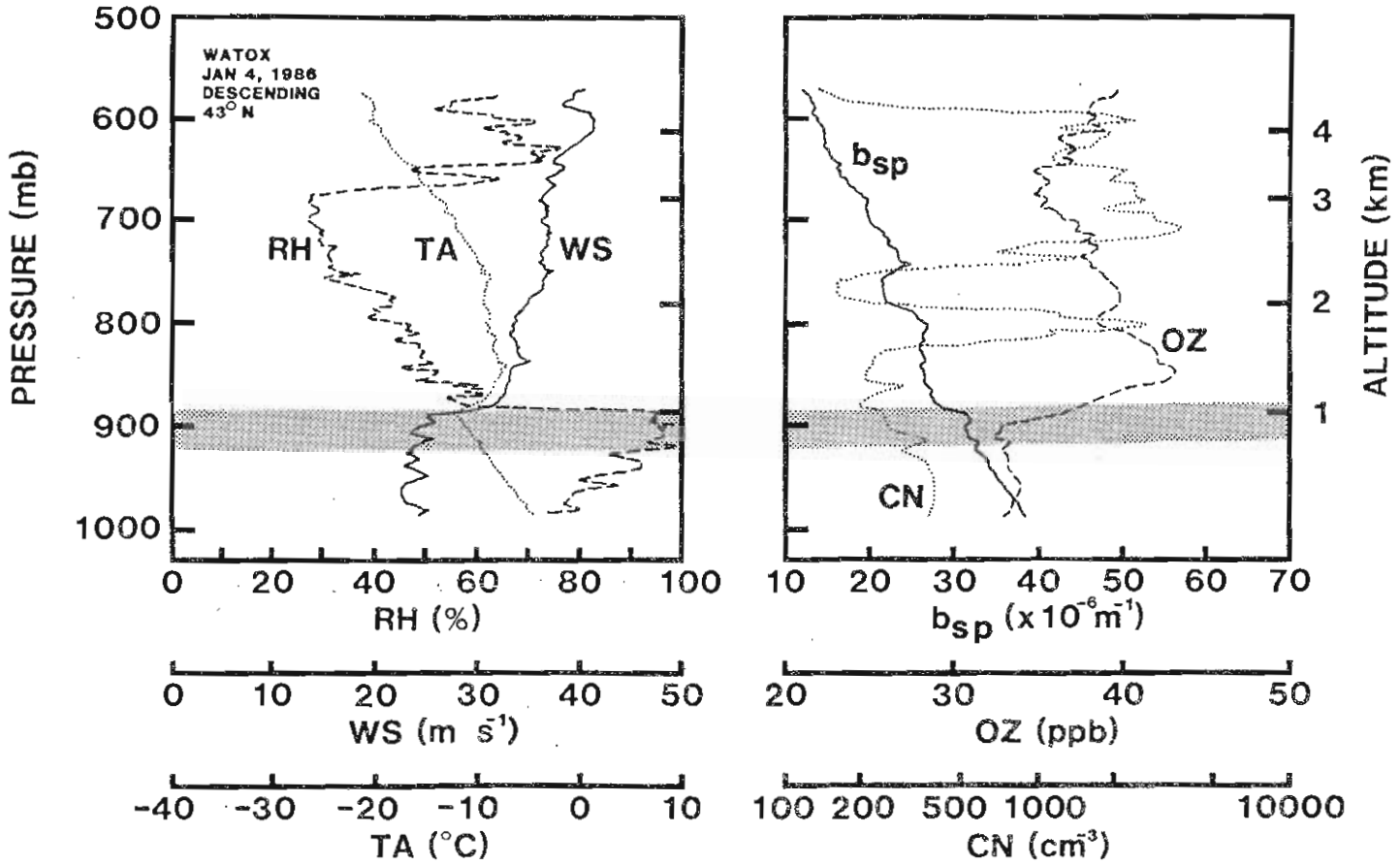

Figure 1.5--An example of vertical profiles of relative humidity, ambient temperature, wind speed, CN concentration, b_{sp}, and ozone, January 4, 1986 at 43°N latitude. The elevated CN concentrations as > 3 km were associated with a haze layer moving over the area from the north. The shaded area represents the cloud layer, capped by the marine boundary layer inversion.

northwest. Aerosol b_{sp} decreased slightly at 750 mb, coincident with a layer of minimum CN concentration.

There is a sharp increase in ozone mixing ratio above the marine boundary layer and the largest ozone values occur just above the temperature inversion. The lower ozone values in the boundary layer are at concentrations expected for air modified by destruction of ozone within the layer. There appears to be some ozone depletion in the free troposphere at 800 mb and between 700-600 mb, coincident with relatively elevated CN concentrations. Data from profiles such as those in fig. 1.5, and data from level aircraft runs, were used to plot the atmospheric cross sections presented in this report.

1.6 Atmospheric Cross Sections

Latitude-altitude meteorological cross sections for a plane approximately parallel to the coast were constructed from data recorded by the aircraft for potential temperature and winds, as shown in fig. 1.6, and for water vapor mixing ratios, as shown in fig. 1.7. In both figures, dashed lines represent the aircraft flight track with time of day (GMT) given at several positions along the flight track. In fig. 1.6 winds are given in m s^{-1} and isentropes at 2-K intervals. Figure 1.7 shows lines of constant water vapor mixing ratio in g kg^{-1}. As determined from the isentropes, the top of the boundary layer was approximately 900 mb, and sloped down from north to south. As expected, the atmosphere was more stable above the boundary layer.

The winds were primarily from the W or NW and were stronger to the north closer to the center of the low-pressure system. The strongest water vapor mixing-ratio gradient occurred just above the cloud layer. Mixing ratios were generally less than 1 to 2 g kg^{-1} above 900 mb. Below 900 mb and south of 40°N latitude, mixing ratios were greater than 4 g kg^{-1}, and exceeded 5 g kg^{-1} near the Gulf Stream south of 38°N.

The spatial distribution of westerly air fluxes perpendicular to the flight track averaged for 15-min segments is shown in fig. 1.8. The dominant feature is a flux of 30 to 40 kg m^{-2} s^{-1} between 43 and 44°N, above the marine boundary layer inversion. Westerly fluxes diminish consistently toward the southern end of the flight track, eventually becoming weak easterly in the marine boundary layer south of 39°N. The marine boundary layer inversion appeared to have no influence on the vertical structure of the air fluxes. A numerical list of the flux calculations is presented in Appendix B.

1.7 Cross Sections of CN Concentration and b_{sp}

Figure 1.9 presents a CN concentration cross section along the flight track, and includes several distinct features of interest. At 43 to 44°N and 600 to 800 mb, a large patch of visibly dark haze yielded CN concentrations between 1000 and 6500 cm^{-3}. This layer was not typical of free tropospheric conditions and probably originated from anthropogenic sources in the higher northern latitudes of North America, as suggested by trajectories described in sec. 1.3. It is associated with the maximum air flux, shown in fig. 1.8. A

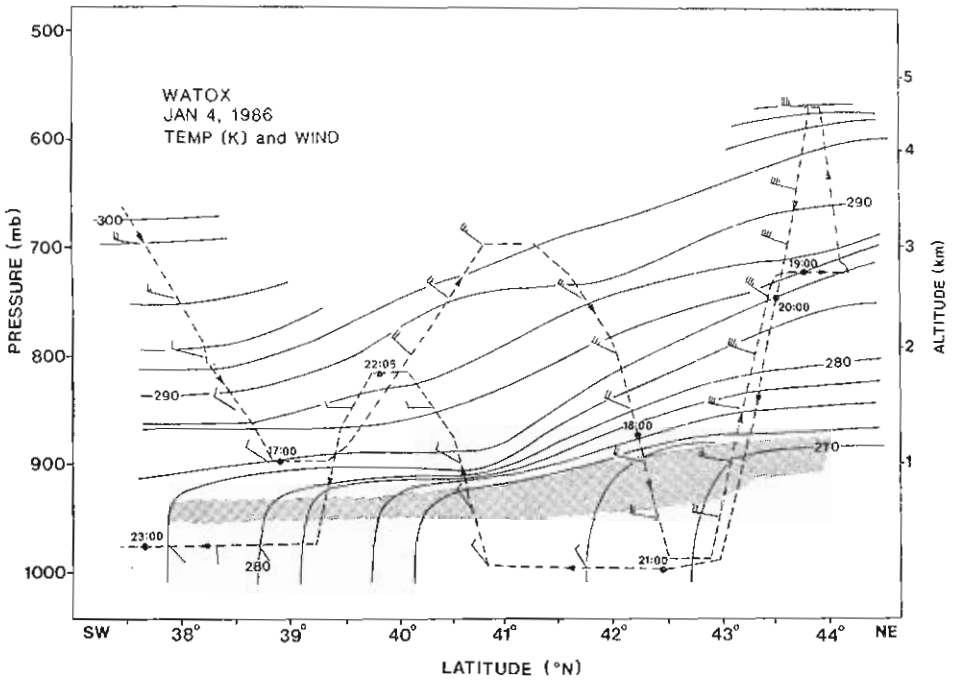

Figure 1.6--Latitude-altitude cross section of potential temperature and wind (full barb = 10 m s^{-1}) along the WP-3D flight track parallel to the coast, January 4, 1986. The stippled area represents the cloud layer. The flight track is shown by the dashed line.

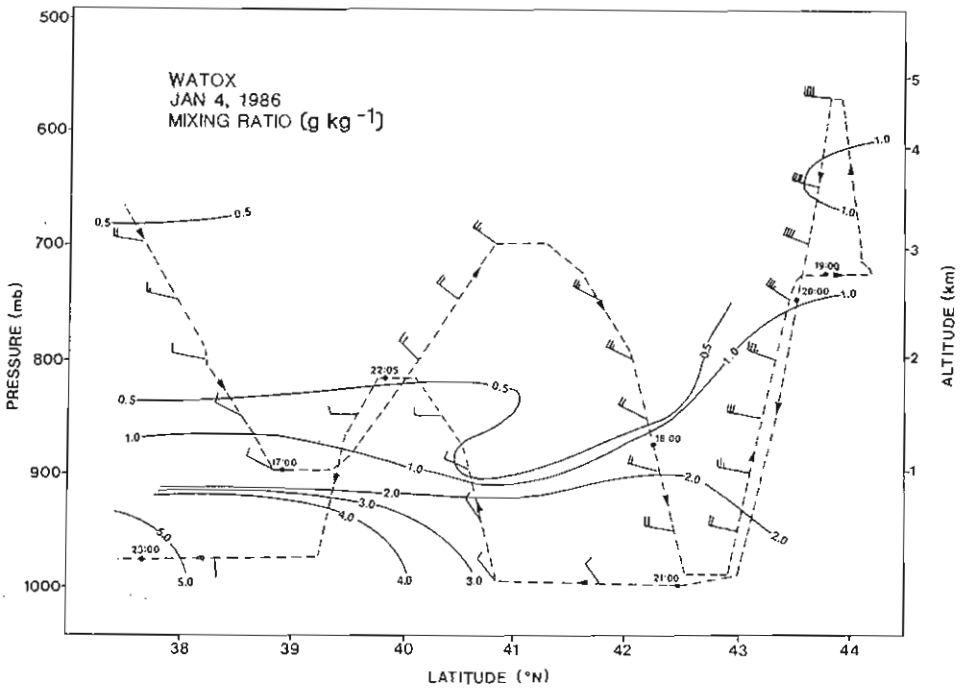

Figure 1.7--Latitude-altitude cross section of water vapor mixing ratio and wind (full barb = 10 m s^{-1} January 4, 1986. The flight track is shown by the dashed line.

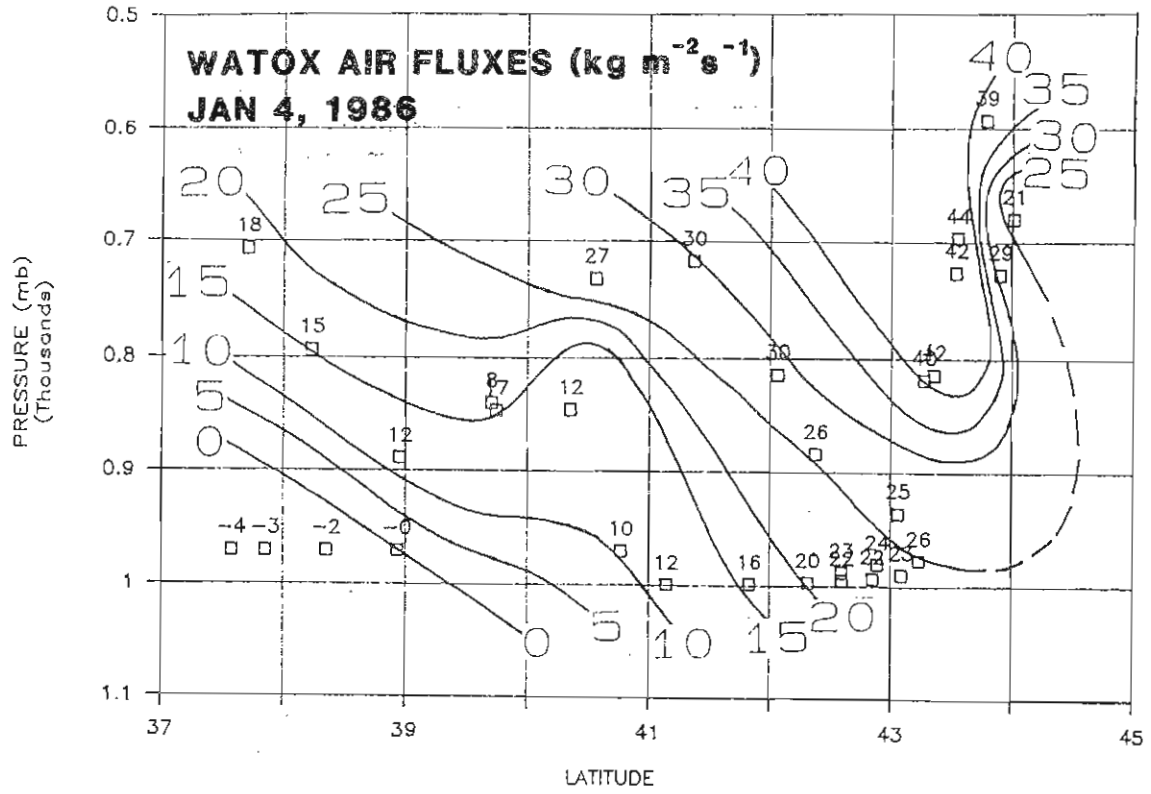

Figure 1.8--Air fluxes perpendicular to the aircraft flight track, January 4, 1986.

secondary CN peak of 3000 cm^{-3} occurred at 890 mb and 39°N, and probably was a remnant of the previous day's marine boundary layer. CN concentrations of less than 500 cm^{-3} at 42 to 43°N in the boundary layer were associated with cleaner subsiding air from the upper troposphere. In the marine boundary layer, higher CN concentrations were measured at the SW end of the transit. Aside from the two CN peaks in the free troposphere, marine boundary layer CN concentrations were about 3 times higher than those in the free troposphere.

A cross-section of b_{sp} is presented in fig. 1.10. Maximum b_{sp} concentrations were observed at the SW end of the flight track, probably associated with transport of anthropogenic particulate matter from sources in the central eastern United States. The spatial pattern of b_{sp} in the free troposphere bears little relationship to the pattern of CN concentrations.

1.8 Aerosol Size Distributions

Number and volume spectra of aerosol particles measured by the ASASP and FSSP probes are presented in fig. 1.11 for the free troposphere, cloud layer, and marine boundary layer respectively. The measurement locations are indicated in fig. 1.9 by letters associated with each individual spectrum.

Free troposphere aerosol spectra generally reflect the CN concentration pattern, in that lowest particle concentrations were observed in the sub-

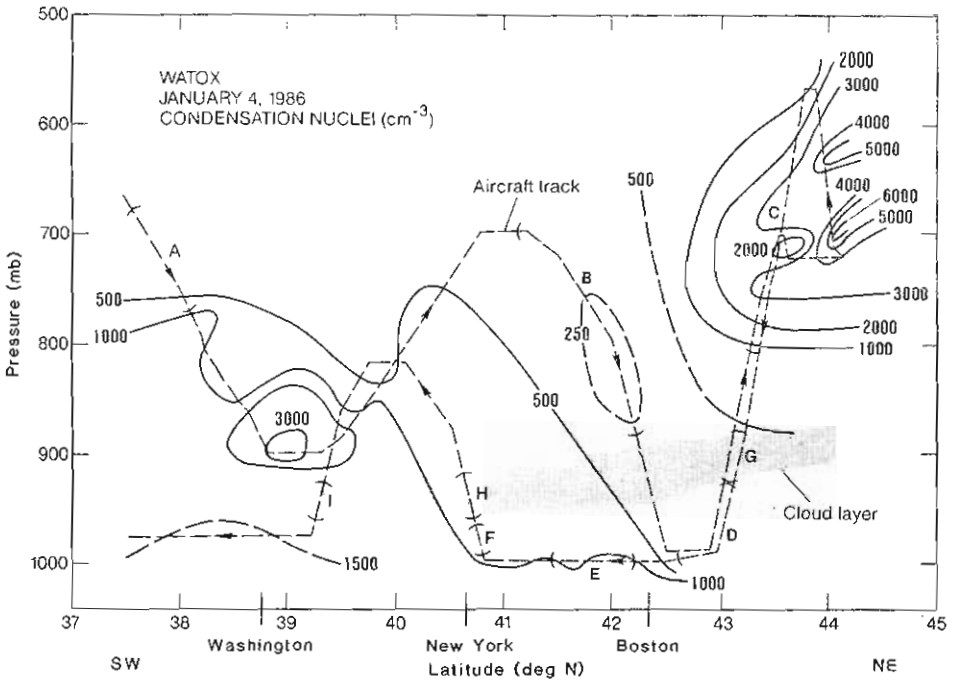

Figure 1.9--NE-SW cross section of CN concentration over the western Atlantic Ocean, January 4, 1986. Letters and brackets on the flight track indicate measurement locations for fig. 1.11. The thick dashed lines emphasize maximum or minimum values.

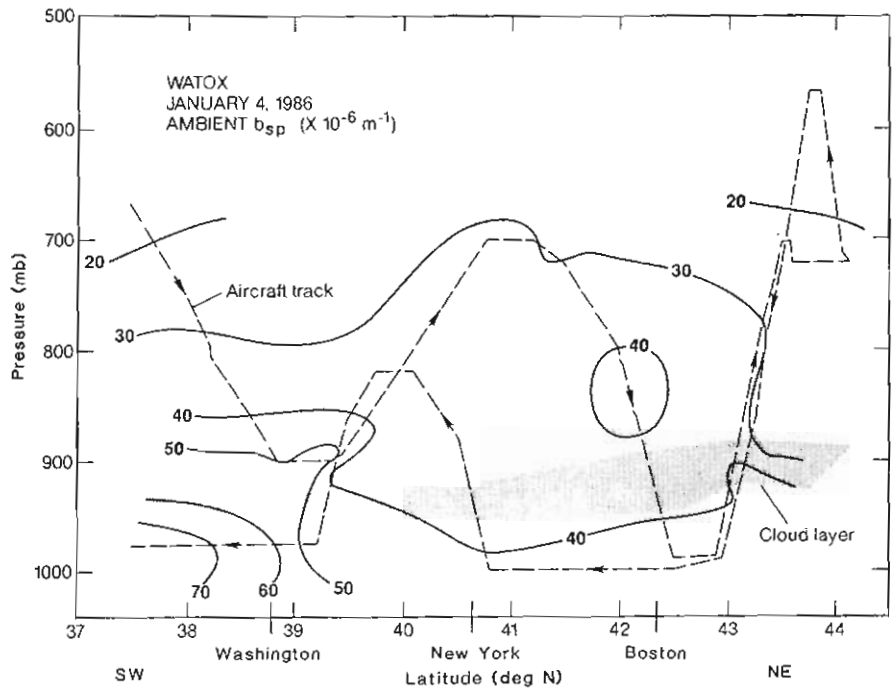

Figure 1.10--NE-SW cross section of b_{sp}, January 4, 1986.

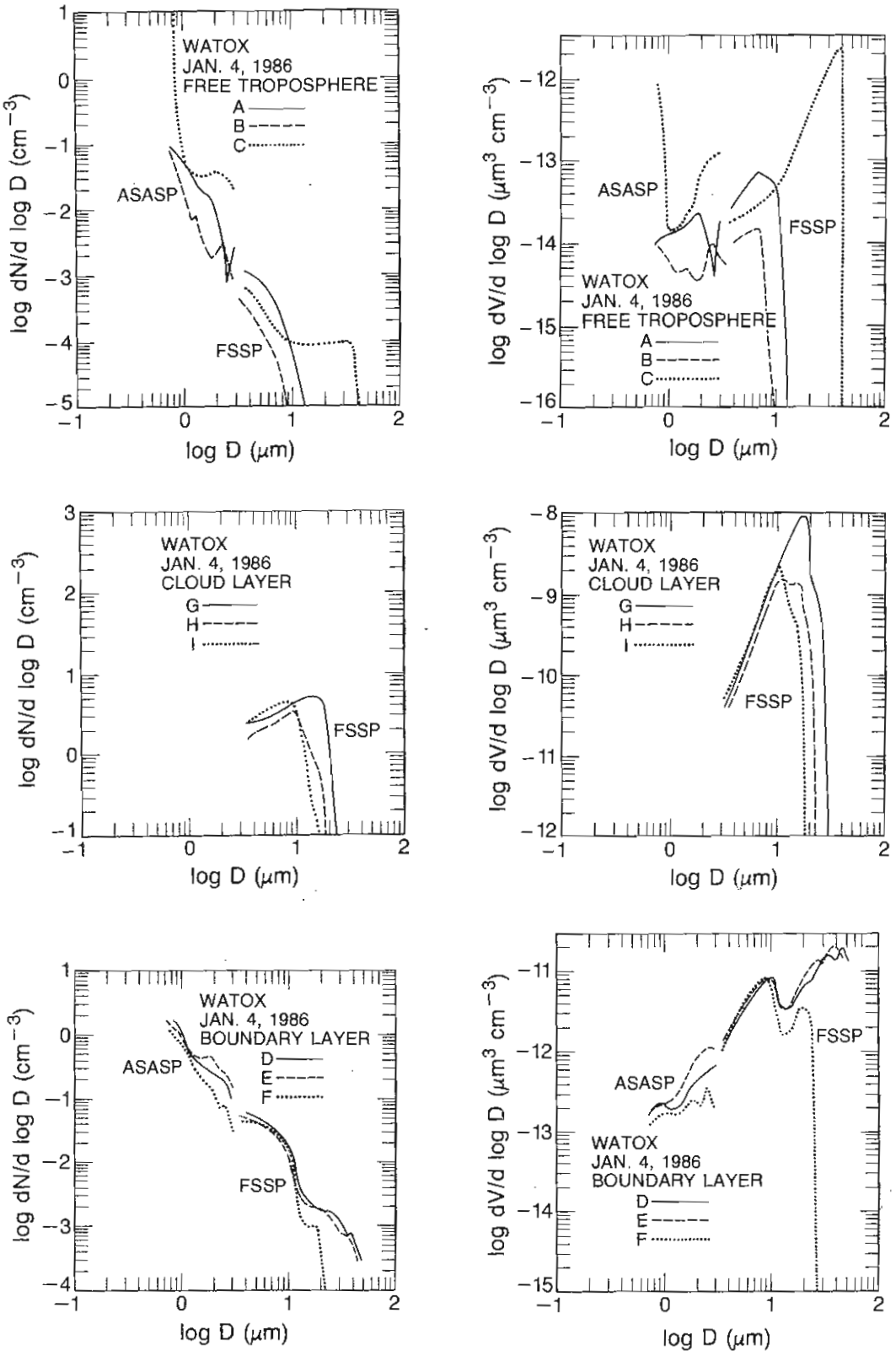

Figure 1.11--Number (left column) and volume (right column) aerosol size spectra at various aircraft locations, January 4, 1986. The letters associated with the spectra refer to locations shown in fig. 1.9.

siding (clean) air at 42°N (curve B) and the highest concentrations in the haze layer at 43-44°N (curve C), particularly in the smaller size ranges (0.645-0.820 μm diameter). This haze layer also contained more large particles (>10 μm) than were observed in background air. The high-altitude haze layer also exhibits peaks at 7-μm diameter and at 30-μm diameter.

Cloud layer droplets exhibit peaks in both number and volume spectra in the 10-20 μm diameter range and show little difference between the three widely separated sampling locations. These distributions are typical for marine stratus clouds.

Aerosol number-size distributions in the boundary layer were an order of magnitude greater than in the free troposphere. The dN/dlogD curves exhibit a steady decrease with particle size, similar to a theoretical Jungean curve. There is little difference in the spectra along the flight track. The dV/dlogD curves exhibit two peaks, one at 8-9 μm, probably associated with sea salt, and another at 30 μm (at the northern end of the flight track). The existence of larger particles in the westerly flow in the northerly region of the flight most likely reflects increased sea salt injected into the atmosphere from sea spray generated by strong winds.

2. WATOX FLIGHT 2, JANUARY 6, 1986

2.1 Flight Track

The aircraft flew SE from McGuire Air Force Base to 38°N, 73°W, then NE to the northern end of the flight track at 41.3°N, 66.5°W, by 1400 GMT. The aircraft then flew SW to 31.5°N, 77°W, before retracing its path NE to 35°N, 72°W and then turning NW to home. During the flight, the aircraft crossed the boundary between the free troposphere and the marine boundary layer eight times. Total flight time was 10 hours, 4 minutes.

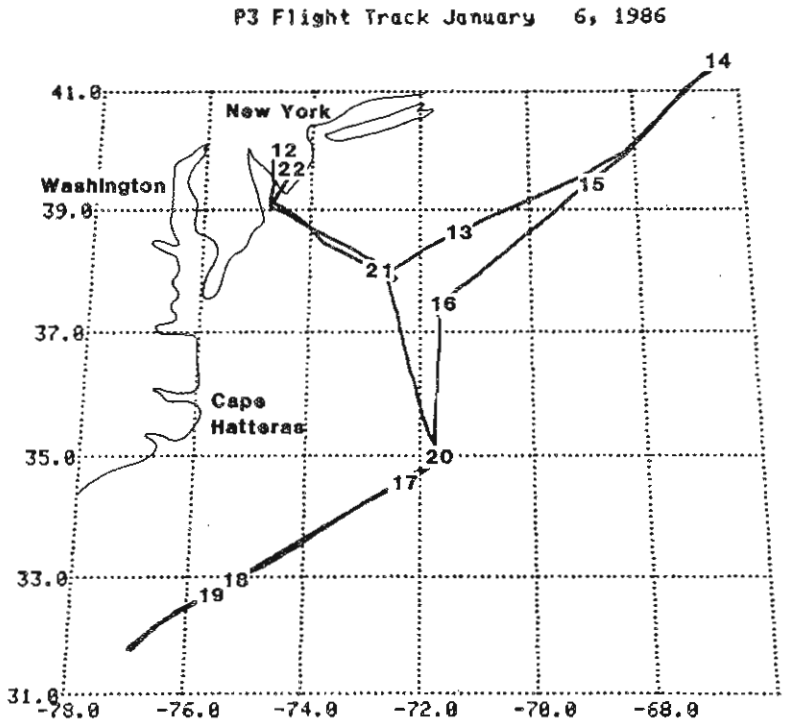

Figure 2.1--Horizontal projection of the flight track on a latitude-longitude grid, for January 6, 1986. The numbers on the flight track are hours (GMT).

2.2 Synoptic Situation

At 1200 GMT January 6, a cold front, associated with a deep low-pressure system (976 mb) centered just west of Newfoundland (fig. 2.2), extended over New York, Pennsylvania, Ohio, and to the west. Strong pressure gradients with W to SW surface winds prevailed over northeastern U.S. and into eastern Canada. High pressure and weak pressure gradients dominated the southeastern U.S.

The 850- and 700-mb charts exhibited a similar airflow pattern, with a closed low over the Gulf of St. Lawrence. Strong W winds prevailed throughout the lower troposphere over much of the eastern U.S.

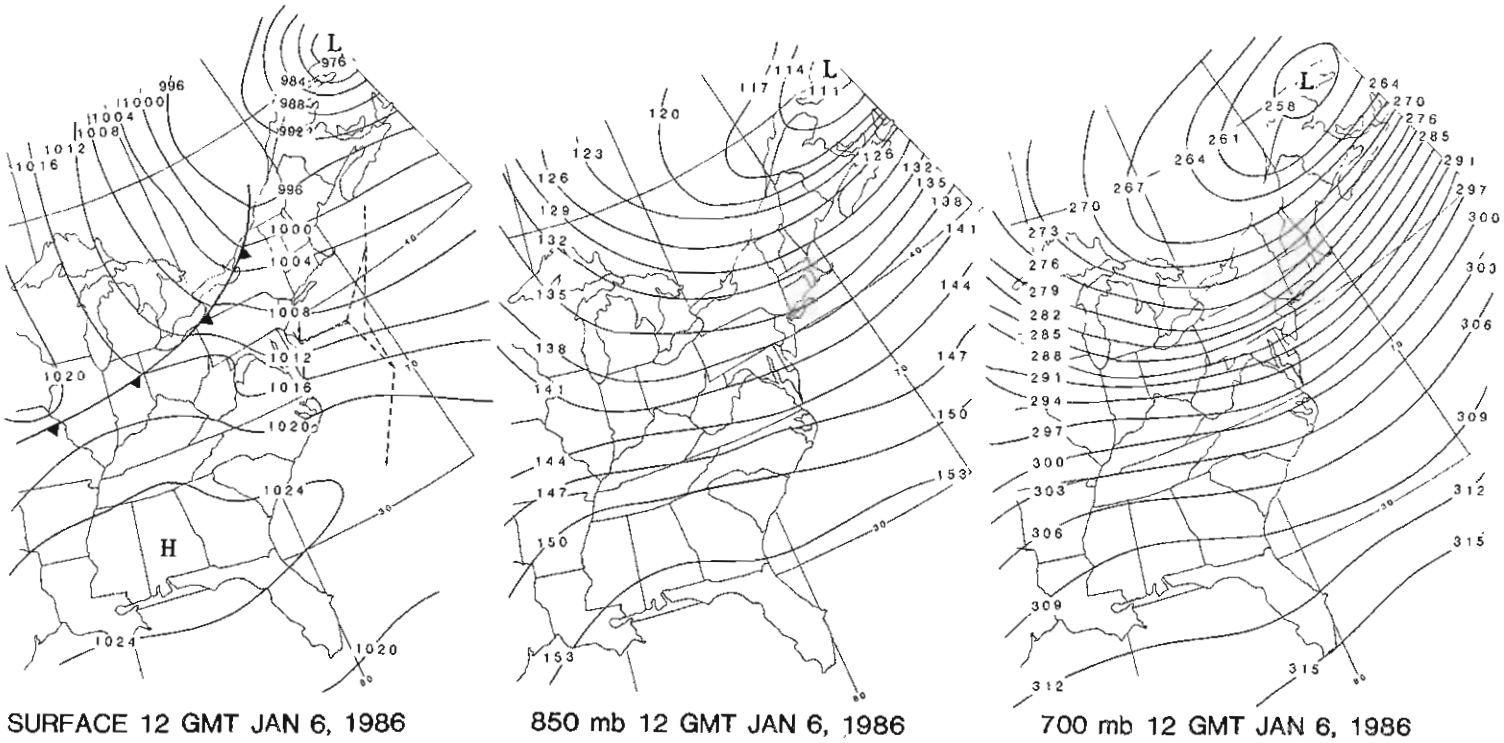

Figure 2.2--Surface (pressure, mb), and 850 and 750 mb (geopotential height, decameters) synoptic analyses for 1200 GMT, January 6, 1986. The flight track is shown by the dashed line on the surface map.

2.3 Air-Parcel Back-Trajectories

Isobaric (850 mb and 700 mb) air-parcel back-trajectories arriving at points A to F at 1200 GMT January 6 are given in figs. 2.3 and 2.4. At 850 mb, trajectories A and B came from more southerly locations than the other trajectories. Trajectory C crossed northeastern Ohio. Trajectories D-F suggest the air parcels were in the Ohio River Valley region about 12 to 24 hours before reaching their end points. The 700-mb trajectories are fairly uniform, crossing south of the Great Lakes on an easterly course and extending off the coast. Greater wind speeds were evident to the north, closer to the center of the low, for the 12-h period before arriving at points A-F. Air parcels from over the Ohio River Valley region reached the trajectory starting points in 12 to 18 hours.

A comparison of results from three trajectory methods is presented in Appendix A.

2.4 Flight Log, January 6, 1986

1210 GMT	Takeoff
1210-1225	Climb SE to 571 mb; 4581 m; clear skies, light to moderate winds.
1248	Flight track now NE, 37°N.
1257-1326	Descend to bottom of cloud layer, 887 mb, 1100 m, 39.5°N; cloud tops 2700 m; cloud base above 1100 m; higher CN patches, 1250 cm^{-3}.
1336-1350	Climb through cloud layer to 3066 m, 695 mb; air much cleaner.
1401	Flight track turns SW, 41°N.
1403-1423	Descend to 985 mb, 238 m, 41°N, in boundary layer; cloud tops 2200 m; cloud base 850-880 m.
1423-1600	In boundary layer, 40.5-37°N; CN 800-1300 cm^{-3}.
1600-1617	Climb through boundary layer to 778 mb, 2165 m, 37°N; cloud base 1800 m; cloud tops 2040 m; clouds dissipating to south.
1622-1638	Descend into boundary layer to 998 mb, 122 m, 36°N; clouds scattered with tops 1950 m.
1638-1830	In boundary layer 35.5-32°S; CN 900-1200 cm^{-3}; 900-1000 mb; flight track varies SE to SW.
1830-1852	Climb to 704 mb, 2963 m, 32°N; flight track changes to NE; few scattered stratocumulus between 1220 and 1370 m.
2000	Flight track NW.
2011	Plane level at 799 mb, 2135 m, 35.5°N; just above cloud tops.
2032-2056	Climb to 696 mb, 3047 m, 37°N.

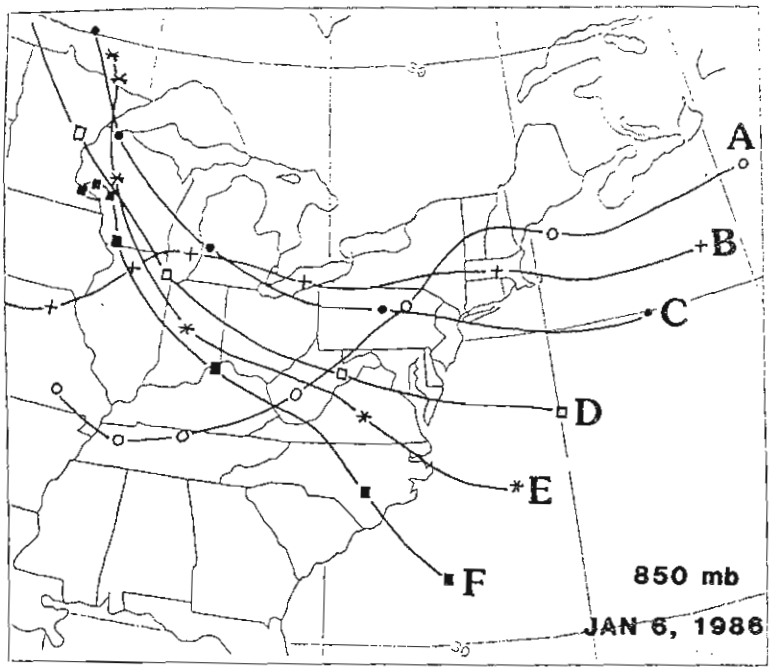

Figure 2.3--850-mb isobaric back-trajectories arriving at point A-F at 1200 GMT, January 6, 1986. Successive symbols indicate 12-h intervals.

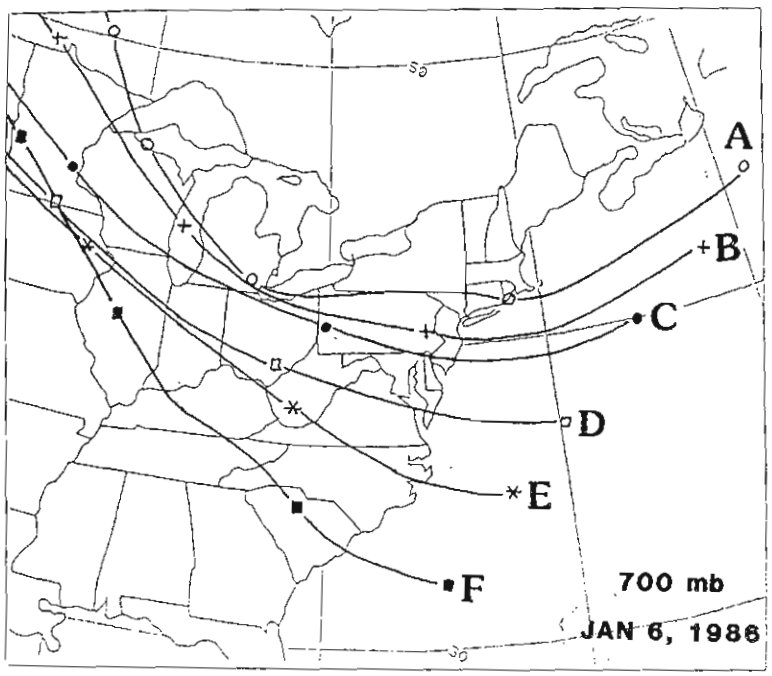

Figure 2.4--700-mb isobaric back-trajectories arriving at points A-F at 1200 GMT, January 6, 1986. Successive symbols indicate 12-h intervals.

2056-2116 Descend to 992 mb, 170 m; few stratocumulus clouds and high cirrus.

2125-2133 Climb to 755 mb, 2407 m.

2200-2214 Descend to surface and land.

2.5 Vertical Profiles Across the Marine Boundary Layer Inversion

Profiles of CN concentration, b_{sp}, ozone, wind speed, wind direction, and relative humidity at 37°N on January 6 exhibited a distinct change upon crossing the boundary layer inversion. As observed in fig. 2.5, relative humidity dropped from greater than 90% at the top of the boundary layer to 10% in the space of 100 m, and CN concentrations dropped from 1600 cm^{-3} to 200 cm^{-3} over the same distance. The temperature profile indicates that this inversion was slightly weaker than that observed on January 4. Aerosol b_{sp} also decreases across the inversion from about 50 × 10^{-6} m^{-1} to 30 × 10^{-6} m^{-1}.

The variations in ozone are similar to those observed on January 4 (fig. 1.5). At 800 mb, above the boundary layer inversion, there is a narrow layer of higher ozone, about 15% greater than that found in the boundary layer. Above 2 km, the ozone decreases to near boundary layer values again. Two profiles slightly to the north which also penetrated the cloud layer, also show an increase of ozone at the same altitude, but on the order of 3-5%.

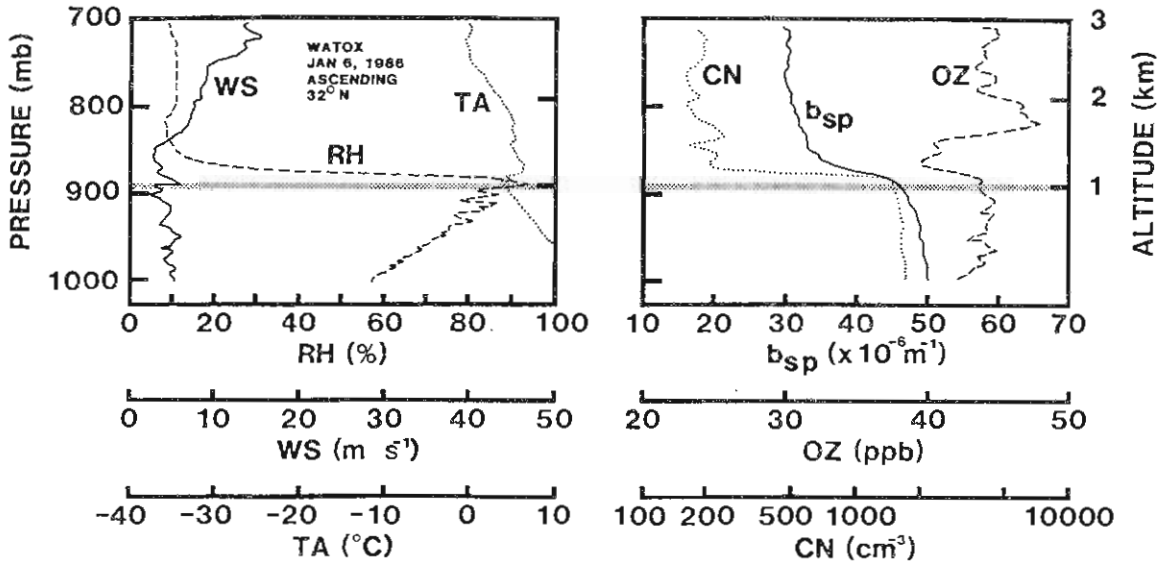

Figure 2.5--An example of vertical profiles of relative humidity, ambient temperature, wind speed, CN concentration, b_{sp}, and ozone, January 6, 1986. The shaded region represents the cloud layer, capped by the marine-boundary layer inversion.

2.6 Atmospheric Cross Sections

Latitude-altitude cross sections of potential temperature, wind speed, and water vapor mixing ratio approximately parallel to the coast were constructed from dropwindsonde and aircraft data along the flight track, as shown in figs. 2.6 and 2.7. The top of the boundary layer increased from about 880 mb at the south end of the track to about 780 mb at the north end. West winds dominated the area throughout the flight and were strongest in the north, closer to the center of the low-pressure system. The cloud layer at the top of the boundary layer was quite shallow except at the northern end of the flight track. The strong water vapor mixing ratio gradient occurred above the cloud layer except in the southern portion of the flight. Mixing ratios were generally less than 1 g kg^{-1} above the boundary layer and greater than 2 g kg^{-1} in the boundary layer. The largest mixing ratio of 6 g kg^{-1} was observed near the surface over the Gulf Stream at 33°N latitude. A relatively dry area was observed near the top of the boundary layer, and also near 33°N latitude.

Westerly air fluxes (kg m^{-2} s^{-1} at STP) perpendicular to the flight track are presented in fig. 2.8 for January 6, 1986. For latitudes 36°N and higher, fluxes increase relatively uniformly with height, peaking at 31 kg m^{-2} s^{-1} in the free troposphere at 700 mb, 37.7°N. Fluxes diminish toward the southern end of the flight track, as also observed on January 4 (fig. 1.8). Overall fluxes of air in the northern half of the flight track were 10 to 15 kg m^{-2} s^{-1} less than on January 4. A tabular list of calculated fluxes is presented in Appendix B.

2.7 Cross Sections of CN Concentration and b_{sp}

Figure 2.9 presents the spatial distribution of CN along the main NE to SW flight track, between 39 and 42°N. CN_3 concentrations in the free troposphere ranged from less than 200 cm^{-3} at the SW end of the flight track to about 500 cm^{-3} at some altitudes at 32-41°N. Unlike January 4, there were no visible haze layers. Between 36 and 41°N, CN concentrations greater than 1000 cm^{-3} occurred just above the marine boundary layer inversion, and the highest CN concentration of >1500 cm^{-3} was observed at the top of the cloud layer at 35.9°N. The streaky pattern of the higher CN concentrations in the cloud layer is probably indicative of anthropogenic plume sources from the continent. Marine boundary layer CN concentrations were measured at 1000 ± 200 cm^{-3} along most of the flight track; slightly lower concentrations were measured at 34-35°N and slightly higher concentrations at 37°N.

Aerosol b_{sp} (fig. 2.10) generally decreased with altitude, with the exception of a slightly elevated area between 750 and 850 mb at 33 to 35°N. The higher concentration areas in the cloud and boundary layers that were observed for CN were not observed for b_{sp}.

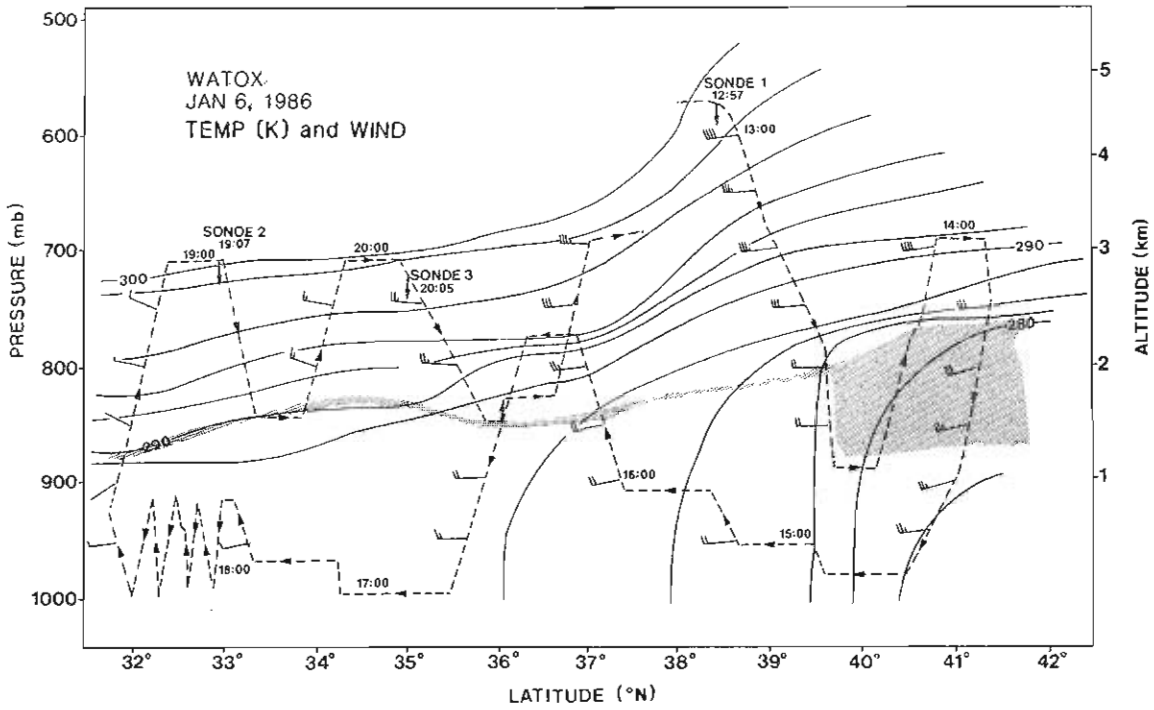

Figure 2.6--Latitude-altitude cross section of potential temperature and wind (full barb = 10 m s^{-1}) along the WP-3D flight track parallel to the coast, January 6, 1986. The stippled area represents the cloud layer. The flight track is shown by the dashed line.

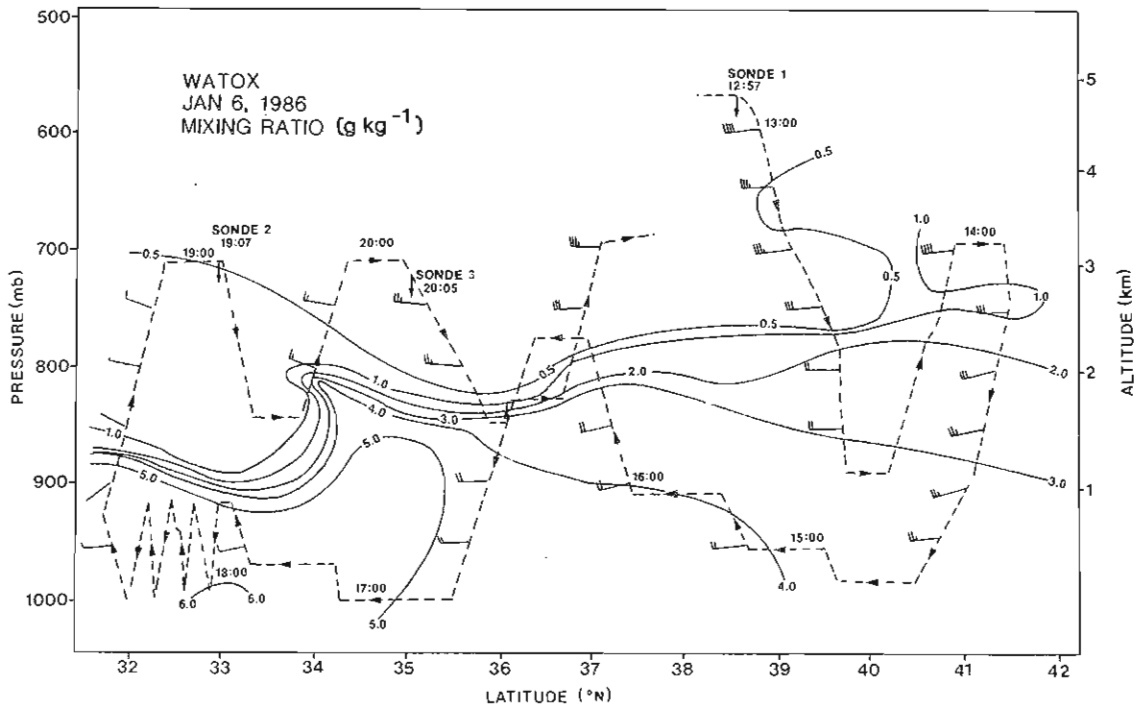

Figure 2.7--Latitude-altitude cross section of water vapor mixing ratio and wind (full barb = 10 m s^{-1}) January 6, 1986. The flight track is shown by the dashed line.

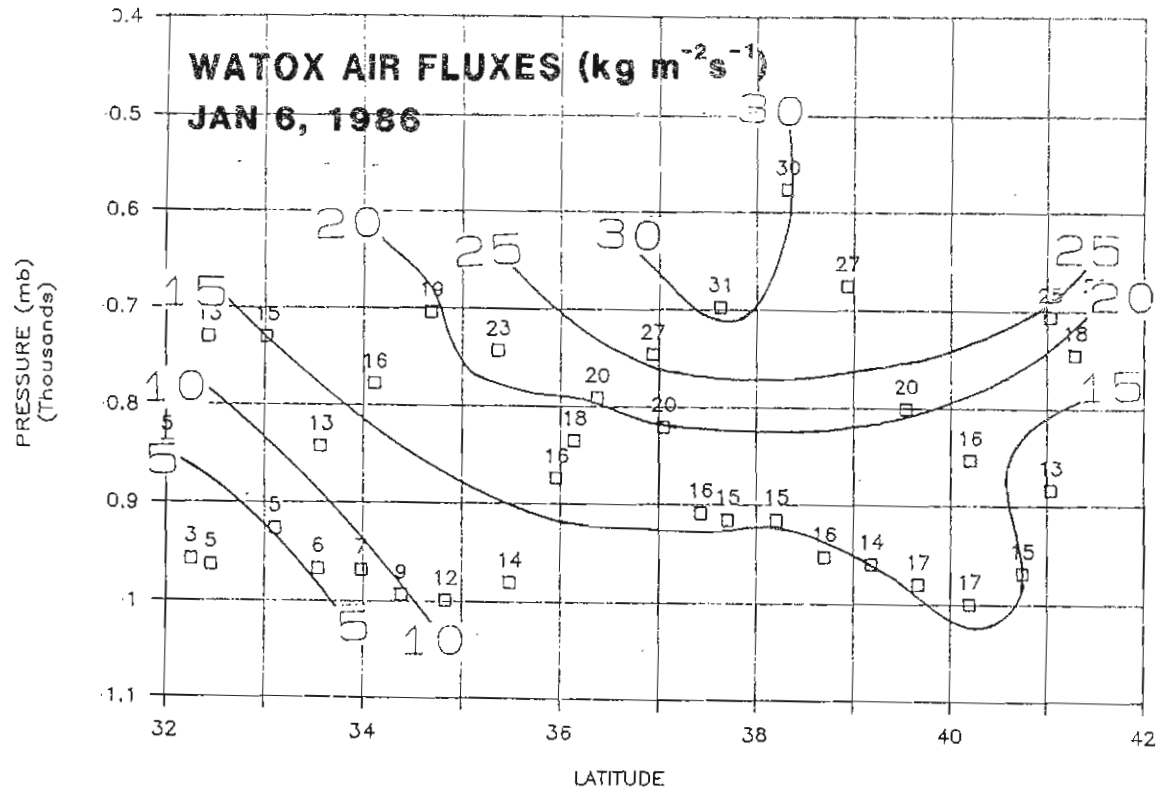

Figure 2.8--Air fluxes perpendicular to the aircraft flight track, January 6, 1986.

2.8 Aerosol Size Distributions

Aerosol size distributions in the free troposphere on January 6 (fig. 2.11) were similar to those outside the haze layers on January 4 (fig. 1.11). The letters on the size distribution spectra refer to locations on fig. 2.9. There is a small but distinct indication of a spatial variation in particle concentration along the flight track represented by higher concentrations in the central region at 36 to 37°N (curve B), and lower concentrations at either end of the track (curves A and C). This is roughly similar to the CN spatial distribution. Both number and volume spectra show considerable variation in aerosol numbers by diameter range. The main peak in the volume spectra occurs at 10-μm diameter.

Cloud layer spectra exhibit a weak bimodal distribution. The mode associated with smaller droplets is typical of a partially evaporating cloud in which entrainment of drier air will diminish the smallest cloud droplets first. The mode at 10 μm represents older, more stable cloud droplets, developed during passage to the top of the cloud.

Aerosol size distributions in the marine boundary layer exhibit a distinct spatial pattern, increasing in concentration from south to north (curves F to D). All spectra retain similar shape characteristics, and volume shows a peak at 8-9 μm, most likely sea salt, reflecting higher wind speeds and a more agitated sea state in the north.

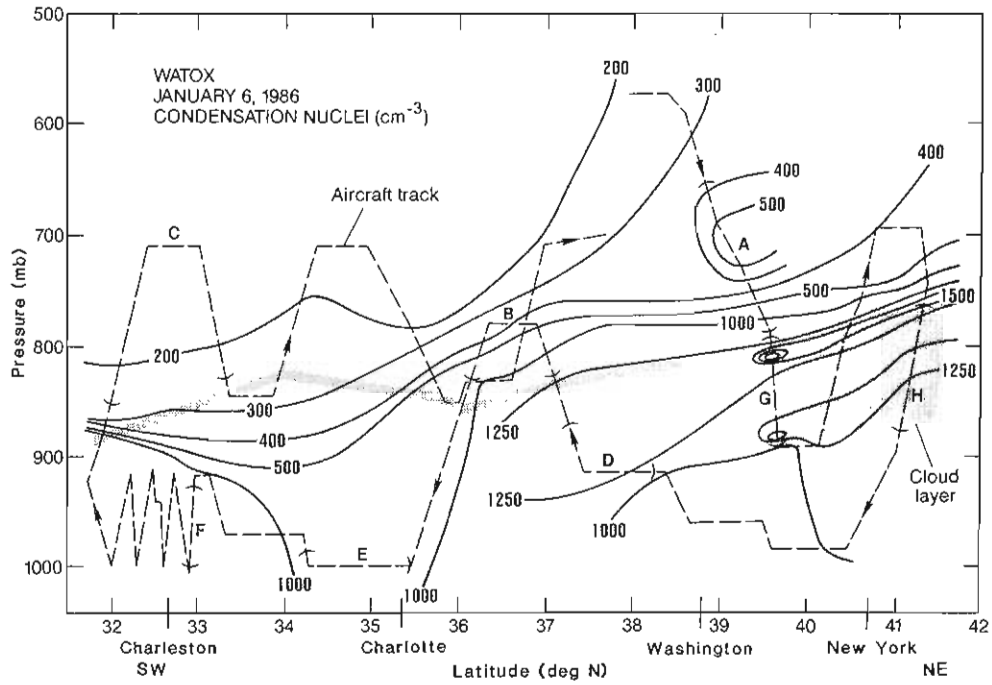

Figure 2.9--NE-SW cross section of CN concentration over the western Atlantic Ocean, January 6, 1986. Letters and brackets on the flight track indicate measurement locations for fig. 2.11.

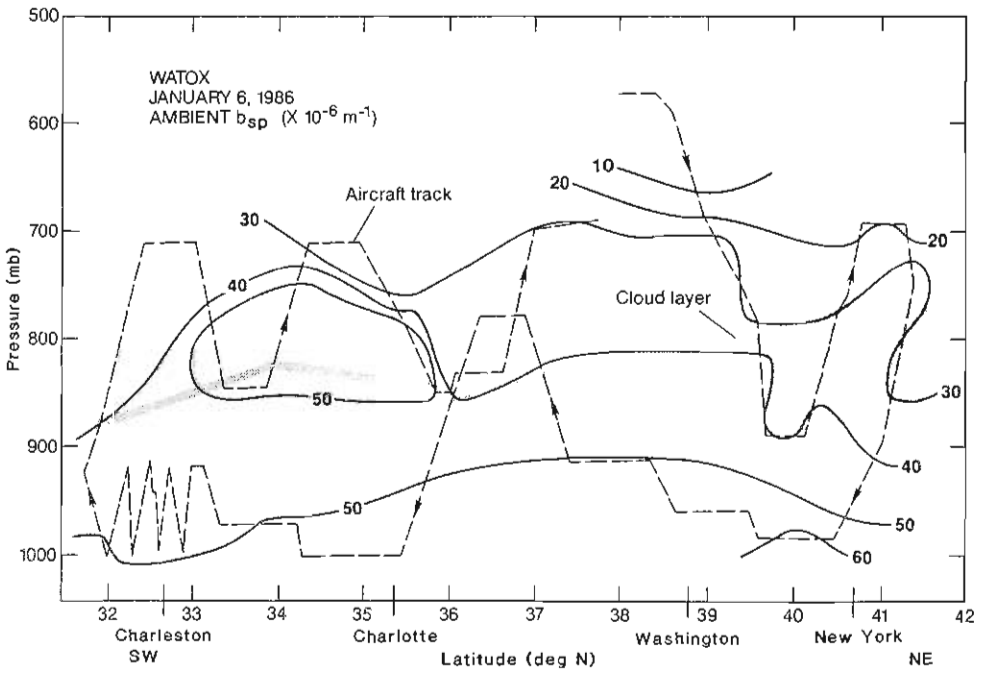

Figure 2.10--NE-SW cross section of b_{sp}, January 6, 1986.

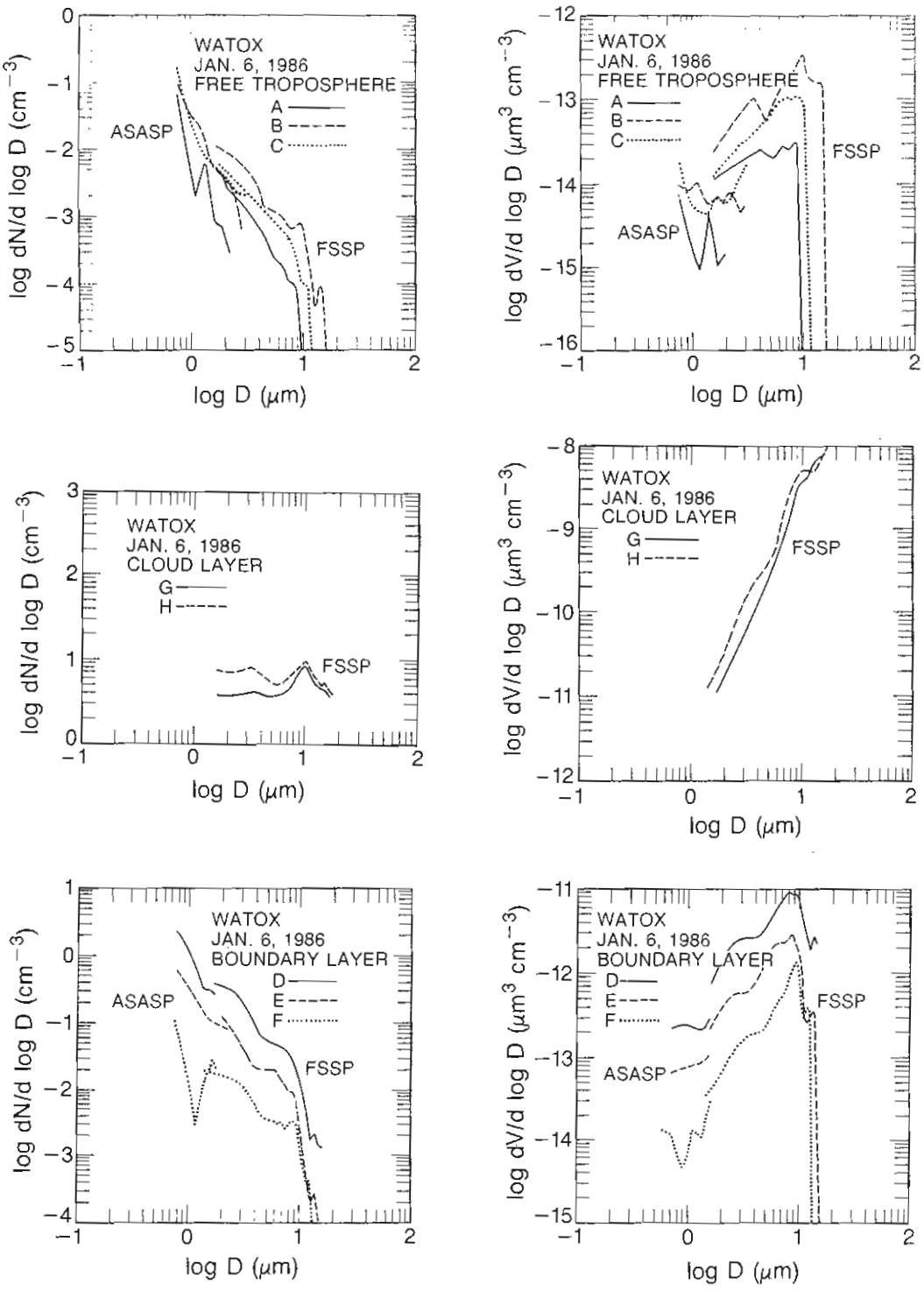

Figure 2.11--Number (left column) and volume (right column) aerosol size spectra at various aircraft locations, January 6, 1986. The letters associated with the spectra refer to locations shown in fig. 2.9.

3. WATOX FLIGHT 3, JANUARY 8, 1986

3.1 Flight Track

The WP-3D aircraft flew NE from McGuire Air Force Base to near Boston, where an in-flight instrument intercomparison was conducted with the NOAA King Air. The WP-3D then flew SE to 41°N, 67°W. After turning SW it flew a long leg to 33°N, 74°W. It then reversed direction, flying NE to 39°N, 70°W, and from there SW to 37.5°N, 71.5°W. It then flew NW to base. The aircraft crossed from the free troposphere to marine boundary layer only once, at the southern end of the flight track. Flight time was 9 hours, 46 minutes.

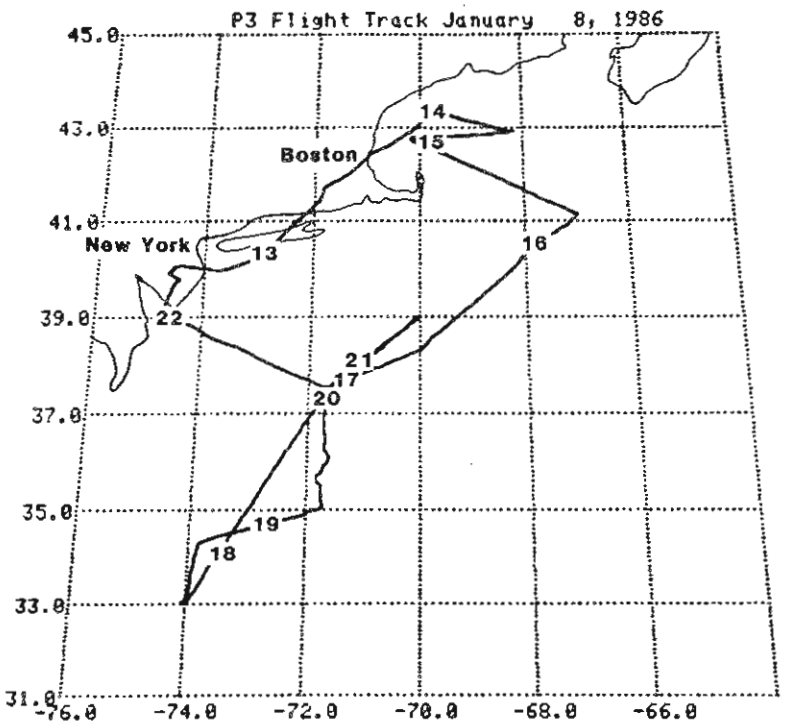

Figure 3.1--Horizontal projection of the flight track on a latitude-longitude grid, January 8, 1986. The numbers on the flight track are hours (GMT)

3.2 Synoptic Situation

At 1200 GMT January 8 the predominant surface feature was a strong high-pressure system (1045 mb) centered over Illinois (fig. 3.2). Winds were N to NW along the east coast and were stronger over New England than to the south. A frontal zone lay about 1000 km off the east coast.

The 850 mb chart indicates strong NW flow over New England and weak winds over the southeastern states. The pattern is similar at 700 mb except that the region of strong NW winds extends farther south than at 850 mb.

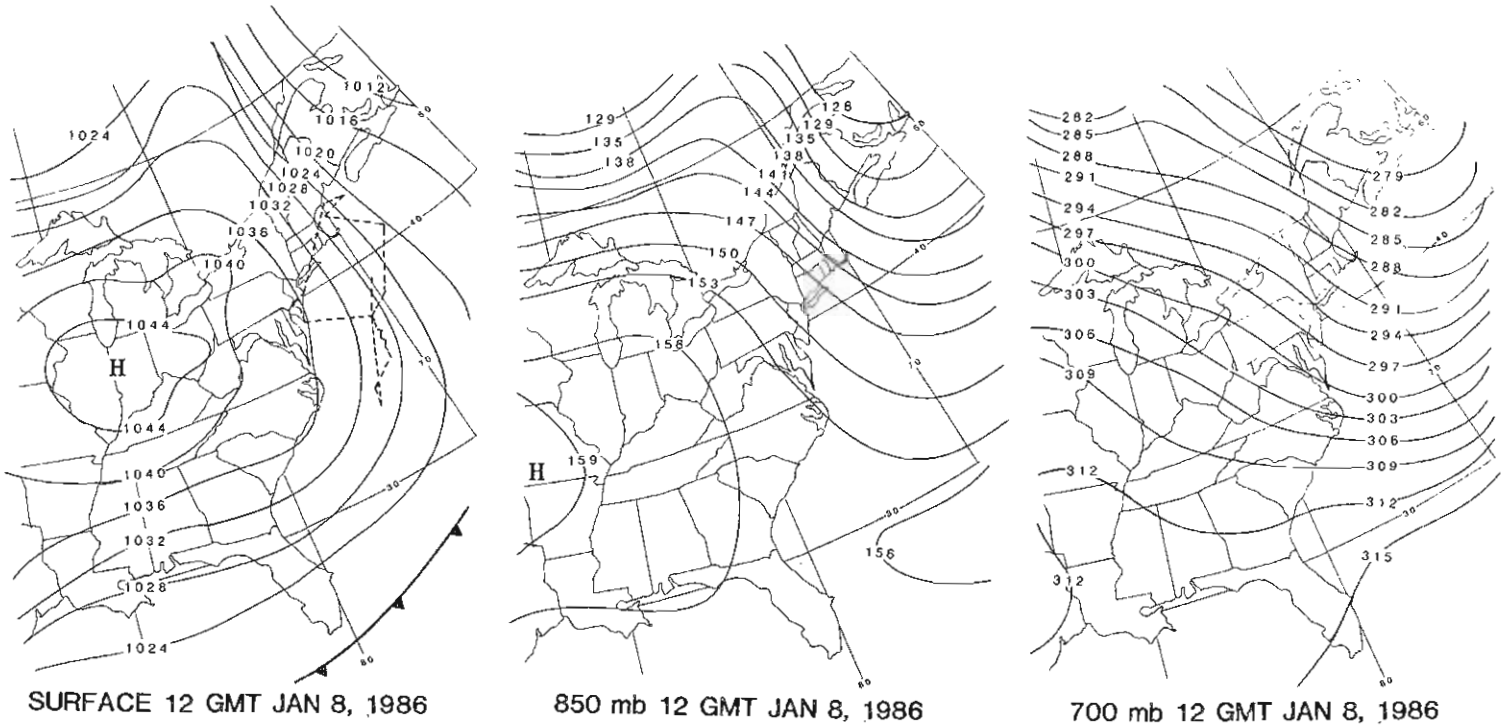

Figure 3.2--Surface (pressure, mb), and 850 and 700 mb (geopotential height, decameters) synoptic analyses for 1200 GMT, January 8, 1986. the flight track is shown by the dashed line on the surface map.

3.3 Air-Parcel Back-Trajectories

Isobaric (850 mb and 700 mb) air-parcel back-trajectories arriving at 1200 GMT January 8 are given in figs. 3.3 and 3.4. In general the flow for both pressure levels was from the N or NW. Air parcels arriving at points A, B, and C generally traveled over New England; those arriving at points D and E generally traveled over Ohio, Pennsylvania, or New York, coming from the N or NW. Air parcels arriving at point F came from the W over North Carolina and South Carolina at 850 mb, and from the W over South Carolina and Georgia at 700 mb. A comparison of results from three trajectory methods is presented in Appendix A.

3.4 Flight Log, January 8, 1986

1239 GMT	Takeoff.
1239-1256	Climb to 587 mb, 4364 m; E-NE flight track; no clouds.
1337	Offshore near Boston.
1338-1358	Descend to 860 mb, 1358 m, 43°N; intercomparison with King Air; scattered stratocumulus (sc) at 975 m.
1426	Flight track now WSW, 42.9°N.
1428-1433	Descend through cloud deck to 972 mb, 341 m, 42.9°N.
1502-1528	Climb through cloud deck to 699 mb, 3015 m, 42.5°N; flight track SE at 1506; remained in free troposphere between 699 and 795 mb until 1819.
1547	Flight track SE, 41°N.
1605	Cloud tops 1830 m, 40°N.
1700	Cloud tops 2440 m, 37.7°N.
1730	Cloud tops 2590 m, 36°N.
1818	Flight track N.
1819-1830	Descend into boundary layer to 925 mb, 757 m, 33°N; remain below 925 mb until 2128; CN peak in cloud >3000 cm^{-3}.
1830	Cloud tops 2225 m, 33.6°N.
1841	Cloud base just above 760 m; flight track NE.
1905	Intermittent light clouds.
1914	Flight track N, then NE, 35°N.
1922	Intermittent light showers; flight track variations to avoid showers

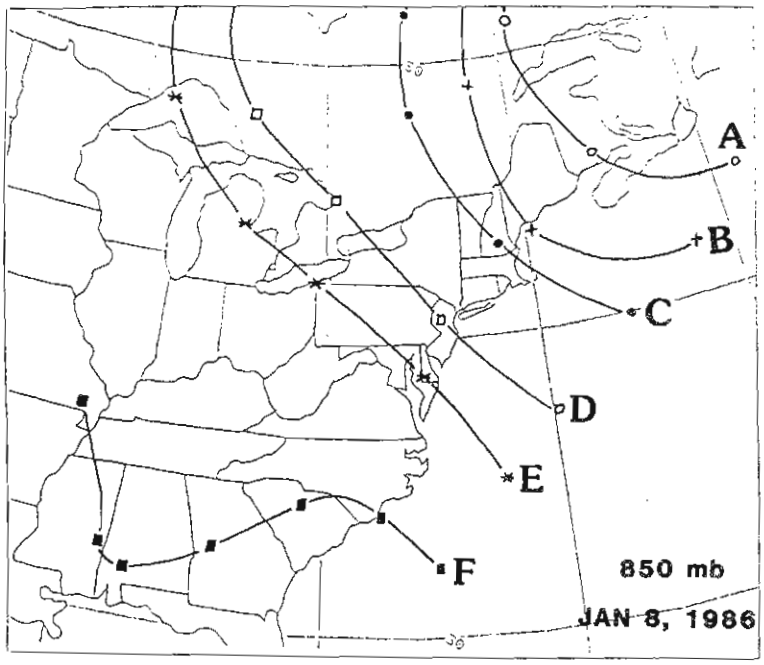

Figure 3.3--850-mb isobaric back-trajectories arriving at points A-F at 1200 GMT, January 8, 1986. Successive symbols indicate 12-h intervals.

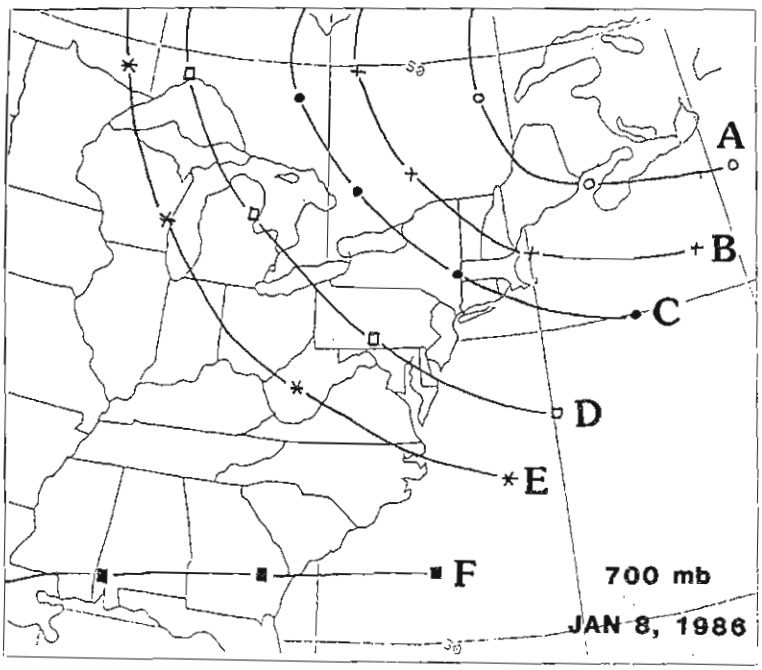

Figure 3.4--700-mb isobaric back-trajectories arriving at points A-F at 1200 GMT, January 8, 1986. Successive symbols indicate 12-h intervals.

1940 Cloud base 686 m, 36.3°N.

2039 Flight track SW, 39°N.

2041 Cloud base 595 m, 38.9°N.

2113 Flight track NW, 37.6°N.

2128-2139 Climb to 754 mb, 2429 m, 38°N; cloud base 854 m; cloud tops 1677 m.

2203-2225 Descend to base.

3.5 Atmospheric Cross Sections

Latitude-altitude cross sections of potential temperature and water vapor mixing ratio approximately parallel to the coast were constructed from dropwindsonde and aircraft data along the main part of the flight track off the coast as shown in figs. 3.5 and 3.6. The winds were N to NW and generally weaker to the south in the region of the high-pressure system. Winds were weaker than for the first two WP-3D flight days. The cloud layer was relatively deep, having a thickness of nearly 1 km. The water vapor mixing ratio gradient capping the cloud layer was weaker than in the first two flights. Above the cloud layer the mixing ratio was generally less than 1 g kg^{-1}. Within the boundary layer, the mixing ratio was between 1 and 3 g kg^{-1} over much of the cross section, and 3 to 4 g kg^{-1} for the southern part of the flight, near the Gulf Stream.

As shown in fig. 3.7 air fluxes (kg m^{-2} s^{-1} at STP) generally increase regularly with height and are lower in the marine boundary layer south of 35°N than on any other portion of the flight track. A tabular list of calculated fluxes is included in Appendix B.

It was possible to construct additional atmospheric cross sections from coastal rawinsonde sites and aircraft data for the part of the flight track along the coast, upwind of the cross section shown in fig. 3.5. The information from one set of these additional cross sections, shown in figs. 3.8 and 3.9, should provide a tool for determining the gradients of meteorological and chemical quantities off the east coast using measured rather than modeled quantities. One important difference between the meteorological conditions along the coast and farther out is that no clouds were present along the coast. Another difference is that the surface-based inversion is much more shallow along the coast than 200-300 km offshore. For the flight along the coast, water vapor mixing ratios were less than 1 g kg^{-1}, compared with a range of 2 to 4 g kg^{-1} to the southeast over the open sea.

The longitude-altitude cross sections of potential temperature and mixing ratio for the flight track normal to the coast (41-43°N) are given in figs. 3.10 and 3.11. This information may be useful in judging the reliability of isentropic and isobaric back-trajectories generated for this region of the flight. Again, the winds were N to NW. Mixing ratios were at most 1.4 g kg^{-1} along the flight track and the cloud layer at 950 mb was quite shallow. The layer between about 900 mb and 750 mb was less stable than at either higher or lower altitudes.

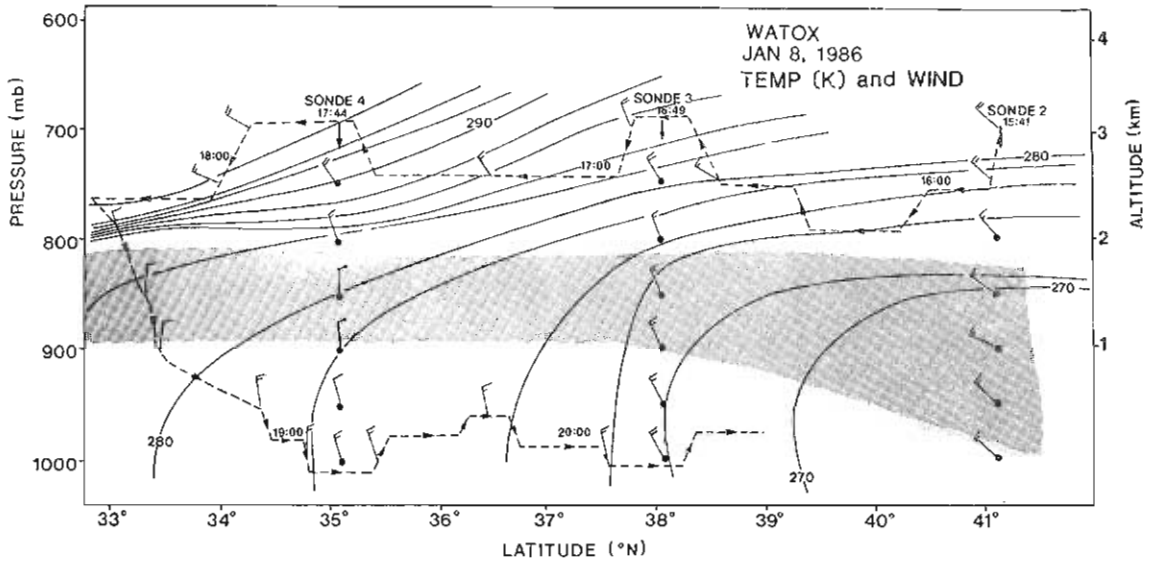

Figure 3.5--Latitude-altitude cross section of potential temperature and wind (full barb = 10 m s^{-1}) along the WP-3D flight track parallel to the coast, January 8, 1986. The stippled area represents the cloud layer. The flight track is shown by the dashed line.

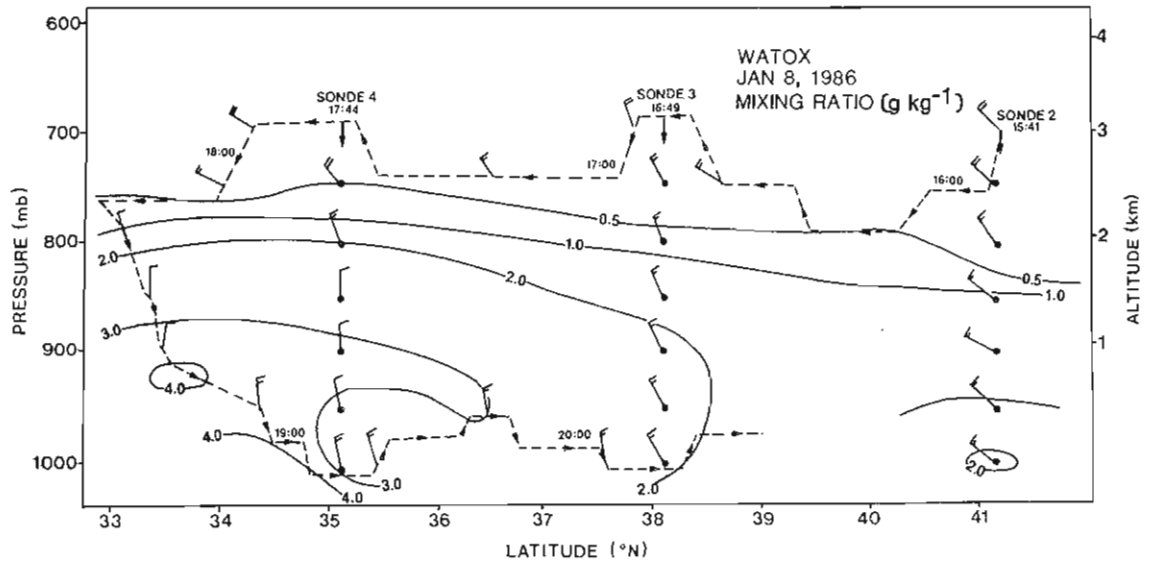

Figure 3.6--Latitude-altitude cross section of water vapor mixing ratio and wind (full barb = 10 m s^{-1}) January 8, 1986. The flight track is shown by the dashed line.

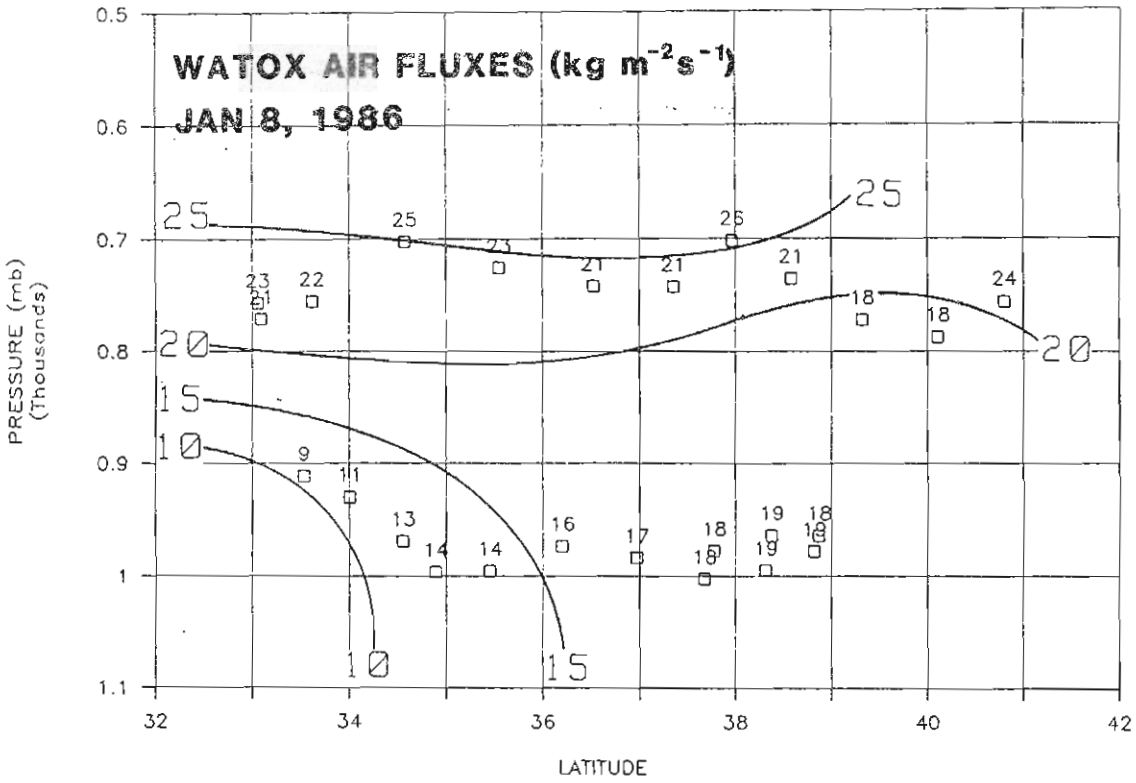

Figure 3.7--Air fluxes perpendicular to the flight track, January 8, 1986.

3.6 Cross Sections of CN Concentration and b_{sp}

On this day the aircraft crossed from free troposphere to boundary layer only once, at the southern end of the flight track. Thus, although dropwindsondes helped establish the location of the cloud, cross section information on CN and b_{sp} is more limited. As depicted in fig. 3.12, CN concentrations decreased fairly regularly with increased altitude from about 1000 cm^{-3} in the marine boundary layer to 100 cm^{-3} in the free troposphere. At the southern end of the flight track (33°N) a sharp CN gradient existed between high concentrations of 3000 cm^{-3} at 800 mb in the cloud layer and 200 cm^{-3} at 770 mb in much cleaner air.

As on the previous days, b_{sp} (fig. 3.13) exhibited higher concentrations in the marine boundary layer, decreasing with altitude. The CN peak at 800 mb and 33°N was matched by a b_{sp} peak of 50 × 10^{-6} m^{-1}, probably indicative of transport of anthropogenic emissions eastward from the continent.

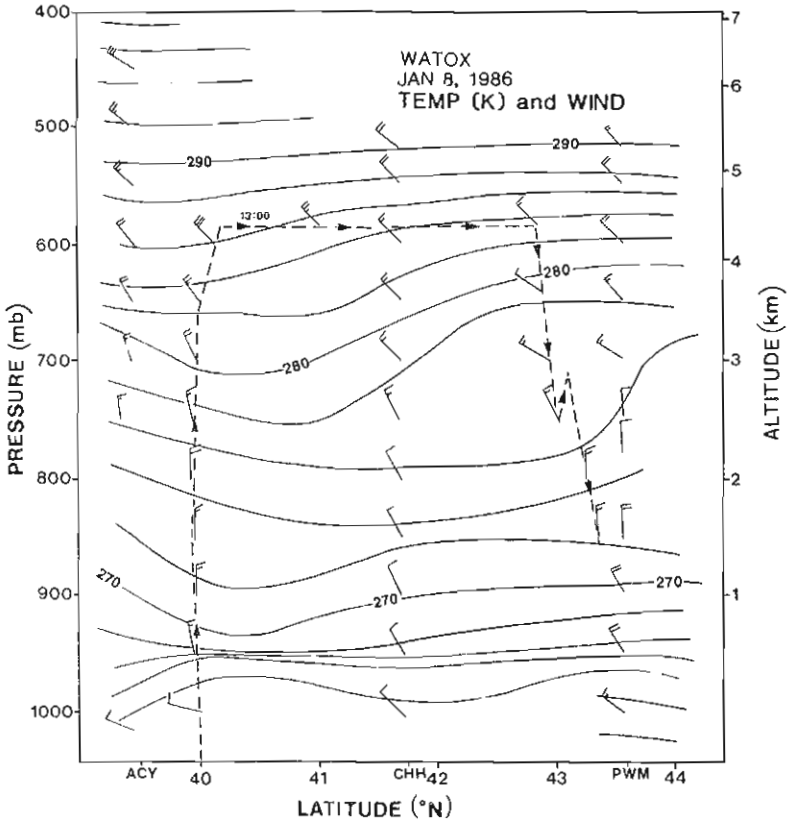

Figure 3.8--Latitude-altitude cross section of potential temperature and wind (full barb = 10 m s^{-1}) for the NE-SW portion of the WP-3D flight track along the coast (Longitude 70-74°W), January 8, 1986. ACY is Atlantic City, New Jersey, CHH, Chatham, Massachusetts, and PWM, Portland, Maine.

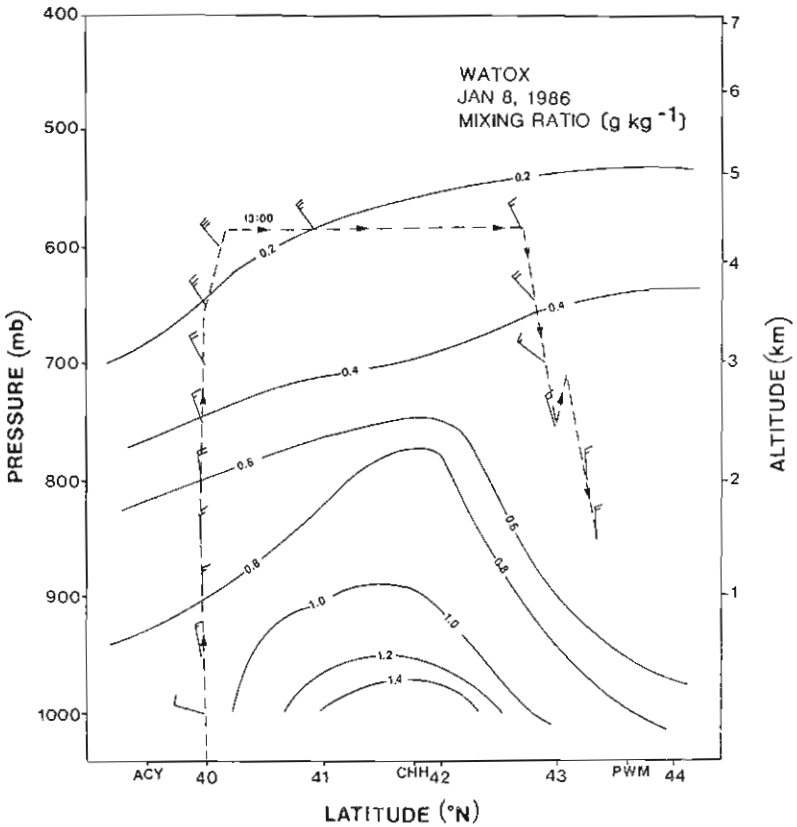

Figure 3.9--Latitude-altitude cross section of water vapor mixing ratio and wind (full barb = 10 m s^{-1}) along the coast, January 8, 1986.

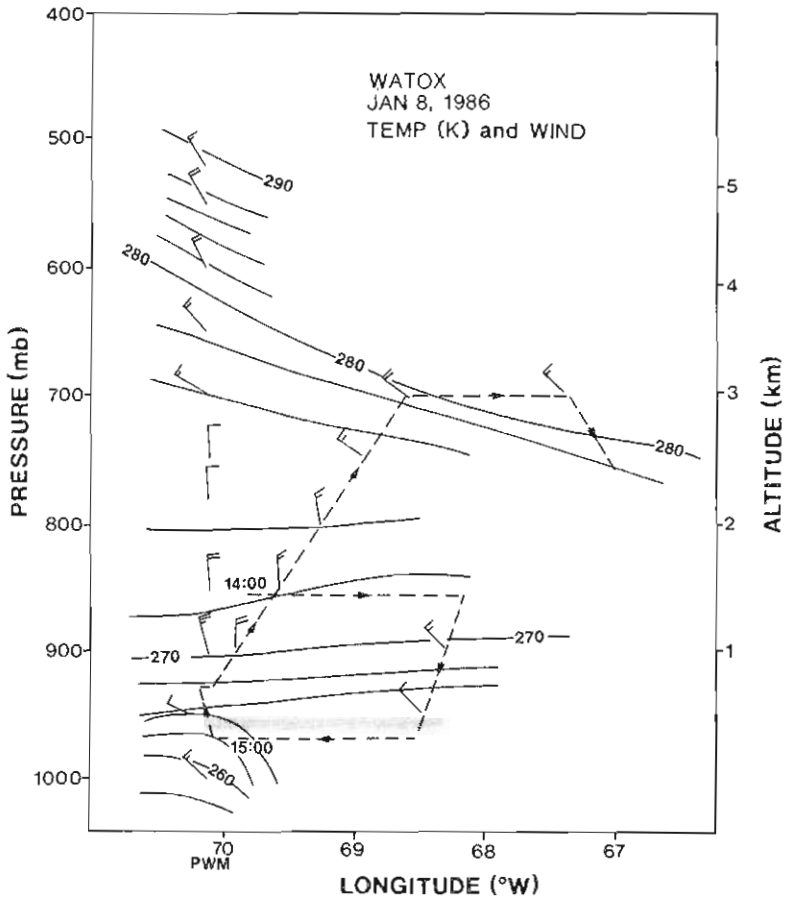

Figure 3.10--Longitude-altitude cross section of potential temperature and wind (full barb = 10 m s^{-1}) along the flight track normal to the coast, latitude 41-43°N, January 8, 1986. PWM is Portland, Maine.

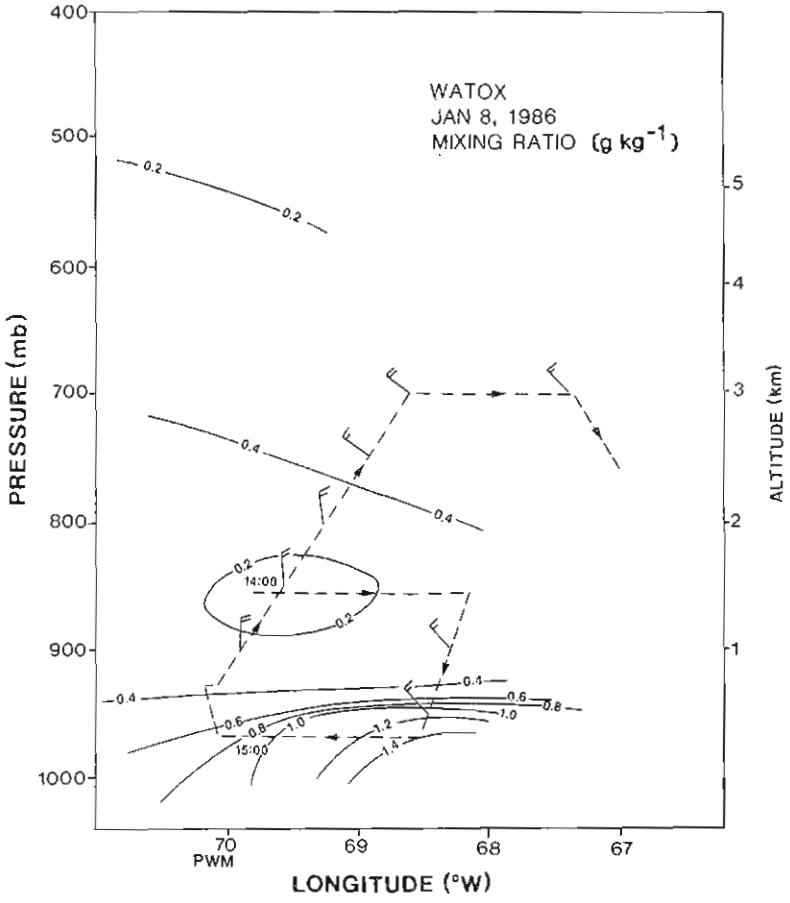

Figure 3.11--Longitude-altitude cross section of water vapor mixing ratio and wind (full barb = 10 m s^{-1}) normal to the coast, January 8, 1986.

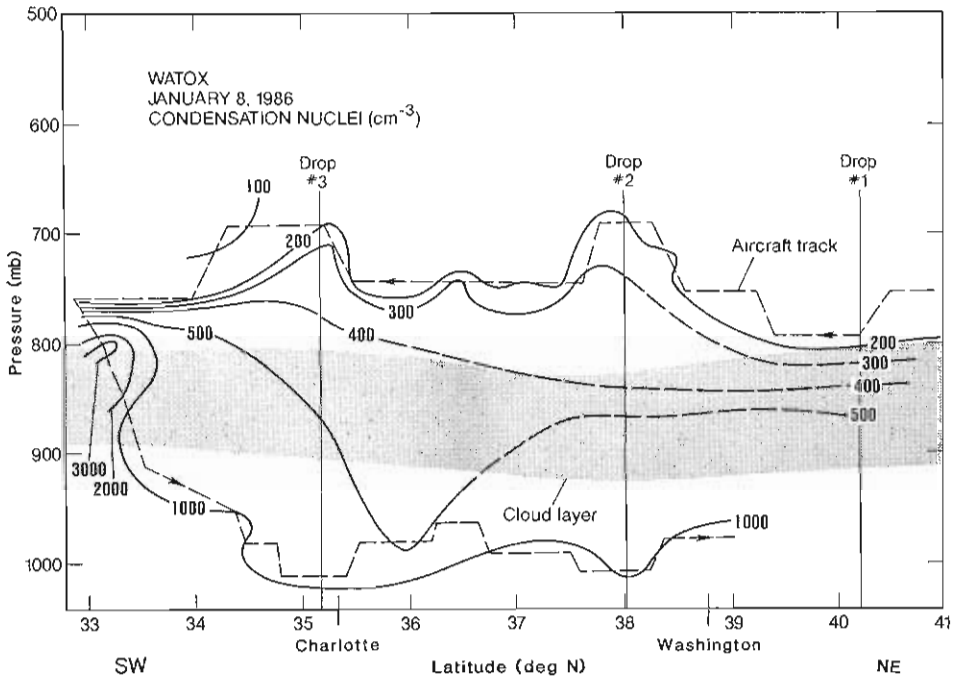

Figure 3.12--NE-SW cross section of CN concentration over the western Atlantic Ocean, January 8, 1986.

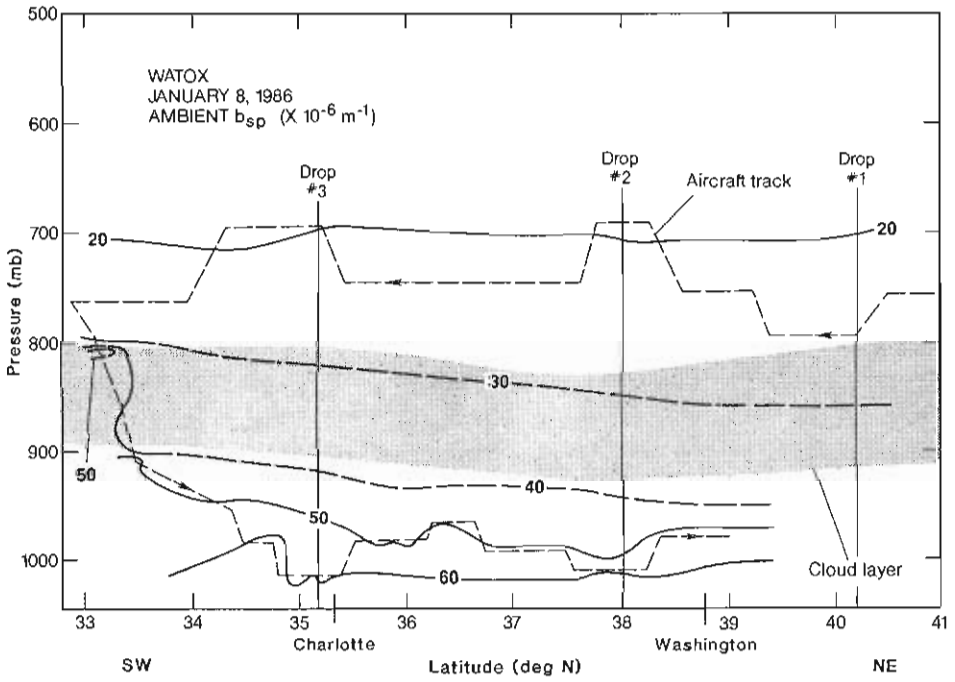

Figure 3.13--NE-SW cross section of b_{sp}, January 8, 1986.

4. WATOX FLIGHT 4, JANUARY 9, 1986

4.1 Flight Track

The aircraft flew E and then SE from McGuire Air Force Base to 37.5°N, 71.5°W, then flew S and SW into a region of high pressure to a southern point of 31.5°N, 74°W. The aircraft then reversed course to 37.5°N, 71.5°W northeast to 40°N, 68.5°W and back to 37.5°N, 71.5°W before returning to base on a NW course. During the flight, the aircraft crossed between the free troposphere and marine boundary layer seven times. It reached a maximum altitude of 7600 m at 39°N while searching for haze layers in the free troposphere. Total flight time was 7 hours, 25 minutes.

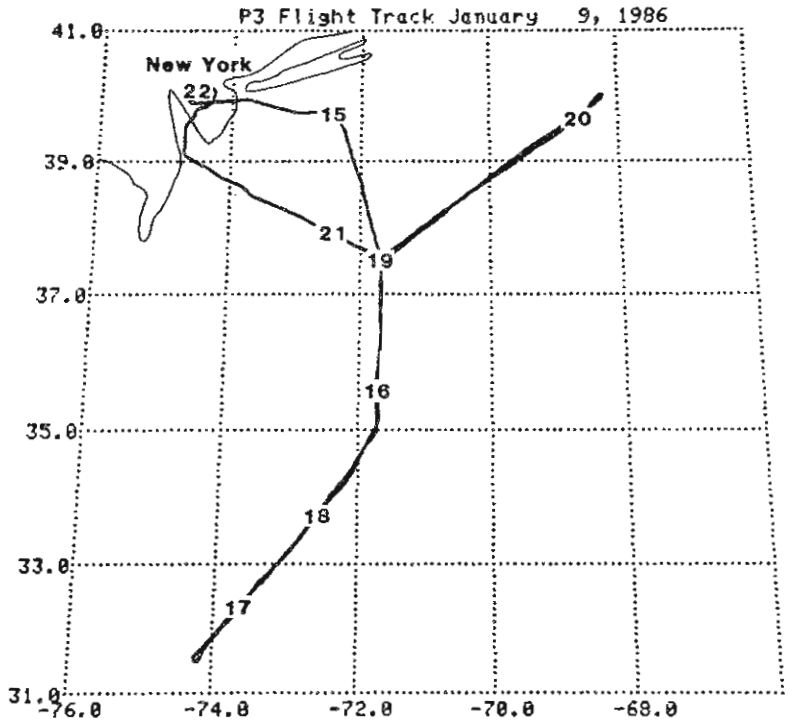

Figure 4.1--Horizontal projection of the flight track on a latitude-longitude, grid, January 9, 1986. The numbers on the flight track are hours (GMT).

4.2 Synoptic Situation

At 1200 GMT January 9 a large area of high pressure was centered over the Carolinas, extending to Texas (fig. 4.2). The pressure gradient was weak south of New Jersey. There were light W winds at the northern part of the WP-3D's flight track and E winds at the southern part. Both the 850-mb and 700-mb charts indicate relatively light W to NW flow off the coast from New Jersey to the south. Winds were weaker to the south.

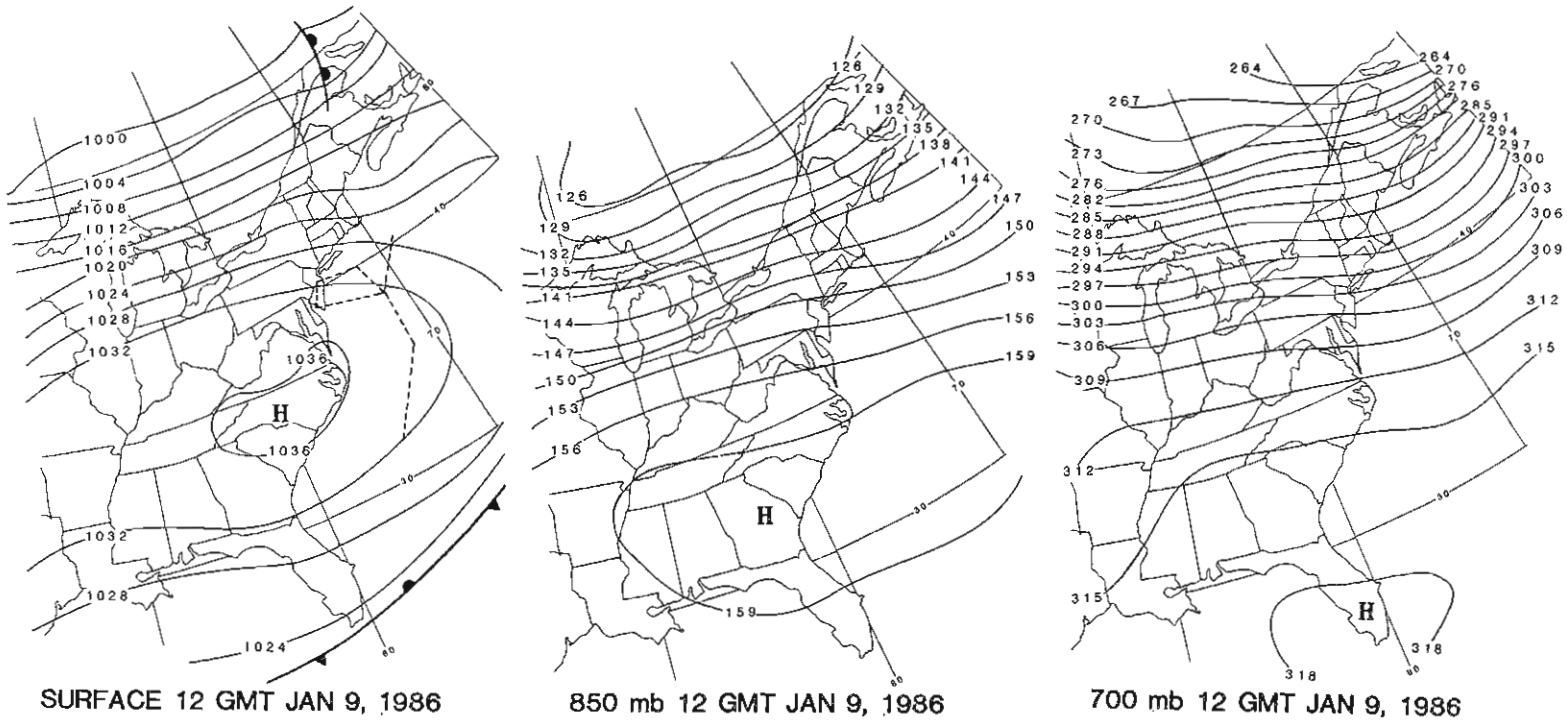

Figure 4.2--Surface (pressure, mb), and 850- and 700-mb (geopotential height, decameters) synoptic analyses for 1200 GMT, January 9, 1986. The flight track is shown by the dashed line on the surface map.

4.3 Air-Parcel Back-Trajectories

Isobaric (850 and 700 mb) air-parcel back-trajectories arriving at 1200 GMT January 9 at points A through F are given in figs. 4.3 and 4.4. Clearly, the transport was generally from the NW. The 850-mb trajectories arriving at points A-F do not extend west of a line between Sault Sainte Marie, Ontario and central Pennsylvania. Similarly those at 700 mb do not extend west of a line between Minnesota and South Carolina. In general, for both 850 mb and 700 mb trajectories arriving at points E and F at 1200 GMT, the transport winds are more N as compared with more W for points A-D.

A comparison of results from three trajectory methods is presented in Appendix A.

4.4 Flight Log, January 9, 1986

1436 GMT Takeoff.

1436-1459 Climb to 538 mb, 5019 m, 40°N; flight track E.

1501 Flight track S, 39.7°N.

1509-1536 Descend to 824 mb, 1701 m, 38.5°N.

1546-1605 Descend through clouds to boundary layer, 1012 mb, 10 m, 36°N; cloud tops 1675 m; cloud base 1065 m.

1609 Flight track SW, 36°N.

1615-1637 Climb to 737 mb, 2598 m, 34.5°N; cloud base 1220 m; cloud tops 2040 m.

1707-1734 Descend to 1011 mb, 22 m, 32°N; cloud tops 1950 m; cloud base 1295 m; CN <200 cm^{-3}; flight track NE, 1716.

1741-1805 Climb to 727 mb, 2715 m, 32.7°N; cloud base 1295 m; cloud tops 1830-1921 m.

1821 Flight track N, 35°N.

1830 Cloud tops 1980 m.

1840-1903 Descend to 1006 mb, 57 m, 36°N; cloud tops 1525 m; CN >1250 cm^{-3} in lower boundary layer; flight track NE, 1901.

1910-2007 Climb to 377 mb, 7600 m, 38-39°N; cloud base 1040 m; cloud top, 1465 m; sharp CN drop from 1500 cm^{-3} to 400 cm^{-3} at cloud top.

1953 Flight track SW.

2008-2052 Descend to 1006 mb, 60 m, 38°-39°N; cloud tops 1340 m; cloud bases 914 m.

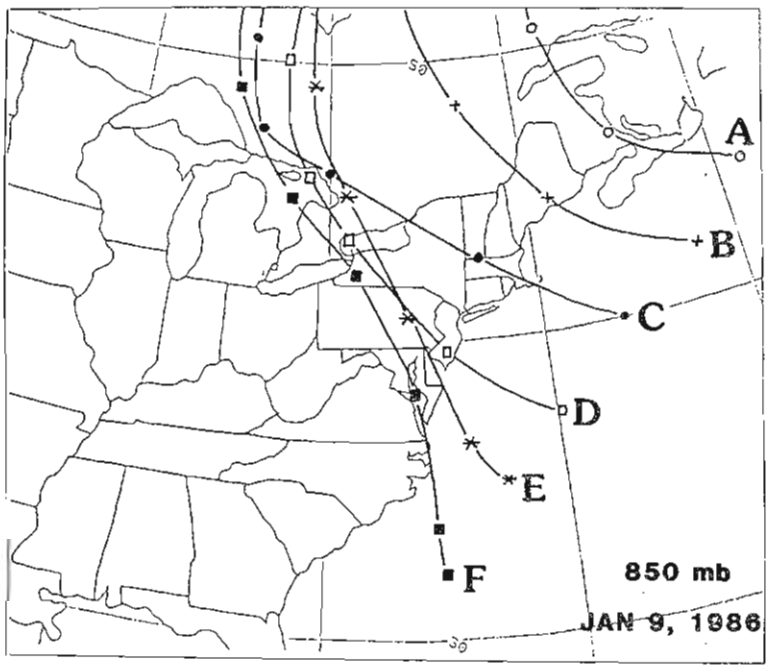

Figure 4.3--850-mb isobaric back-trajectories arriving at points A-F at 1200 GMT, January 9, 1986. Successive symbols indicate 12-h intervals.

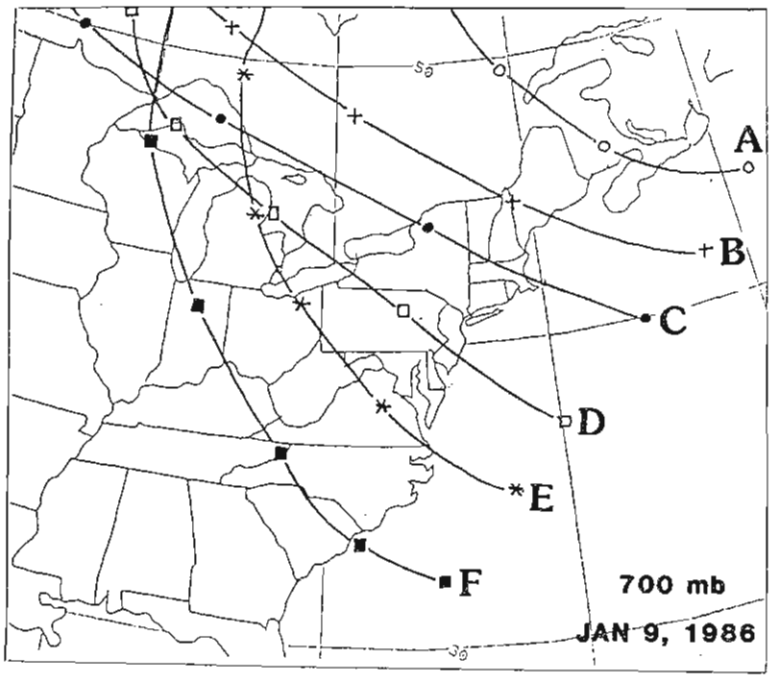

Figure 4.4--700-mb isobaric back-trajectories arriving at points A-F at 1200 GMT, January 9, 1986. Successive symbols indicate 12-h intervals.

2048 Flight track NW, 40°N.

2102-2107 Climb to 723 mb, 2754 m, 38°N.

2142-2200 Descend to base.

4.5 Vertical Profiles Across the Marine Boundary Layer Inversion

The vertical profiles of CN concentration, ozone, b_{sp}, and meteorological variables obtained at the northern end of the flight track are shown in fig. 4.5. As observed on previous occasions (January 4, fig. 1.5; January 6, fig. 2.5), CN concentration and relative humidity decrease strongly above the marine boundary layer inversion; CN concentration and b_{sp} decrease rapidly with height in the free troposphere. In contrast to January 4, the moist layer between 500 and 650 mb on this day contained only slightly higher CN concentrations.

An enhanced ozone layer between the top of the marine boundary layer and the top of the dry layer at about 675 mb was consistently seen in all profiles on this day, although it was most pronounced in the profile shown.

The dry, warm layer above the boundary layer correlates well with this layer of enhanced ozone. This layer of air appears to be subsiding along its path from a source relatively rich in ozone, but of low CN concentration. Such a region might be found at somewhat higher altitudes in the troposphere, at more northerly latitudes where air richer in ozone and lower in aerosols was mixed down from the stratosphere. The boundary layer has ozone mixing ratios slightly greater than those measured above 675 mb.

The role of chemical production of ozone in air into which precursors have been injected and transported cannot be clearly determined on the basis of data given here. It is expected that ozone production would be slow during this time of year, but over longer distances enough production may occur to contribute to the ozone budget and produce a thin layer as seen in fig. 4.5. This layering, apparent in most of the profiles during WATOX, might indicate a more dramatic creation of ozone layers than that envisioned by a slow photochemical production process.

4.6 Atmospheric Cross Sections

Latitude-altitude cross sections of potential temperature, wind speed, and water vapor mixing ratio approximately parallel to the coast were constructed from dropwindsonde and aircraft data along the flight track, as shown in figs. 4.6 and 4.7. Of the four WP-3D flights, the aircraft flew the highest on this flight, reaching above 400 mb. Compared with the WP-3D flight on January 8 (fig. 3.5), the winds were weaker and the cloud layer thinner on this day. The winds were E at the southernmost end of the flight and W during the rest of the flight. Water vapor mixing ratios were generally less than 2 g kg^{-1} above the cloud layer, and had a relative maximum at 650 mb, 39°N latitude. Mixing ratios in the boundary layer were relatively high, e.g., greater than 4 g kg^{-1} over much of the cross section.

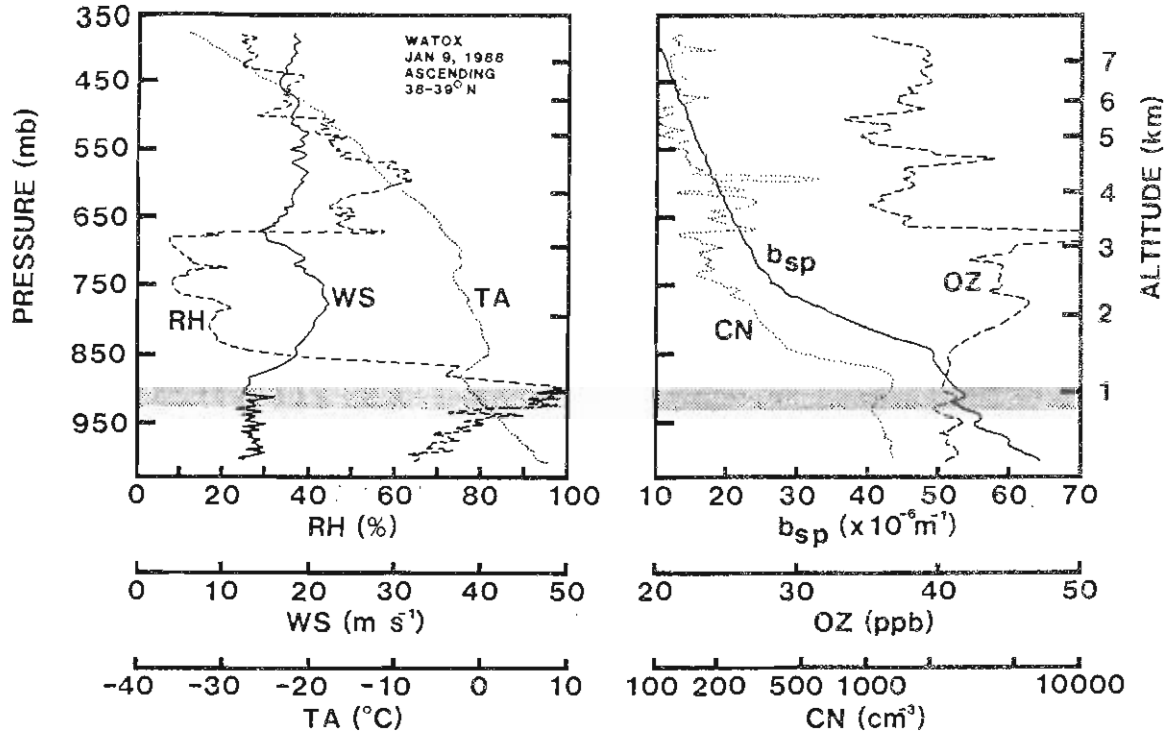

Figure 4.5--An example of vertical profiles of relative humidity, ambient temperature, wind speed, CN concentration, b_{sp}, and ozone, January 9, 1986. The shaded region represents the cloud layer, capped by the marine boundary layer inversion.

Air fluxes on January 9, shown in fig. 4.8, were generally lower than on the other three days. The spatial pattern of higher values farther north continued. Fluxes in the marine boundary layer at 32°N were easterly. The decrease in fluxes compared with the other days and the more even spread of values with latitude reflect the position of the high-pressure system. Tabular calculations of fluxes in 15-min segments are included in Appendix B.

Longitude-altitude cross sections of potential temperature and mixing ratio approximately normal to the coast were constructed from the Atlantic City rawinsonde, aircraft dropwindsondes and from the data recorded by the aircraft along the first and last segments of the flight track. As with the third flight, these normal cross sections (see figs. 4.9 and 4.10) should aid in judging the reliability of trajectories calculated for this period of the flight. The atmospheric stability near the surface was greater closer to the coast than along the main part of the flight track. Winds were also W while the aircraft flew approximately normal to the coast. Water vapor mixing ratios at the surface were smaller closer to the coast. A relative maximum was observed near 675 mb, 73°W longitude shown in fig. 4.10. No clouds were present along the flight segments normal to the coast.

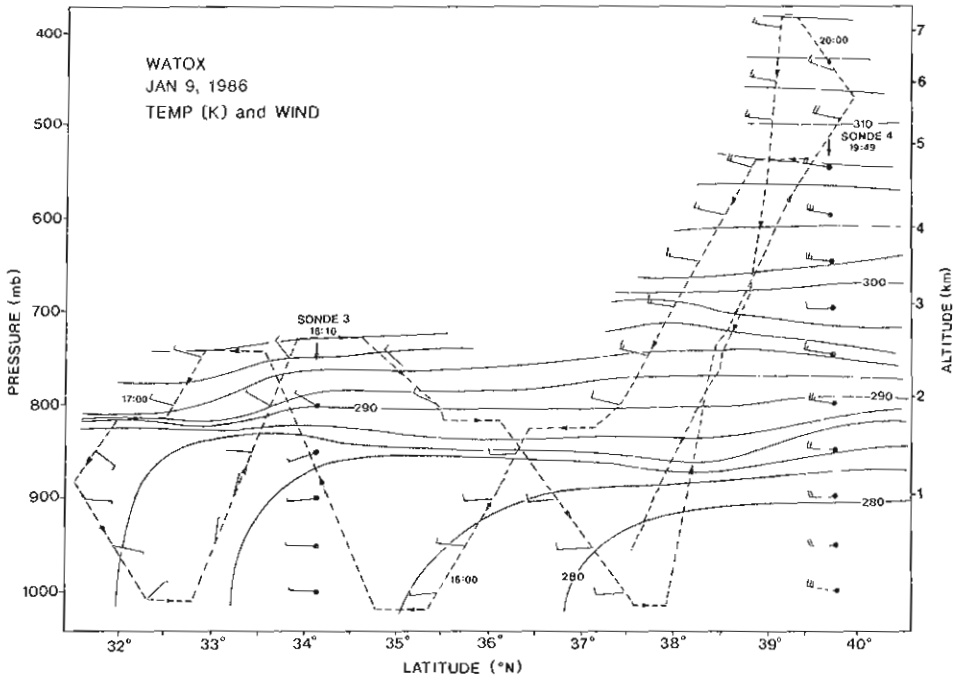

Figure 4.6--Latitude-altitude cross section of potential temperature (K) and wind (full barb = 10 m s^{-1}) along the WP-3D flight track parallel to the coast, January 9, 1986. The stippled area represents the cloud layer. The flight track is shown by the dashed line.

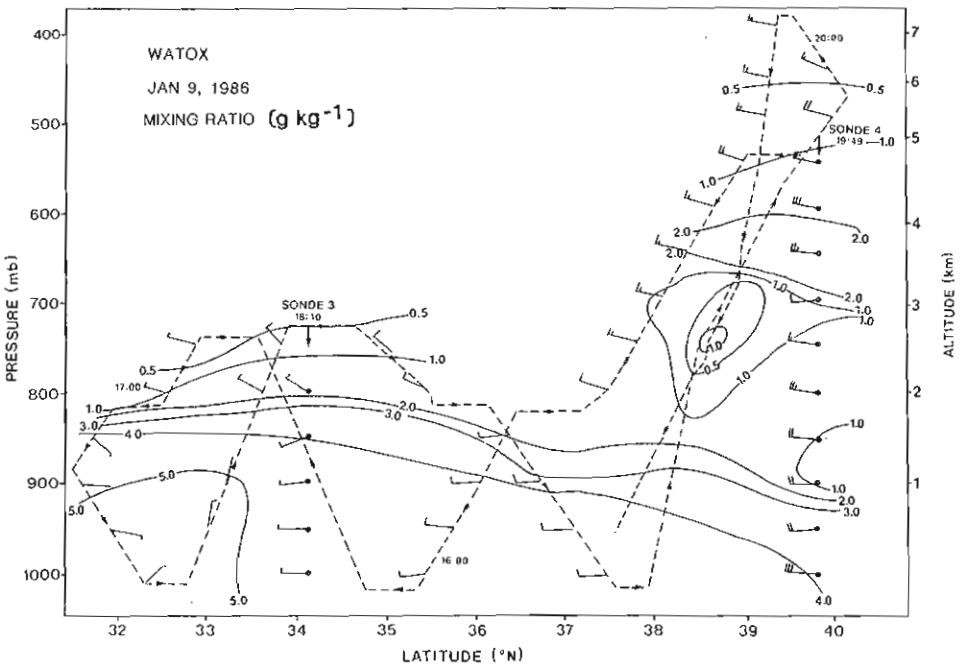

Figure 4.7--Latitude-altitude cross section of water vapor mixing ratio and wind (full barb = m s^{-1}) January 9, 1986. The flight track is shown by the dashed line.

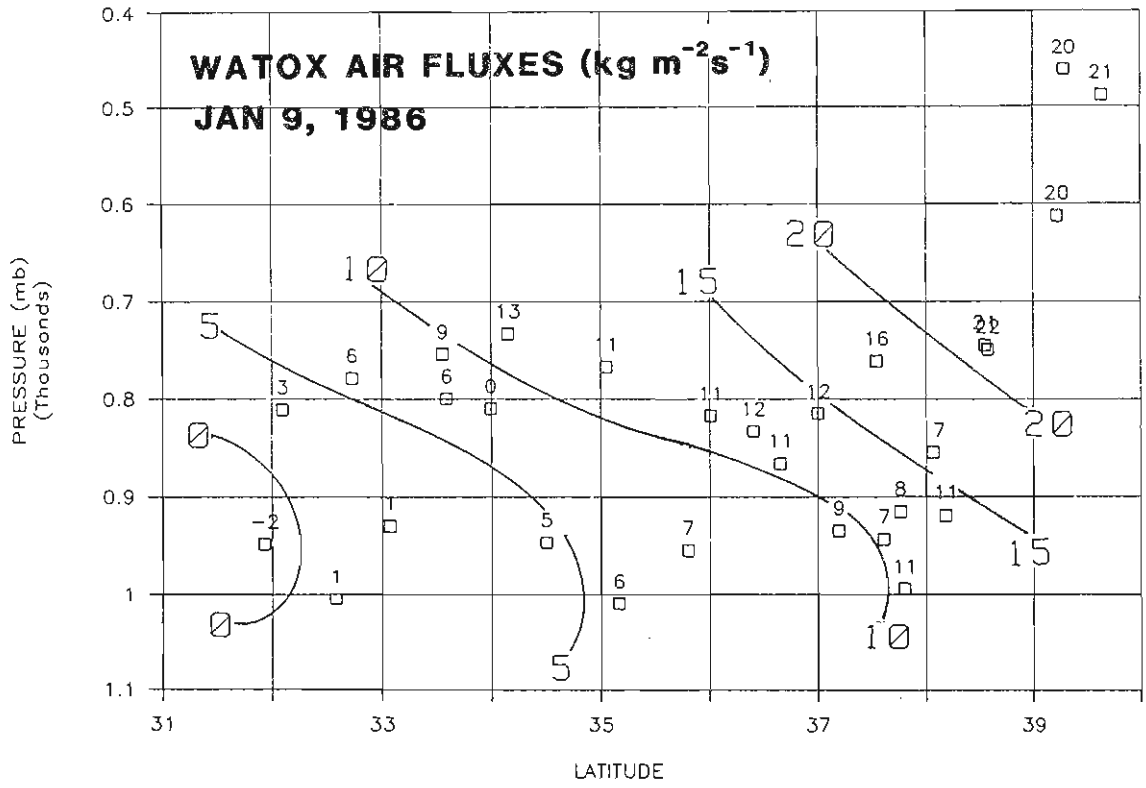

Figure 4.8--Air fluxes (kg m^{-2} s^{-1} at STP) perpendicular to the aircraft flight track, January 9, 1986.

4.7 Cross Sections of CN Concentration and b_{sp}

On this day the lowest CN concentrations were observed in the cloud layer and marine boundary layer at the southern end of the flight track (32°N) within the high-pressure system, as shown in fig. 4.11. Here, subsiding air from the middle troposphere plus E winds from ocean sources contributed to the clean air. CN concentrations increased steadily at more northerly locations, attaining levels of more than 1250 cm^{-3} in the marine boundary layer at 37-38°N, probably associated with increased strength of the NW airflow. CN concentrations in the free troposphere exhibited little variation except occasional patches of higher values between 37 and 39°N at high elevations. At 38.2°N the top of the cloud layer was well defined, and there was a sharp gradient in CN concentration, changing from 1500 cm^{-3} to 400 cm^{-3}.

Aerosol b_{sp} again exhibited generally decreasing values with altitude (fig 4.12). There is a slight trend toward higher values to the NE, particularly with altitude in the free troposphere at 38°N, but neither the impact of the high-pressure system nor the vertical variations evident in the CN cross sections are apparent in the b_{sp} data.

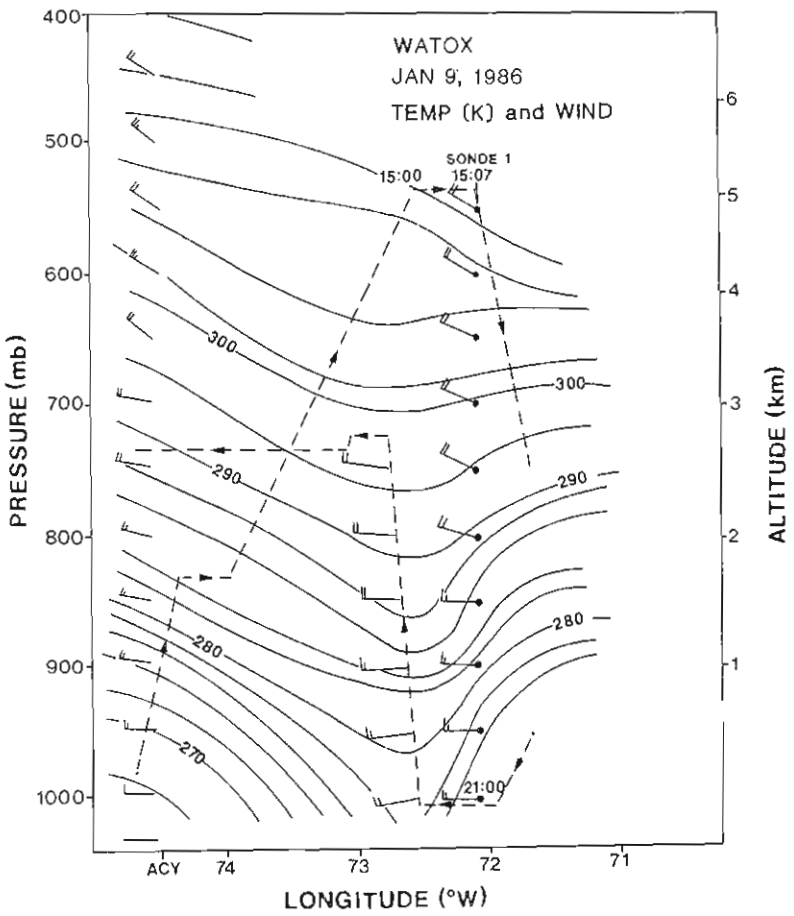

Figure 4.9--Longitude-altitude cross section of potential temperature (K) and wind (full barb = 10 m s^{-1}) along the WP-3D flight track normal to the coast, latitude 37.5-39°N, January 9, 1986. ACY is Atlantic City, New Jersey.

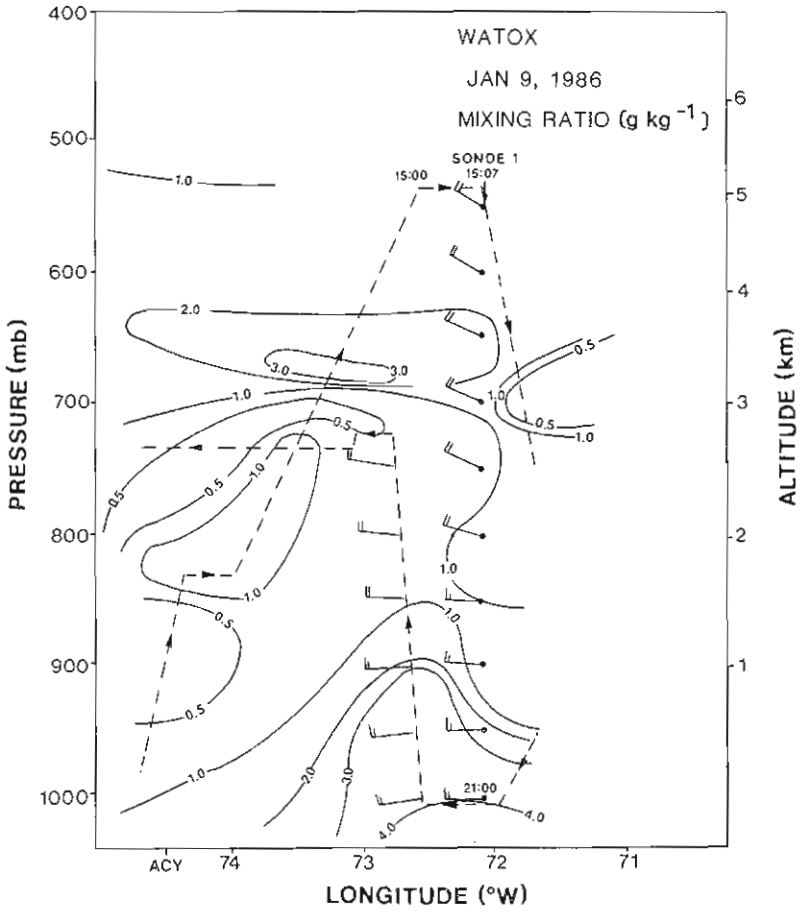

Figure 4.10--Longitude-altitude cross section of water vapor mixing ratio and wind (full barb = 10 m s^{-1}) normal to the coast, January 9, 1986.

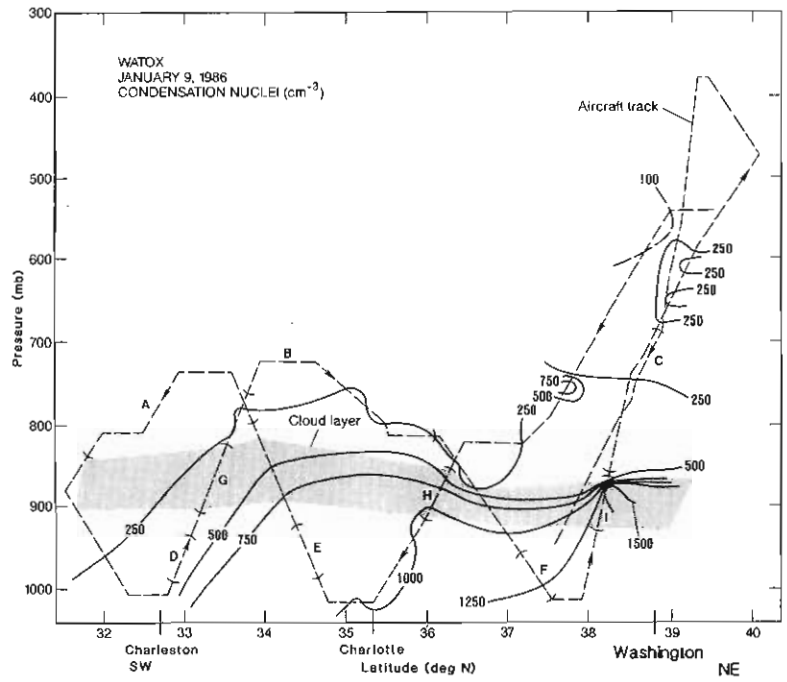

Figure 4.11-NE-SW cross section of CN concentration over the western Atlantic Ocean, January 9, 1986. Letters and brackets on the flight track indicate measurement locations for fig. 4.13.

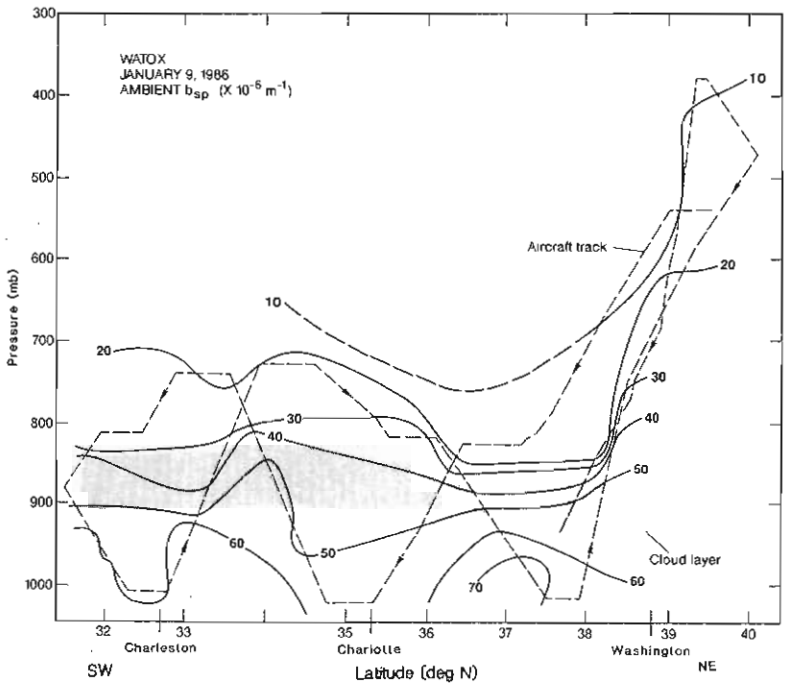

Figure 4.12--NE-SW cross section of b_{sp}, January 9, 1986.

4.8 Aerosol Size Distributions

Aerosol size distributions measured on January 9, shown in fig. 4.13, were broadly similar to those on previous days, but exhibited smaller variations with location along the flight track. Letters associated with each curve indicate locations on fig. 4.11. In the free troposphere (fig. 4.13), size distributions in the center of the high-pressure system (curves A and B) were essentially the same as those in the NW airflow farther north (curve C).

Size distributions in the cloud layer show a well-mixed situation, having a peak in the number and volume spectra at 8-9 μm diameter, and some evaporation of the smallest droplets, typical of small marine stratus clouds.

In the marine boundary layer the higher CN area on the northern end of the flight track (curve F) is matched by a slightly greater overall size spectrum compared with the locations farther south (curves E and F). The volume peak at 8-μm diameter, suggests that a sea-salt component dominates the aerosol spectra.

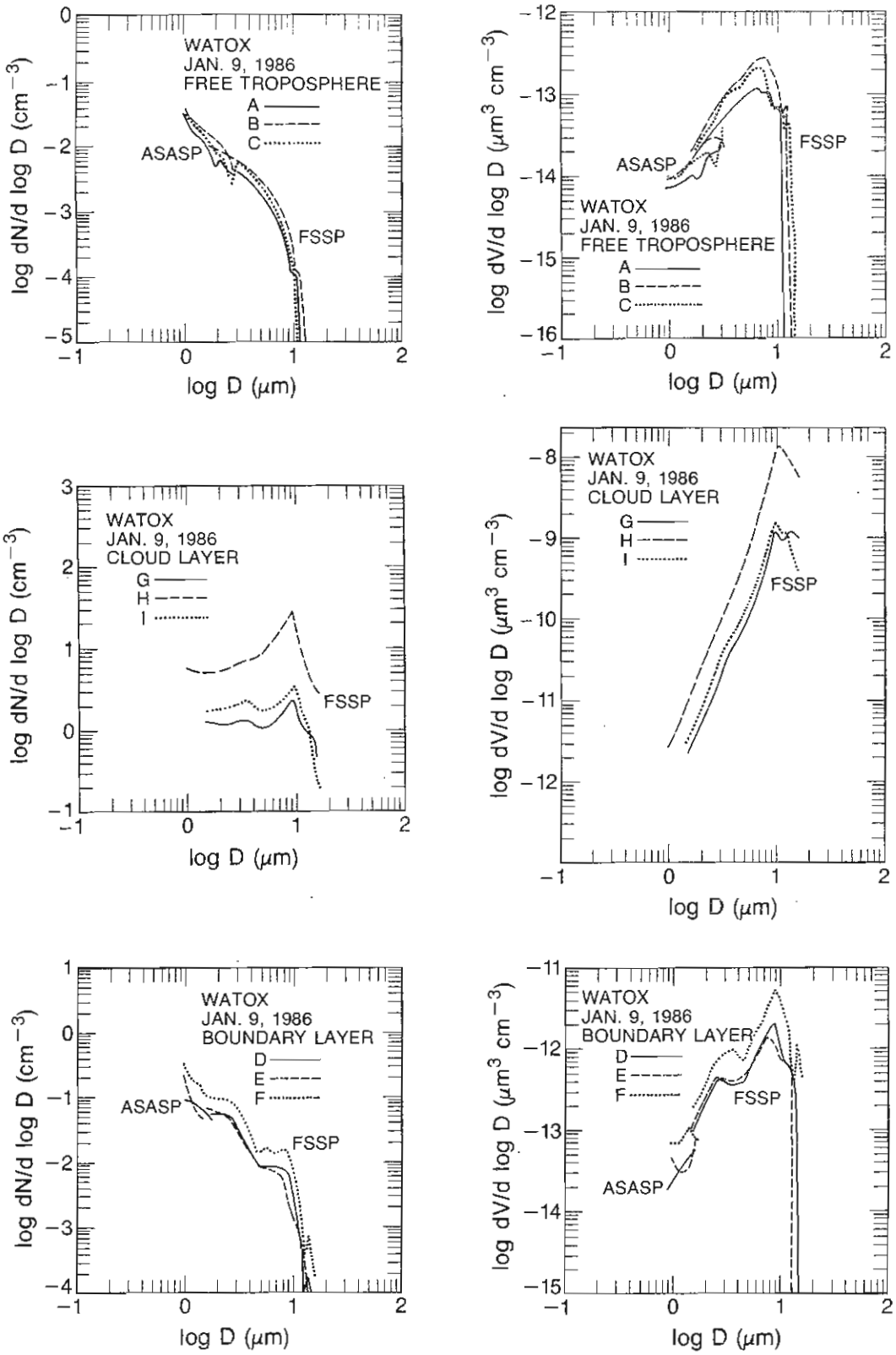

Figure 4.13--Number (left column) and volume (right column) aerosol size spectra at various aircraft locations, January 9, 1986. The letters associated with the spectra refer to locations shown in fig. 4.11.

ACKNOWLEDGMENTS

We thank Joe Boatman, Laureen Gunter, and Stan Wilkison for help with the PMS analysis; Gary Herbert for comments on the meteorological analysis; and Joyce Harris for back-trajectory models. This project was supported by grants from NOAA and NSF, and by the National Acid Precipitation Assessment Program.

REFERENCES

Harris, J.M., 1982. The GMCC atmospheric trajectory program. NOAA Tech Memo ERL-ARL-116, Air Resources Laboratory, Rockville, Maryland, 30 pp.

Harris, J. M., and B. A. Bodhaine (eds.), 1983. Geophysical Monitoring for Climatic Change No. 11 Summary Report 1983. Environmental Research Laboratories, Boulder, CO, 75 pp.

Heffter, J. L., 1983. Branching atmospheric trajectory (BAT) model. NOAA Tech. Memo ERL-ARL-121, NOAA Air Resources Laboratories, Silver Spring, MD, 16 pp.

Schnell, R. C., 1984. Arctic haze and the Arctic Gas and Aerosol Sampling Program (AGASP). Geophys. Res. Lett. 11:361-364.

Schnell, R. C., H. A. Bridgman, P. S. Naegele, and T. Watson, 1987. The NOAA WP-3D meteorological, aerosol, and gas systems, and flight operations during WATOX-86. Global Biogeochemical Cycles, in press, 1987.

Appendix A

AIR PARCEL BACK-TRAJECTORY SUMMARY FOR WATOX-86

A.1 Introduction

In addition to the isobaric trajectories presented in the main text, three other types of back-trajectories have been calculated for particular heights and locations for WATOX-86 WP-3D intensives. The three trajectory models and their appropriate references are (1) the Branching Atmospheric Trajectory (BAT) model run in default mode (Heffter, 1983), (2) the BAT model run in the modified mode (Heffter, NOAA ARL, personal communication, 1987) and the Geophysical Monitoring for Climatic Change (GMCC) Isentropic Trajectory model (Harris and Bodhaine, 1983).

A.2 Model Descriptions

A.2.1 ARL Branching Atmospheric Trajectory (BAT) Model in Default Mode

The default mode of the BAT model incorporates the following features:

(1) Three tropospheric layers identified as surface (lowest 300 m), boundary (variable as determined by the model), and upper.

(2) Transport backward or forward in time at 0000, 0600, 1200, or 1800 GMT.

(3) Transport using the average of observed winds in a layer and inverse distance squared wind weighting.

(4) Branching trajectories at day/night transitions (0300 GMT and 1500 GMT).

The symbols used for the BAT branching trajectories represent the vertical extent of the transport layers and the percentage of the original air mass along the trajectory. Figure A.1 depicts these layers (1N, 2N, 3N, 2D, 3D), where N is a night layer and D is a day layer. Table A.1 defines each symbol with a layer or percentage of original mass.

Table A.1--BAT trajectory layers and percentages of original mass

Type of layer		Percent of start mass	
Layer	Symbol	%	Symbol
2D	-----	80-100	A
3D	00000	60-80	B
1N	°°°°°	40-60	C
2N	- - -	20-40	D
3N	+++++	5-20	E

A.2.2 ARL Branching Atmospheric Trajectory (BAT) Model in Modified Mode

The modified mode of the BAT model incorporates the following features:

(1) A single tropospheric layer specified by the user.

(2) Transport backward or forward in time at 0000, 0600, 1200, or 1800 GMT.

(3) Transport using the average of observed winds in a layer and inverse distance squared wind weighting.

(4) No branching or other treatment of vertical motion.

A.2.3 GMCC Isentropic Trajectory Model

The default mode of the GMCC Isentropic Trajectory model incorporates the following features:

(1) Trajectories calculated on potential temperature surfaces interpolated from gridded wind components at mandatory pressure levels produced by a National Meteorological Center global atmospheric model.

(2) Transport backward or forward in time at 0000 or 1200 GMT.

A.3 Trajectories That Were Run and Graphical Depictions of Each

Table A.2 lists all the back-trajectories that were run during WATOX in January 1986 and includes the model parameters desired, as well as the model parameters actually chosen. Figures A.2-A.9 are examples of each of the trajectories with the appropriate flight track for January 4, 6, 8, and 9, 1986.

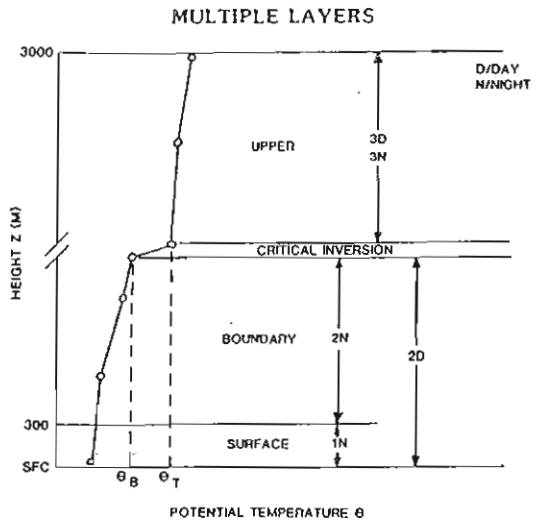

Figure A.1--Multiple atmospheric layers in the BAT model . Critical inversion criteria are 1) $\Delta\theta/\Delta Z \geq .005$ K/m. 2) $\theta_T - \theta_B \geq 2K$.

Table A-2 WATOX January 1986 Back-Trajectories

Date	Lat.	Lon.	Model	Model layer (m)	Model Parameters Desired				Model Parameters Chosen			
					Time (GMT)	P (mb)	θ (K)	Height (m)	Time (GMT)	P (mb)	θ (K)	Height (m)
4	42.86	63.31	BAT	Default mode	2030	PBL	270	171	2100			
4	41.24	66.88	θ*	Isentropic	1735	700	292	2979	0000 (1/5)	767	290	2300
4	41.24	66.88	BAT	2900-3100	1735	700	292	2979	1800			
6	38.99	69.50	BAT	Default mode	1513	PBL	283	4432	1500			
6	40.79	67.24	θ*	Isentropic	1349	700	290	2879	0000 (1/7)	646	290	3400
6	40.79	67.24	BAT	2800-3000	1349	700	290	2879	1200			
8	37.37	71.70	BAT	Default mode	2000	PBL	275	352	2100			
8	40.33	72.89	θ*	Isentropic	1300	580	287	4276	1200	513	290	5200
8	40.33	72.89	BAT	4200-4400	1300	580	287	4276	1200			
9	34.74	71.91	BAT	Default mode	1615	1012	283	180	1500			
9	33.97	72.42	θ*	Isentropic	1630	805	288	2044	1200	798	290	2100
9	33.97	72.42	BAT	1900-2100	1630	805	288	2044	1500			

BAT model parameters chosen within the program.

*Isentropic

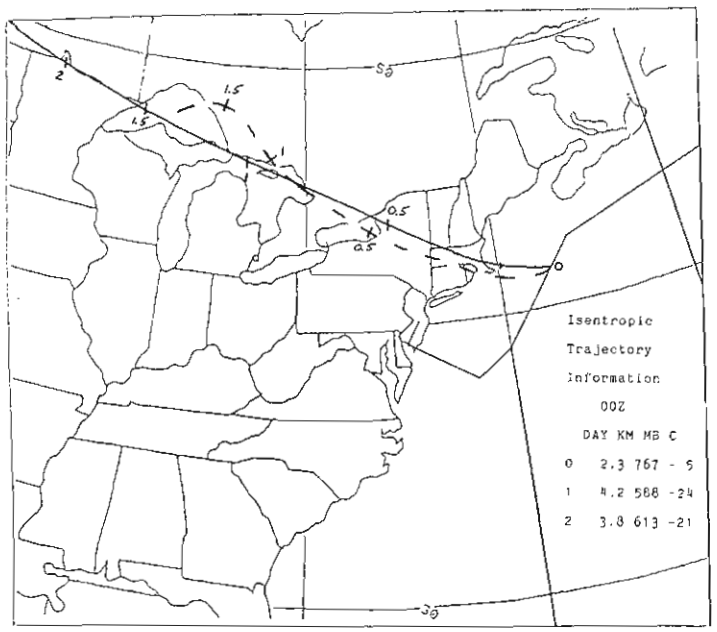

Figure A.2--Backward BAT (modified) trajectory (dashed, 2900-3100 m layer, 1800 GMT on January 4, 1986) and backward isentropic trajectory (solid, θ = 290 K, 0000 GMT on January 5, 1986), originating at 41.24°N, 66.88°W. Each tick mark represents 12 hours (0.5 days).

Figure A.3--Backward BAT trajectory (run in default mode and allowed to branch) originating at 2100 GMT on January 4, 1986, from 42.86°N, 63.31°W. Letters represent 12 hours (0.5 days).

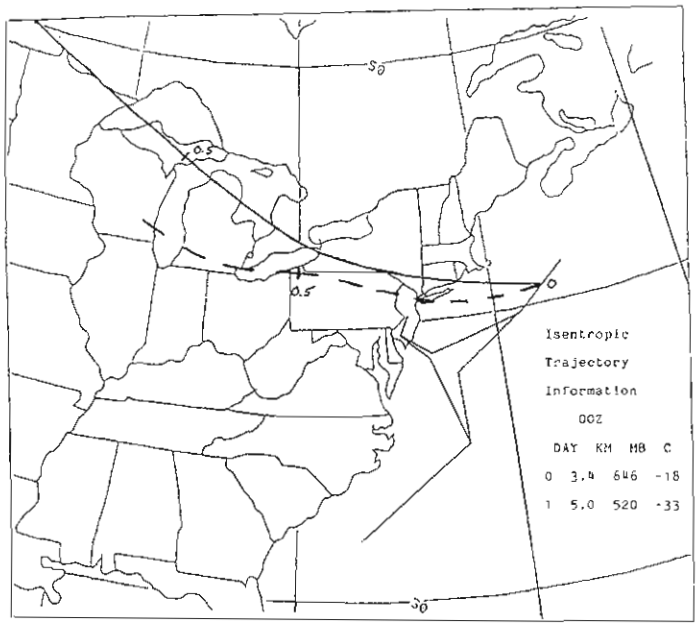

Figure A.4--Backward BAT (modified) trajectory (dashed, 2800-3000 m layer, 1200 GMT on January 6, 1986) and backward isentropic trajectory (solid, θ = 290 K, 0000 GMT on January 7, 1986), originating at 40.79°N, 67.24°W. Each tick mark represents 12 hours (0.5 days).

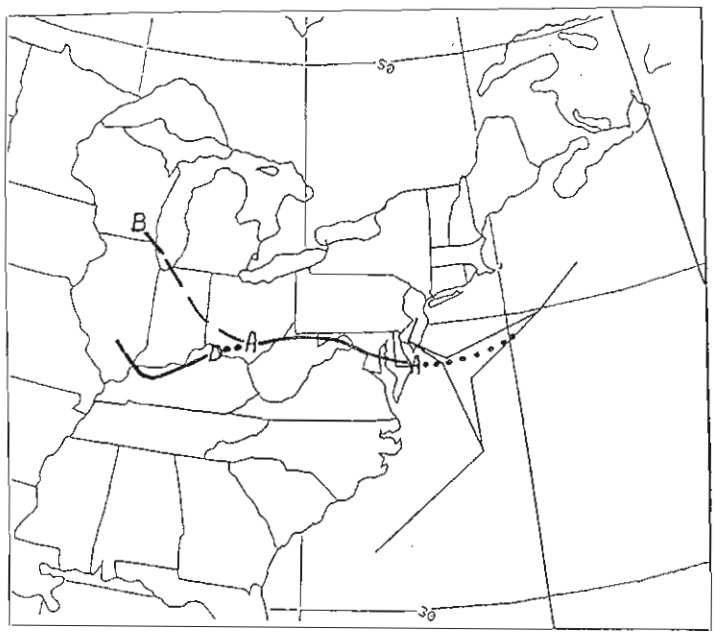

Figure A.5--Backward BAT trajectory (run in default mode and allowed to branch) originating at 1500 GMT January 6, 1986, from 38.99°N, 69.50°W. Letters represent 12 hours (0.5 days).

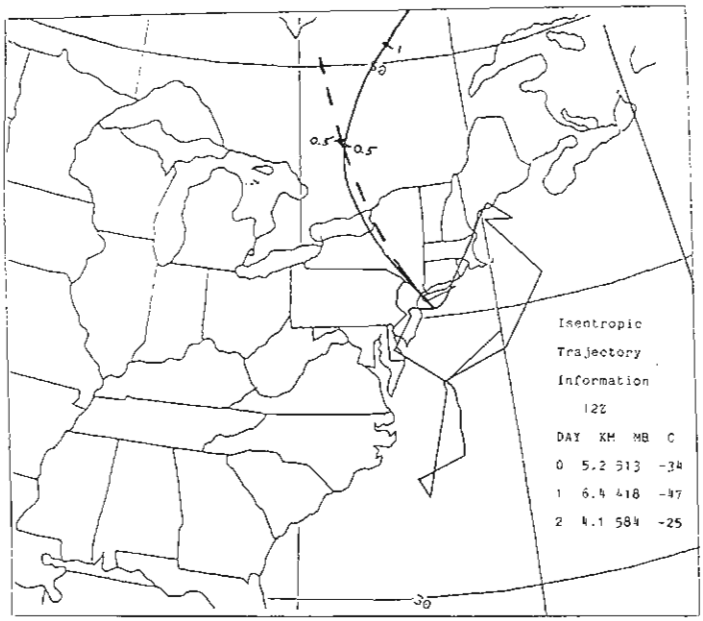

Figure A.6--Backward BAT (modified) trajectory (dashed, 4200-4400 m layer, 1200 GMT on January 8, 1986) and backward isentropic trajectory (solid, θ = 290 K, 1200 GMT on January 8, 1986), originating at 40.33°N, 72.89°W. Each tick mark represents 12 hours (0.5 days).

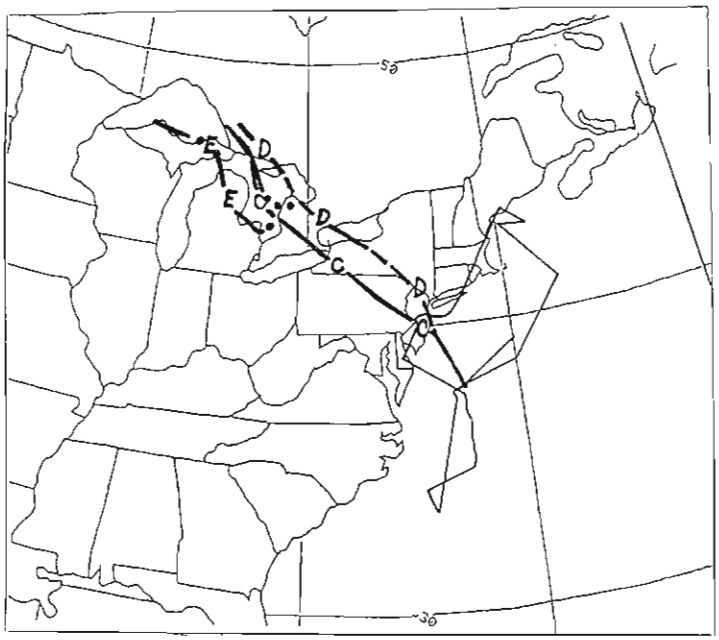

Figure A.7--Backward BAT trajectory (run in default mode and allowed to branch) originating at 2100 GMT on January 8, 1986, from 37.37°N, 71.70°W. Letters represent 12 hours (0.5 days).

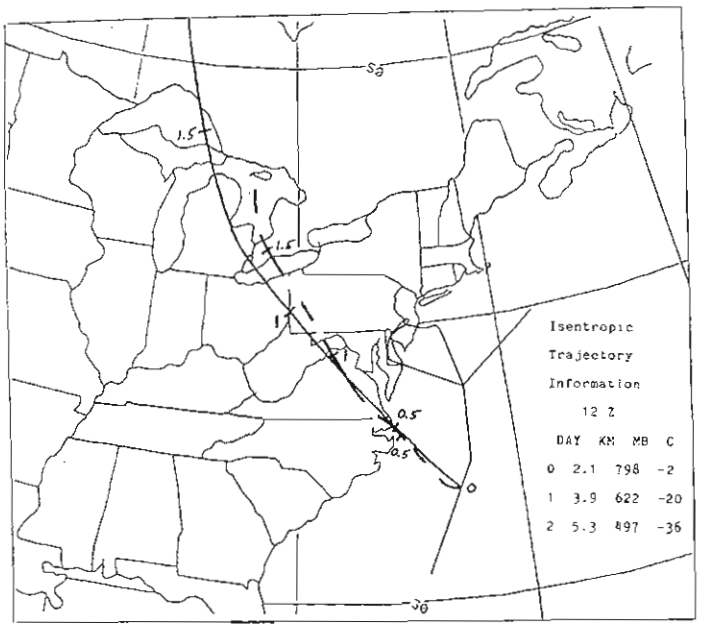

Figure A.8--Backward BAT (modified) trajectory (dashed, 1900-2100 m layer, 1500 GMT on January 9, 1986) and backward isentropic trajectory (solid, θ = 290 K, 1200 GMT on January 9, 1986), originating at 33.97°N, 72.42°W. Each tick mark represents 12 hours (0.5 days).

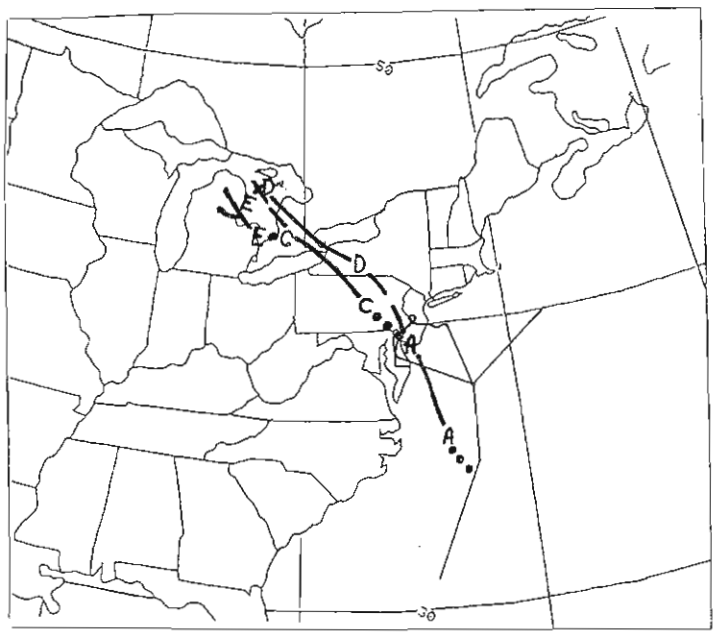

Figure A.9--Backward BAT trajectory (run in default mode and allowed to branch) originating at 1500 GMT on January 9, 1986, from 34.74°N, 71.91°W. Letters represent 12 hours (0.5 days).

Appendix B
WATOX AIR FLUX CALCULATIONS

B.1 Introduction

Air fluxes perpendicular to the WP-3D flight track were calculated and tabulated on approximately 15-min-average segments. In addition, spatial distributions were prepared for the $\overline{U}$ and $\overline{V}$ wind components relative to the idealized NW-SE flight track.

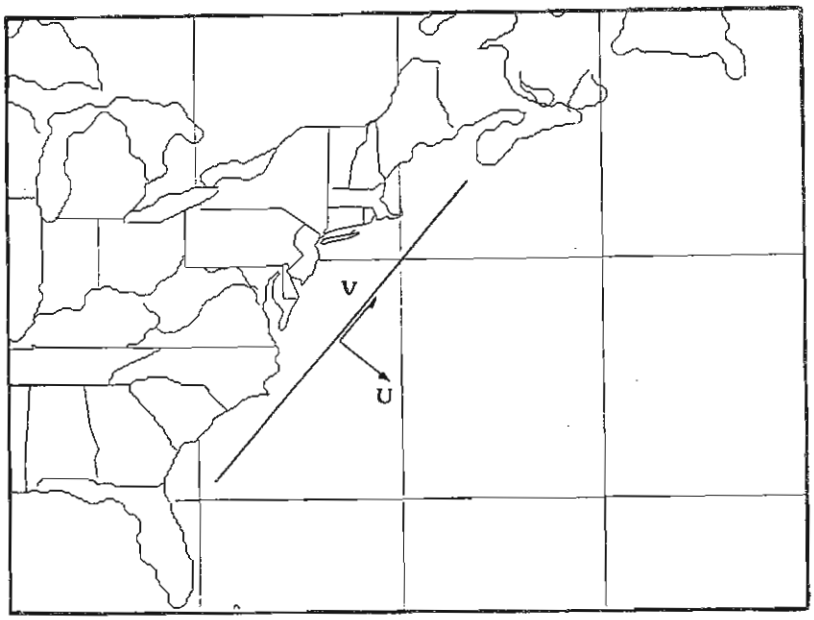

Figure B.1--Parameterization of the $\overline{U}$ and $\overline{V}$ air fluxes relative to an idealized WATOX flight track.

B.2 Definitions of Terms in the Tables.

TIME S	Start time, hours, minutes, seconds, of the averaging segment.
TIME E	End time, hours, minutes, seconds, of the averaging segment.
LAT S	Starting latitude (°N) of the averaging segment.
LAT E	Ending latitude (°N) of the averaging segment.
LAT AVE	Average latitude of the segment.
LON S	Starting longitude (°W) of the averaging segment.
LON E	Ending longitude (°W) of the averaging segment.
P	Average pressure (mb) of each segment.
PS	Starting pressure level (mb) of each segment.

PE	Ending pressure level (mb) of each segment
RALT S	Starting radar altitude (m) of segment.
RALT E	Ending radar altitude (m) of segment.
T	Average temperature (°C) of each segment.
U	Average northwesterly component of the wind for each segment. -U means southeasterly wind component.
V	Average southwesterly component of the wind for each segment. -V means northeasterly wind component.
FLUX STP ($kg\ m^{-2}\ s^{-1}$)	Northwesterly flux (kilograms per square meter per second) of air for the segment into the flight track adjusted to standard temperature (25°C) and pressure (1013 mb).
FLUX AMBIENT ($kg\ m^{-2}\ s^{-1}$)	Northwesterly flux (kilograms per square meter per second) of air for the segment into the flight track for ambient (unadjusted conditions.
FLUX STP ($m^3\ s^{-1}$)	Northwesterly flux (cubic meters per second) of air for the segment into the flight track adjusted to standard temperature (25°C) and pressure (1013 mb).
FLUX AMBIENT ($m^3\ s^{-1}$)	Northwesterly flux (cubic meters per second) of air for the segment into the flight track for ambient (unadjusted) conditions.
MAX FLUX STP ($kg\ m^{-2}\ s^{-1}$)	Maximum northwesterly flux (kilograms per square meter per second) of air for the segment adjusted to standard temperature and pressure.
MIN FLUX STP ($kg\ m^{-2}\ s^{-1}$)	Minimum northwesterly flux (kilograms per square meter per square meter per second) of air for the segment adjusted to standard temperature and pressure.
FLUX STD STP ($kg\ m^{-2}\ s^{-1}$)	Standard deviation of the northwesterly flux (kilograms per square meter per second) of air for the segment adjusted to standard temperature and pressure.

B.3 Tables of Air Flux and Meteorological Values, and Spatial Distributions of $\overline{U}$ and $\overline{V}$ Wind Components

Tabular calculations of air flux perpendicular to the WP-3D flight track are presented here for January 4, 6, 8, and 9, 1986, plus relevant meteorological information in approximately 15-min-average segments. Spatial distributions of the $\overline{U}$ and $\overline{V}$ wind components are also included for each day, relative to the idealized NW-SE flight track shown in fig. B.1.

WATOX FLIGHT 1, DAY 4

TIME S HHMMSS	TIME E HHMMSS	LAT S	LAT E	LAT AVG	LON S	LON E	P (MB)	PS (MB)	PE (MB)	RALT S (M)	RALT E (M)	T (C)	U (M/S)	V (M/S)	FLUX STP kg/m2/s	FLUX AMBIENT kg/m2/s	FLUX STP m3/s	FLUX AMBIENT m3/s	MAX FLUX STP kg/m2/s	MIN FLUX STP kg/m2/s	FLUX STD STP kg/m2/s
162035	163000	37.50	37.91	37.71	71.61	70.85	706.30	673.4	735.4	3396	2685	-3.21	14.29	7.78	18.44	13.01	20.25	14.29	20.24	16.04	1.27
163015	164455	37.92	38.54	38.23	70.83	69.71	794.40	737.2	852.7	2662	1479	1.29	11.45	3.44	14.78	11.53	14.67	11.45	17.39	10.31	1.77
164500	165955	38.55	39.35	38.95	69.70	68.90	888.80	854.3	897.4	1467	1052	2.16	9.18	0.72	11.85	10.31	10.55	9.18	15.08	10.31	1.17
170005	171455	39.35	40.14	39.75	68.90	68.04	846.20	897.5	789.4	1049	2071	0.55	13.53	3.52	17.46	14.56	16.23	13.53	22.67	12.77	3.02
171500	173000	40.15	40.97	40.56	68.03	67.16	732.70	787.7	699.6	2082	2990	-6.70	20.91	4.89	26.99	20.01	28.20	20.91	30.98	22.58	2.42
173015	174455	40.98	41.75	41.37	67.15	66.27	717.10	699.6	762.4	2990	2291	-8.50	23.19	7.14	29.93	21.87	31.74	23.19	31.17	28.43	0.64
174500	175955	41.76	42.36	42.06	66.26	65.20	814.40	763.5	887.0	2280	1161	-5.69	22.91	6.81	29.57	24.28	27.90	22.91	32.19	25.72	1.94
180005	180035	42.37	42.38	42.38	65.19	65.15	884.00	878.6	892.0	1145	1028	-8.05	20.48	5.98	26.43	23.77	22.78	20.48	27.95	25.26	0.73
180315	181455	42.46	42.73	42.60	64.92	63.91	987.80	947.9	992.4	553	163	-3.17	17.65	8.32	22.78	22.47	17.89	17.65	25.33	19.93	1.21
181500	182955	42.73	43.05	42.89	63.91	62.58	980.30	992.4	944.7	163	533	-5.06	18.46	9.73	23.82	23.49	18.72	18.46	26.47	21.06	1.19
183000	183055	43.05	43.07	43.06	62.57	62.49	935.40	942.5	931.2	550	646	-9.05	19.24	11.71	24.83	23.71	20.15	19.24	25.51	23.99	0.46
183435	184455	43.16	43.38	43.27	62.16	61.14	818.50	884.8	762.1	1031	2166	-10.30	30.72	10.30	39.65	33.29	36.59	30.72	44.60	30.38	3.31
184500	185950	43.38	43.69	43.54	61.13	59.58	726.30	760.5	727.4	2182	2493	-11.92	32.25	8.15	41.62	31.20	43.02	32.25	46.32	32.89	3.87
190000	191500	43.69	44.12	43.91	59.58	57.99	727.60	727.4	727.6	2493	2467	-13.51	22.09	18.78	28.51	21.54	29.23	22.09	43.60	16.22	8.10
191510	192950	44.13	43.89	44.01	57.97	58.76	679.00	727.6	572.2	2467	4294	-14.51	16.63	29.93	21.46	15.19	23.49	16.63	31.35	10.96	5.62
193000	194450	43.89	43.67	43.78	58.77	59.83	592.30	572.3	640.6	4296	3488	-18.93	29.91	25.10	38.60	24.25	47.61	29.91	43.07	28.67	3.80
194500	195950	43.66	43.43	43.55	59.84	60.90	696.20	641.8	748.2	3478	2345	-12.44	34.43	13.21	44.43	32.00	47.82	34.43	46.42	40.68	1.53
200000	200930	43.43	43.27	43.35	60.91	61.52	814.00	749.1	881.3	2334	1087	-8.43	32.43	10.88	41.85	34.70	39.11	32.43	45.92	33.98	2.38
201240	211450	43.25	43.21	43.23	61.73	61.88	977.10	948.2	989.9	529	183	-5.09	19.80	12.65	25.55	25.12	20.14	19.80	27.12	24.59	0.82
201500	202950	43.21	42.96	43.09	61.89	62.85	989.80	989.6	989.9	185	203	-3.69	17.76	11.60	22.92	22.70	17.93	17.76	26.95	19.00	1.63
203000	204450	42.96	42.74	42.85	62.86	63.81	993.30	989.9	994.8	203	180	-3.41	17.37	9.08	22.42	22.26	17.49	17.37	23.84	19.49	0.80
204500	205950	42.73	42.46	42.60	63.82	64.79	994.70	994.8	994.6	180	197	-2.47	17.01	5.39	21.95	21.75	17.17	17.01	24.31	19.39	1.08
210000	211450	42.46	42.17	42.32	64.81	65.79	997.00	994.6	997.7	197	183	-1.98	15.43	2.38	19.91	19.74	15.56	15.43	22.36	17.34	1.07
211500	212950	42.16	41.50	41.83	65.79	66.57	998.10	997.7	998.4	183	196	-1.31	12.26	0.50	15.82	15.67	12.38	12.26	18.98	14.00	0.97
213000	214450	41.49	40.80	41.15	66.58	67.34	999.30	998.4	987.9	196	289	-0.39	9.29	-0.50	11.99	11.84	9.40	9.29	14.84	9.34	1.37
214500	214630	40.80	40.73	40.77	67.34	67.42	969.60	983.9	955.5	323	562	-2.35	7.47	-1.89	9.64	9.31	7.74	7.47	10.87	8.86	0.67
214840	215950	40.63	40.08	40.36	67.54	68.09	845.10	919.0	814.6	873	1855	0.07	9.50	6.37	12.26	10.23	11.39	9.50	14.84	9.80	0.95
220000	221440	40.07	39.34	39.71	68.10	68.91	839.40	814.6	926.0	1855	835	-0.30	6.54	5.47	8.44	7.00	7.88	6.54	11.07	0.68	2.33
221650	222950	39.24	38.62	38.93	69.03	69.64	970.30	965.0	970.1	499	455	3.38	-0.30	-0.85	-0.39	-0.37	-0.32	-0.30	1.75	-2.95	0.93
223000	224450	38.61	38.09	38.35	69.65	70.50	970.30	970.1	970.3	455	451	5.25	-1.78	1.28	-2.30	-2.16	-1.89	-1.78	-1.18	-4.16	0.58
224500	225950	38.08	37.63	37.86	70.51	71.47	970.30	970.3	970.4	451	445	6.73	-2.24	0.64	-2.89	-2.70	-2.40	-2.24	-1.15	-5.00	0.75
230000	230330	37.63	37.52	37.58	71.48	71.71	970.20	970.4	970.3	445	446	8.68	-3.35	1.39	-4.32	-4.01	-3.61	-3.35	-3.05	-5.32	0.61

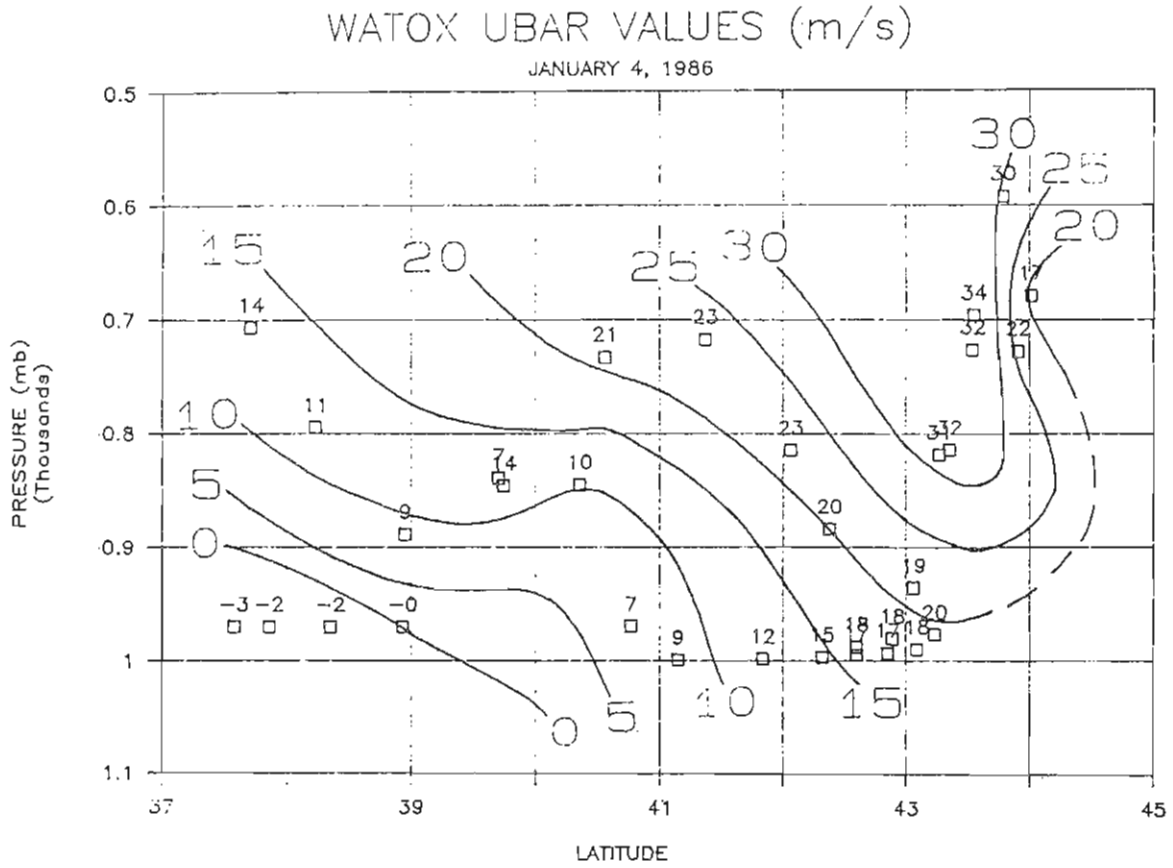
WATOX UBAR VALUES (m/s)
JANUARY 4, 1986
PRESSURE (mb)
(Thousands)
0.5
0.6
0.7
0.8
0.9
1
1.1
37
39
41
43
45
LATITUDE

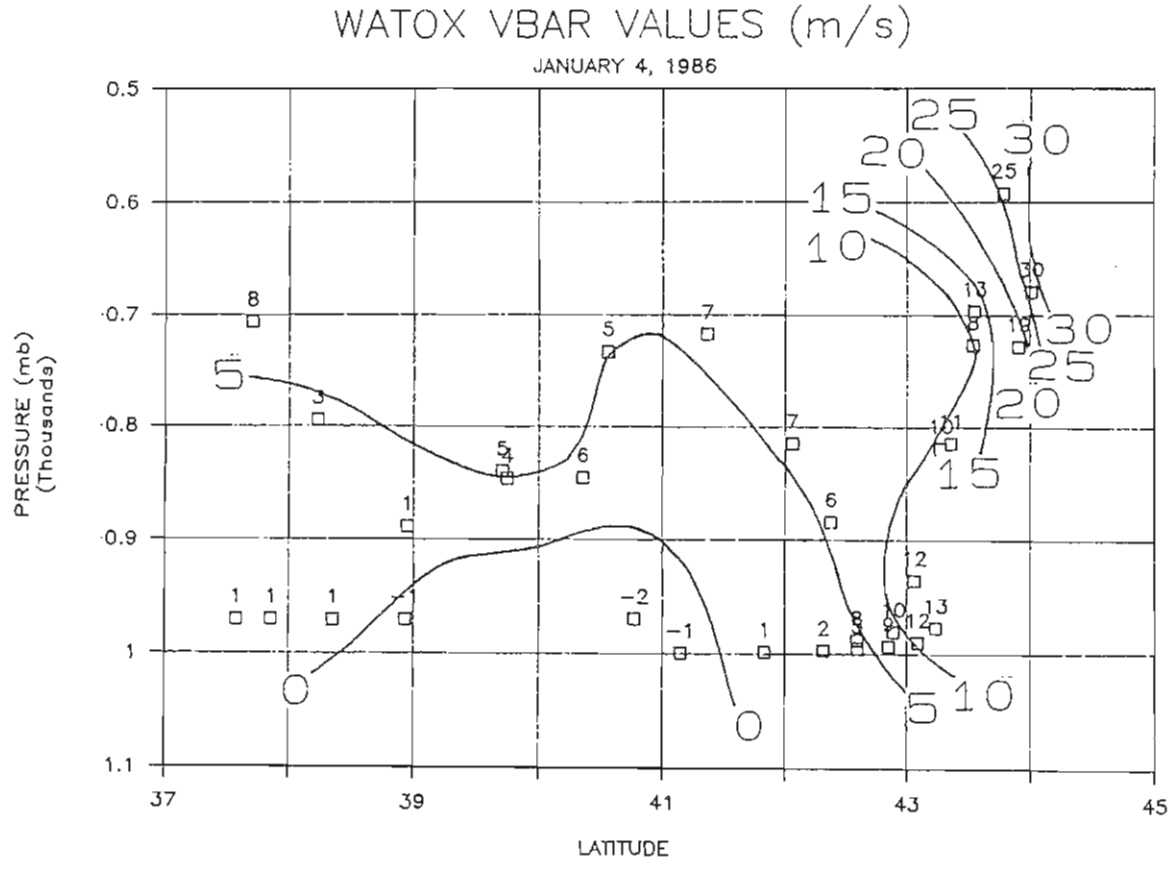
WATOX VBAR VALUES (m/s)
JANUARY 4, 1986
PRESSURE (mb)
(Thousands)
0.5
0.6
0.7
0.8
0.9
1
1.1
37
39
41
43
45
LATITUDE

WATOX FLIGHT 2, DAY 6

TIME S HHMMSS	TIME E HHMMSS	LAT S	LAT E	LAT AVG	LON S	LON E	P (MB)	PS (MB)	PE (MB)	RALT S (M)	RALT E (M)	T (C)	U (M/S)	V (M/S)	FLUX STP kg/m2/s	FLUX AMBIENT kg/m2/s	FLUX STP m3/s	FLUX AMBIENT m3/s	MAX FLUX STP kg/m2/s	MIN FLUX STP kg/m2/s	FLUX STD STP kg/m2/s
124800	125950	38.02	38.61	38.32	72.49	71.34	576.70	572.7	599.6	4523	4148	-17.21	23.62	30.05	30.48	18.52	38.88	23.62	31.77	27.38	1.05
130000	131450	38.62	39.24	38.93	71.32	69.79	674.70	601.1	720.0	4127	2718	-10.56	20.67	29.49	26.68	18.48	29.83	20.67	34.03	24.1	1.95
131500	132950	39.24	39.83	39.54	69.77	68.45	800.90	719.5	887.0	2725	1067	-6.23	15.74	21.31	20.31	16.44	19.45	15.74	26.04	14.27	3.59
133000	134450	39.83	40.57	40.20	68.44	67.79	853.20	887.1	766.7	1067	2187	-5.39	12.26	20.10	15.82	13.59	14.27	12.26	19.89	1.95	2.5
134500	135950	40.58	41.48	41.03	67.48	66.41	705.50	764.4	695.0	2208	2905	-11.26	19.30	31.74	24.91	18.09	26.57	19.30	28.34	17.23	2.17
140000	140020	41.49	41.50	41.50	66.40	66.37	695.20	695.0	695.8	2905	2904	-12.97	16.10	30.77	20.78	14.97	22.35	16.10	21.1	20.25	0.38
140030	141450	41.50	41.07	41.29	66.35	66.95	744.30	700.8	867.5	2850	1215	-10.56	13.77	25.64	17.77	13.58	18.02	13.77	23.78	10.69	4.26
141500	141700	41.07	41.00	41.04	66.96	67.03	883.80	870.4	898.4	1187	939	-4.24	9.96	20.87	12.85	11.39	11.24	9.96	16.17	8.27	2.05
141710	142950	40.99	40.50	40.75	67.04	67.55	967.80	900.4	989.0	920	172	2.54	11.58	19.42	14.95	14.15	12.23	11.58	17.25	12.81	1.07
143000	144450	40.49	39.90	40.20	67.55	68.18	999.00	989.0	988.9	172	183	5.10	13.27	16.45	17.13	16.58	13.71	13.27	20.93	14.21	1.28
144500	150000	39.90	39.42	39.66	68.18	68.88	979.20	988.9	959.4	183	443	6.37	12.81	16.49	16.53	15.62	13.56	12.81	21.56	11.72	1.86
150000	151450	39.42	38.93	39.18	68.89	69.58	959.40	959.4	959.2	443	446	6.30	10.60	16.87	13.68	12.66	11.45	10.60	16.95	10.16	1.46
151500	152950	38.92	38.47	38.70	69.58	70.25	951.80	959.2	914.7	446	850	5.71	12.26	15.33	15.82	14.56	13.32	12.26	18.41	12.51	1.16
153000	154450	38.46	37.95	38.21	70.26	70.95	914.80	914.4	913.9	852	867	3.67	11.36	16.57	14.66	13.06	12.75	11.36	17.4	12.16	1.01
154500	155950	37.95	37.46	37.71	70.95	71.58	915.10	913.9	916.1	867	858	4.52	11.64	14.63	15.02	13.35	13.10	11.64	17.53	12.22	1.01
160000	160110	37.45	37.40	37.43	71.59	71.64	908.40	916.2	901.1	858	997	4.06	12.38	18.29	15.98	14.12	14.01	12.38	17.54	14.26	1.14
160120	161450	37.40	36.69	37.05	71.64	71.66	820.40	897.9	779.0	1020	2178	-1.11	15.13	17.99	19.53	15.88	18.61	15.13	24.92	13.52	2.66
161500	162620	36.68	36.06	36.37	71.66	71.69	790.40	779.0	838.5	2178	1606	-1.08	15.64	18.27	20.18	15.81	19.97	15.64	23.16	15.74	1.72
162700	162950	36.03	35.88	35.96	71.69	71.71	873.80	849.1	899.2	1506	1043	2.50	12.25	13.88	15.81	13.51	14.33	12.25	18.66	13.45	1.49
163000	164450	35.87	35.09	35.48	71.71	71.74	979.60	902.8	998.1	1008	174	11.71	11.08	11.68	14.30	13.26	11.95	11.08	17.09	10.99	1.32
164500	165950	35.08	34.57	34.83	71.74	72.26	998.50	998.1	998.7	174	178	13.47	9.07	8.86	11.71	11.00	9.66	9.07	14.98	8.95	1.29
170005	171455	34.57	34.19	34.38	72.26	73.00	992.60	998.7	967.8	178	452	12.97	7.06	8.12	9.11	8.52	7.55	7.06	12	6.43	1.27
171500	172955	34.19	33.76	33.98	73.01	73.72	967.60	967.8	967.7	452	456	10.83	5.37	7.78	6.93	6.37	5.84	5.37	9.32	4.92	0.78
173000	174455	33.76	33.32	33.54	73.72	74.43	966.40	967.7	944.4	456	662	10.58	4.50	7.21	5.81	5.33	4.90	4.50	7.86	3.99	0.88
174500	175955	33.31	32.90	33.11	74.44	75.21	925.70	941.2	973.1	692	354	7.30	3.80	6.42	4.90	4.36	4.27	3.80	6.44	1.94	0.81
180005	181455	32.40	32.51	32.46	75.21	75.98	962.20	976.0	934.0	388	760	10.00	3.66	6.14	4.72	4.33	3.99	3.66	6.29	2.84	0.68
181500	182955	32.50	32.01	32.26	75.98	76.67	957.00	931.8	998.4	779	207	9.66	2.52	5.22	3.25	2.97	2.76	2.52	6.13	1.12	0.98
183000	183635	32.00	31.75	31.88	76.68	76.90	958.10	1003.7	915.4	207	937	9.70	1.60	4.13	2.06	1.89	1.75	1.60	4.81	0.56	0.77
183645	184000	31.75	31.90	31.83	76.89	76.75	907.80	919.7	883.8	898	1210	5.54	1.81	3.51	2.34	2.05	2.06	1.81	4.3	0.74	1.01
184015	184455	31.90	32.12	32.01	76.74	76.56	843.40	881.5	810.4	1233	1919	5.47	3.88	2.34	5.01	4.09	4.75	3.88	7.46	2.66	1.58
184500	185955	32.13	32.72	32.43	76.55	75.56	729.40	807.8	706.7	1937	3024	1.72	10.17	7.57	13.13	9.39	14.21	10.17	16.79	7.56	2.61
190005	191455	32.73	33.30	33.02	75.55	74.57	729.40	706.7	809.6	3024	1924	-0.34	11.95	9.93	15.42	11.12	16.58	11.95	16.86	12.49	1.4
191500	192955	33.30	33.83	33.57	74.56	73.65	842.60	812.4	844.7	1895	1571	3.55	9.83	8.36	12.69	10.42	11.97	9.83	14.22	10.68	0.88
193000	194455	33.84	34.38	34.11	73.64	72.69	777.70	844.7	703.5	1571	3037	0.77	12.58	10.04	16.24	12.43	16.43	12.58	19.31	12.65	1.98
194500	195955	34.39	34.97	34.68	72.68	71.66	703.70	703.6	703.9	3037	3024	-1.23	14.94	16.39	19.28	13.45	21.41	14.94	20.55	17.87	0.54
200005	201455	34.98	35.74	35.36	71.66	71.98	743.40	703.9	811.0	3024	1875	-0.86	17.56	15.79	22.66	16.68	23.85	17.56	26.2	16.61	1.62
201500	202955	35.75	36.53	36.14	71.98	72.22	834.90	813.9	831.9	1845	1651	0.33	14.22	17.32	18.35	15.11	17.27	14.22	21.67	12.81	1.83
203000	204455	36.54	37.33	36.94	72.22	72.42	745.50	831.9	969.7	1651	3047	-2.53	20.73	21.46	26.75	19.87	27.91	20.73	32.07	15.84	4.62
204500	205525	37.34	37.91	37.63	72.42	72.61	696.80	696.7	696.8	3047	3024	-5.62	23.97	23.29	30.94	21.73	34.13	23.97	32.28	28.3	1.18

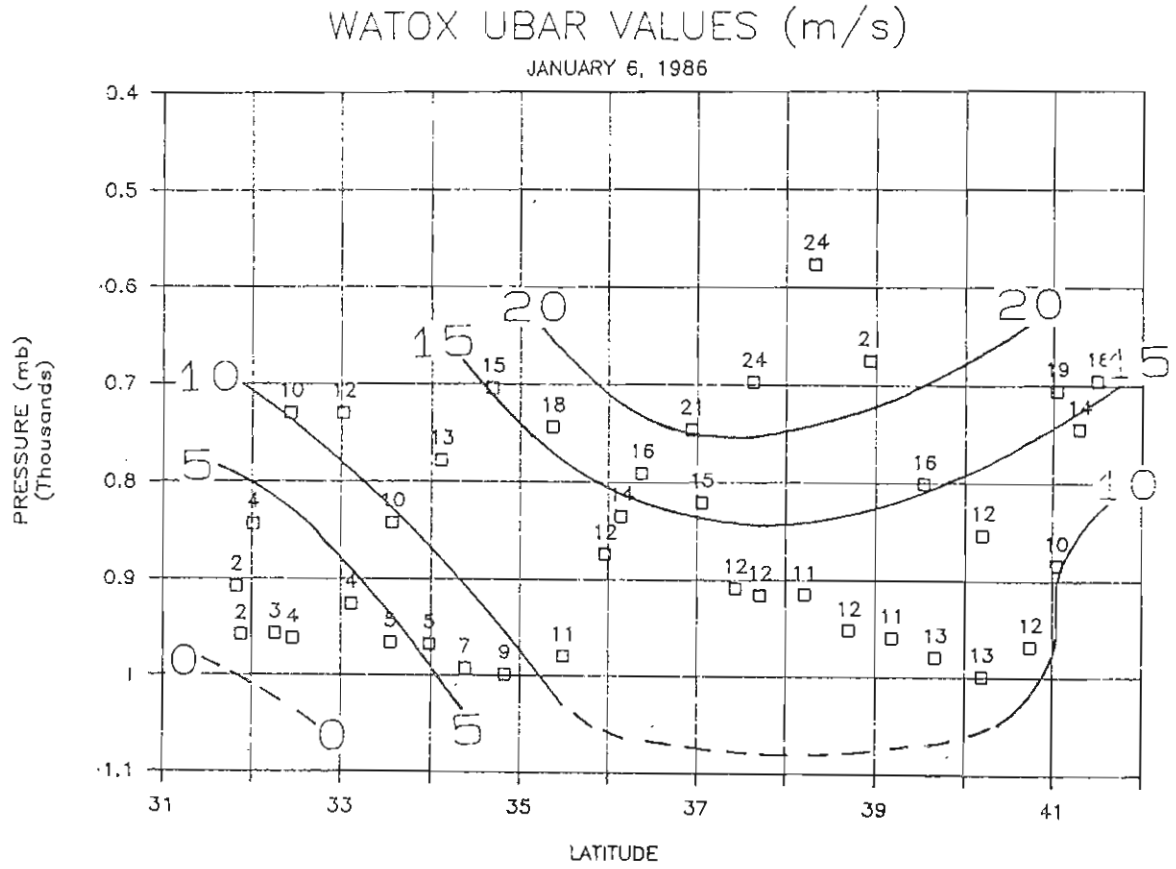
WATOX UBAR VALUES (m/s)
JANUARY 6, 1986
PRESSURE (mb)
(Thousands)
0.4
0.5
0.6
0.7
0.8
0.9
1
1.1
31
33
35
37
39
41
LATITUDE

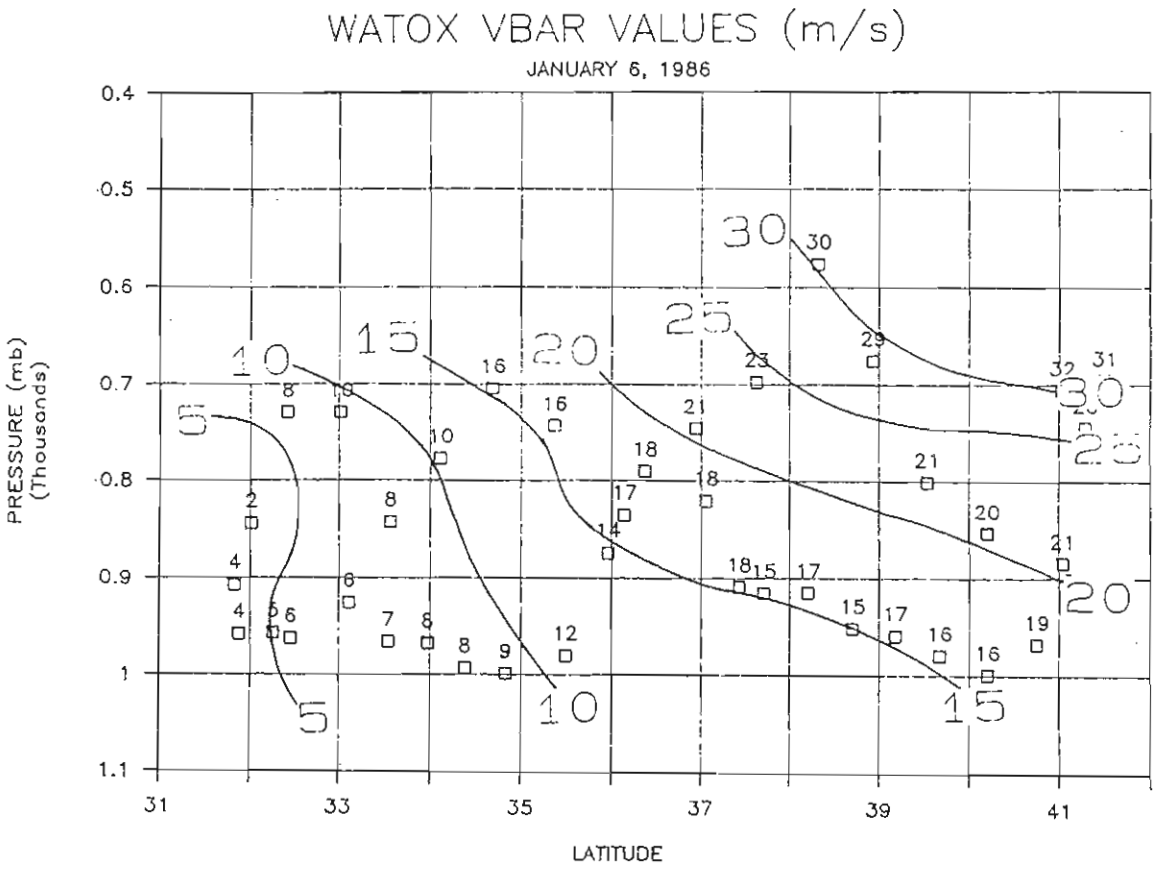
WATOX VBAR VALUES (m/s)
JANUARY 6, 1986
PRESSURE (mb)
(Thousands)
0.4
0.5
0.6
0.7
0.8
0.9
1
1.1
31
33
35
37
39
41
LATITUDE

WATOX FLIGHT 3, DAY 8

TIME S HHMMSS	TIME E HHMMSS	LAT S	LAT E	LAT AVG	LON S	LON E	P (MB)	PS (MB)	PE (MB)	RALT S (M)	RALT E (M)	T (C)	U (M/S)	V (M/S)	FLUX STP kg/m2/s	FLUX AMBIENT kg/m2/s	FLUX STP m3/s	FLUX AMBIENT m3/s	MAX FLUX STP kg/m2/s	MIN FLUX STP kg/m2/s	FLUX STD STP kg/m2/s
154700	155950	41.09	40.52	40.81	67.00	67.84	756	757.7	756.2	2339	2376	-17.18	18.67	-4.49	24.09	19.19	23.44	18.67	26.61	20.94	1.07
160000	161450	40.51	39.70	40.11	67.85	68.55	788	756.2	795.9	2376	2002	-15.65	13.65	-0.99	17.62	14.53	16.55	13.65	21.96	15.07	1.92
161500	162950	39.69	38.94	39.32	68.56	69.35	772	795.9	753.4	2002	2439	-16.24	14.23	1.34	18.36	14.88	17.56	14.23	21.49	14.17	1.96
163000	164450	38.93	38.23	38.58	69.36	70.18	736	753.4	698.2	2439	3040	-15.73	16.54	1.53	21.35	16.45	21.46	16.54	24.08	17.53	1.53
164500	165950	38.22	37.71	37.97	70.19	71.28	702	698.2	737.7	3040	2641	-15.34	19.94	-2.68	25.73	18.89	27.17	19.94	27.19	21.99	1.28
170000	171450	37.70	37.01	37.36	71.29	71.93	744	741.0	743.7	2604	2593	-12.51	16.00	-3.48	20.65	15.88	20.80	16.00	23.99	19.2	1.14
171500	172950	37.00	36.05	36.53	71.94	72.46	743	743.7	737.7	2593	2672	-10.47	16.49	-0.98	21.28	16.23	21.63	16.49	24.36	19.38	1.18
173000	174450	36.04	35.05	35.55	72.47	72.96	726	737.8	699.4	2609	3115	-8.01	17.94	0.98	23.15	17.10	24.29	17.94	26.99	19.87	1.88
174500	175950	35.04	34.10	34.57	72.97	73.46	703	699.4	732.8	3115	2769	-4.66	19.29	4.66	24.90	17.56	27.34	19.29	27.65	21.79	1.58
180000	181450	34.09	33.14	33.62	73.46	73.92	756	734.4	757.5	2749	2512	-0.24	16.71	2.67	21.57	16.11	22.37	16.71	25.43	17.58	2
181500	181730	33.13	32.98	33.06	73.90	74.02	757	757.5	757.3	2512	2512	1.07	18.00	2.79	23.23	17.30	24.18	18.00	24.43	22.37	0.53
181740	182200	32.98	33.20	33.09	74.04	73.97	772	757.5	798.0	2506	2093	0.27	16.23	-0.30	20.95	15.94	21.33	16.23	25.16	10.24	4.04
182610	182950	33.43	33.64	33.54	73.94	73.93	911	899.3	925.6	1147	910	0.02	7.19	-9.25	9.28	8.35	7.99	7.19	11.26	7.94	1.01
183000	184450	33.65	34.36	34.01	73.93	73.68	930	925.5	941.8	916	769	0.49	8.16	-8.68	10.53	9.65	8.91	8.16	13.03	6.55	1.17
184500	185950	34.39	34.71	34.55	73.63	72.66	969	942.8	979.1	763	444	3.38	9.78	-6.90	12.62	11.92	10.35	9.78	16.03	9.83	1.39
190000	191450	34.71	35.07	34.89	72.65	71.73	996	979.1	1008.5	444	187	5.56	10.87	-6.78	14.02	13.52	11.28	10.87	17.82	9.08	1.49
191500	192950	35.08	35.82	35.45	71.73	71.74	995	1008.5	978.6	187	443	5.10	11.17	-6.08	14.41	13.90	11.58	11.17	17.43	11.79	1.08
193000	194450	35.83	36.57	36.20	71.73	71.70	973	978.6	962.9	443	574	1.93	12.17	-5.18	15.71	14.98	12.76	12.17	18.73	13.54	1.19
194500	195950	36.58	37.36	36.97	71.70	71.69	983	962.9	989.6	574	352	1.19	13.23	-5.16	17.07	16.50	13.69	13.23	19.65	13.47	1.57
200000	201450	37.36	37.99	37.68	71.70	71.15	1002	989.6	1009.6	352	183	0.87	13.98	-5.87	18.04	17.79	14.18	13.98	21.36	14.45	1.47
201500	202950	38.00	38.63	38.32	71.14	70.43	995	1009.6	977.0	183	444	-1.28	14.47	-4.05	18.67	18.42	14.67	14.47	21.59	14.64	1.39
203000	203900	38.63	39.01	38.82	70.42	70.03	977	977.0	977.6	444	446	-3.60	14.62	-2.37	18.86	18.45	14.95	14.62	21.8	15.73	1.18
203910	204450	39.01	38.73	38.87	70.04	70.30	964	977.6	959.0	446	595	-4.72	14.27	-1.68	18.41	17.83	14.74	14.27	20.11	16.65	0.86
204500	205950	38.72	38.03	38.38	70.31	71.07	963	959.0	976.5	595	462	-3.76	14.57	-3.68	18.80	18.13	15.12	14.57	21	16.48	0.96
210000	211100	38.02	37.53	37.78	71.08	71.67	977	977.8	975.0	451	477	-1.08	13.66	-5.91	17.62	17.07	14.11	13.66	20.07	15.19	1.19

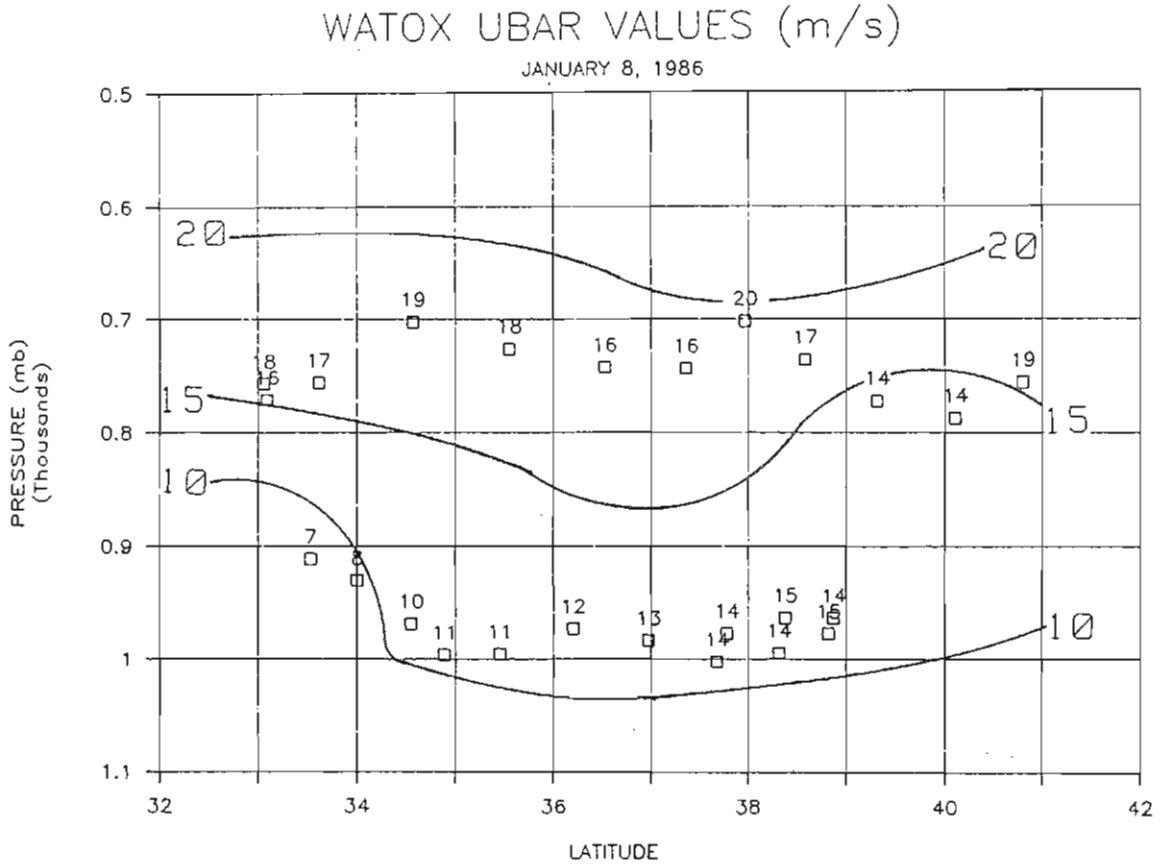
WATOX UBAR VALUES (m/s)
JANUARY 8, 1986
PRESSURE (mb)
(Thousands)
0.5
0.6
0.7
0.8
0.9
1
1.1
32
34
36
38
40
42
LATITUDE
20
15
10

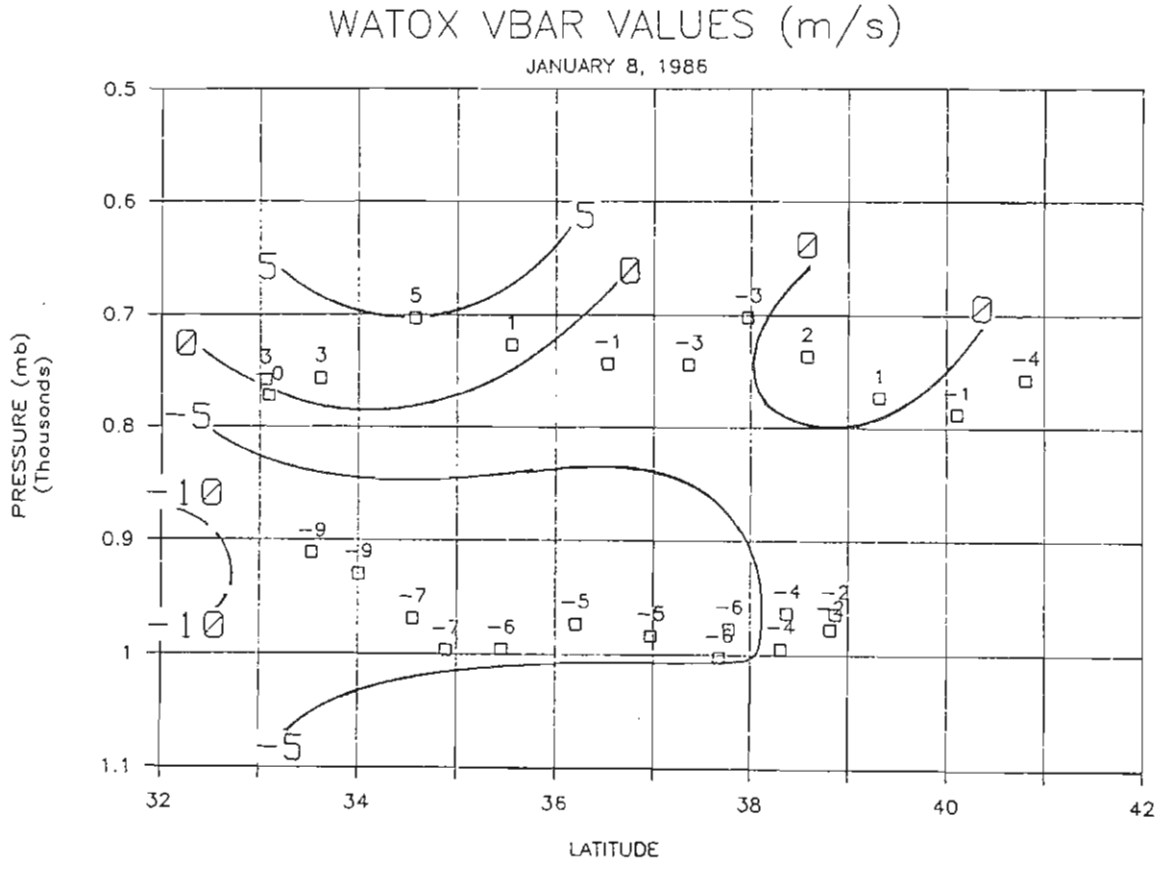
WATOX VBAR VALUES (m/s)
JANUARY 8, 1986
PRESSURE (mb)
(Thousands)
0.5
0.6
0.7
0.8
0.9
1
1.1
32
34
36
38
40
42
LATITUDE
5
0
-5
-10

WATOX FLIGHT 4,DAY9

TIME S HHMMSS	TIME E HHMMSS	LAT S	LAT E	LAT AVG	LON S	LON E	P (MB)	PS (MB)	PE (MB)	RALT S (M)	RALT E (M)	T (C)	U (M/S)	V (M/S)	FLUX STP kg/m2/s	FLUX AMBIENT kg/m2/s	FLUX STP m3/s	FLUX AMBIENT m3/s	MAX FLUX STP kg/m2/s	MIN FLUX STP kg/m2/s	FLUX STD STP kg/m2/s
152900	152950	37.57	37.51	37.54	71.69	71.69	761.00	755.7	768.1	2523	2396	-2.40	12.29	5.45	15.90	12.02	16.22	12.29	16.2	15.6	0.19
153000	154450	37.49	36.51	37.00	71.69	71.68	815.00	768.1	824.8	2396	1835	-1.48	9.39	6.54	12.10	9.80	11.61	9.39	16.39	10.14	1.4
154500	154820	36.50	36.29	36.40	71.68	71.68	833.40	824.8	848.8	1835	1609	-0.74	9.26	6.48	11.90	9.86	11.23	9.26	13.26	7.92	1.42
155300	155950	36.00	35.59	35.80	71.71	71.71	954.60	914.1	979.5	1020	456	4.37	5.39	4.94	7.00	6.45	5.81	5.39	9.33	5.57	0.91
160000	161450	35.58	34.74	35.16	71.71	71.90	1008.60	986.4	1012.3	399	174	9.67	4.57	2.82	5.90	5.67	4.75	4.57	8.94	2.65	1.51
161500	162410	34.73	34.26	34.50	71.91	72.20	946.20	1011.8	882.2	180	1343	5.54	3.48	1.40	4.50	4.11	3.80	3.48	6.97	0.4	1.53
162920	162950	34.00	33.98	33.99	72.40	72.42	809.90	812.8	806.9	1967	2025	-3.55	0.16	3.44	0.20	0.17	0.20	0.16	0.61	-0.19	0.33
163000	164450	33.97	33.13	33.55	72.42	73.00	753.90	805.1	738.4	2044	2744	-0.33	6.88	0.60	8.90	6.62	9.23	6.88	10.94	-1.08	2.38
164500	165950	33.12	32.33	32.73	73.01	73.61	778.80	738.4	809.1	2744	2011	1.35	4.74	1.71	6.10	4.68	6.20	4.74	10.05	0.33	2.59
170000	170820	32.32	31.86	32.09	73.62	73.99	811.00	809.1	823.6	2012	1867	3.21	2.15	0.00	2.80	2.20	2.72	2.15	5.02	-0.74	1.33
171900	172950	31.64	32.21	31.93	74.12	73.76	947.70	900.0	996.4	1148	298	8.63	-1.69	-2.75	-2.20	-1.98	-1.86	-1.69	-0.46	-3.8	0.82
173000	174450	32.22	32.93	32.58	73.75	73.17	1004.10	998.0	960.8	286	603	12.46	0.38	-2.34	0.50	0.46	0.40	0.38	1.9	-1.32	0.79
174500	175020	32.94	33.20	33.07	73.17	72.97	929.20	959.5	894.3	618	1188	5.88	1.00	-3.29	1.30	1.16	1.11	1.00	2.57	-0.06	0.68
175520	175950	33.46	33.71	33.59	72.79	72.60	799.60	826.6	772.6	1819	2361	0.67	4.55	1.97	5.90	4.62	5.78	4.55	7.4	2.15	1.06
180000	181450	33.72	34.58	34.15	72.60	71.98	733.00	770.7	727.1	2383	2842	-0.37	9.74	0.63	12.60	9.11	13.44	9.74	14.19	7.74	1.66
181500	182950	34.59	35.51	35.05	71.97	71.74	766.90	727.1	809.5	2842	1971	-0.51	8.81	1.19	11.40	8.62	11.62	8.81	12.82	9.52	0.93
183000	184450	35.53	36.48	36.01	71.74	71.68	817.10	809.9	847.2	1967	1598	0.25	8.51	5.26	11.00	8.85	10.56	8.51	13.68	8.38	1.54
184500	184950	36.49	36.81	36.65	71.68	71.69	866.00	847.5	885.3	1594	1239	0.05	8.53	8.57	11.00	9.41	9.98	8.53	13.51	7.25	1.62
185140	185950	36.93	37.45	37.19	71.68	71.68	934.40	897.9	982.7	1126	388	1.64	7.16	8.88	9.20	8.47	7.81	7.16	11.18	6.88	0.82
190000	191450	37.47	38.12	37.80	71.68	70.82	993.90	983.3	936.1	378	775	6.15	8.53	9.08	11.00	10.56	8.89	8.53	13.62	8.53	1.1
191500	191700	38.13	38.23	38.18	70.81	70.69	918.70	932.8	906.2	803	1030	0.19	8.80	9.68	11.40	10.29	9.71	8.80	12.56	8.89	0.96
191730	192950	38.25	38.85	38.55	70.66	69.87	744.30	891.6	676.4	1157	3352	-1.95	16.12	10.21	20.80	15.40	21.78	16.12	24.75	9.69	2.96
193000	194450	38.86	39.58	39.22	69.86	68.82	612.40	675.1	550.9	3367	4928	-8.78	15.68	8.66	20.20	12.64	25.10	15.68	23.38	15.18	2.11
194500	195950	39.58	39.69	39.64	68.81	68.61	488.10	549.8	418.9	4943	6962	-19.79	16.58	7.42	21.40	11.12	31.92	16.58	23.69	19.74	0.88
200000	201450	39.68	38.89	39.29	68.62	69.72	461.90	417.4	687.5	6988	3228	-24.18	15.39	9.31	19.90	9.94	30.76	15.39	21.85	16.14	1.54
201500	202950	38.88	38.27	38.58	69.74	70.68	748.70	690.7	808.7	3191	1951	-1.45	16.98	13.50	21.90	16.28	22.85	16.98	25.19	18.67	1.48
203000	203940	38.26	37.86	38.06	70.69	71.24	854.80	810.0	894.8	1938	1142	1.32	12.90	12.46	16.60	13.98	15.36	12.90	21.74	6.76	3.37
204000	204450	37.85	37.66	37.76	71.26	71.51	915.10	896.5	932.2	1127	817	0.82	5.96	12.00	7.70	6.93	6.62	5.96	10.39	5.31	1.18
204500	204820	37.66	37.54	37.60	71.52	71.71	943.20	933.4	958.7	809	587	2.79	5.22	11.15	6.70	6.21	5.66	5.22	9.28	4.85	0.94

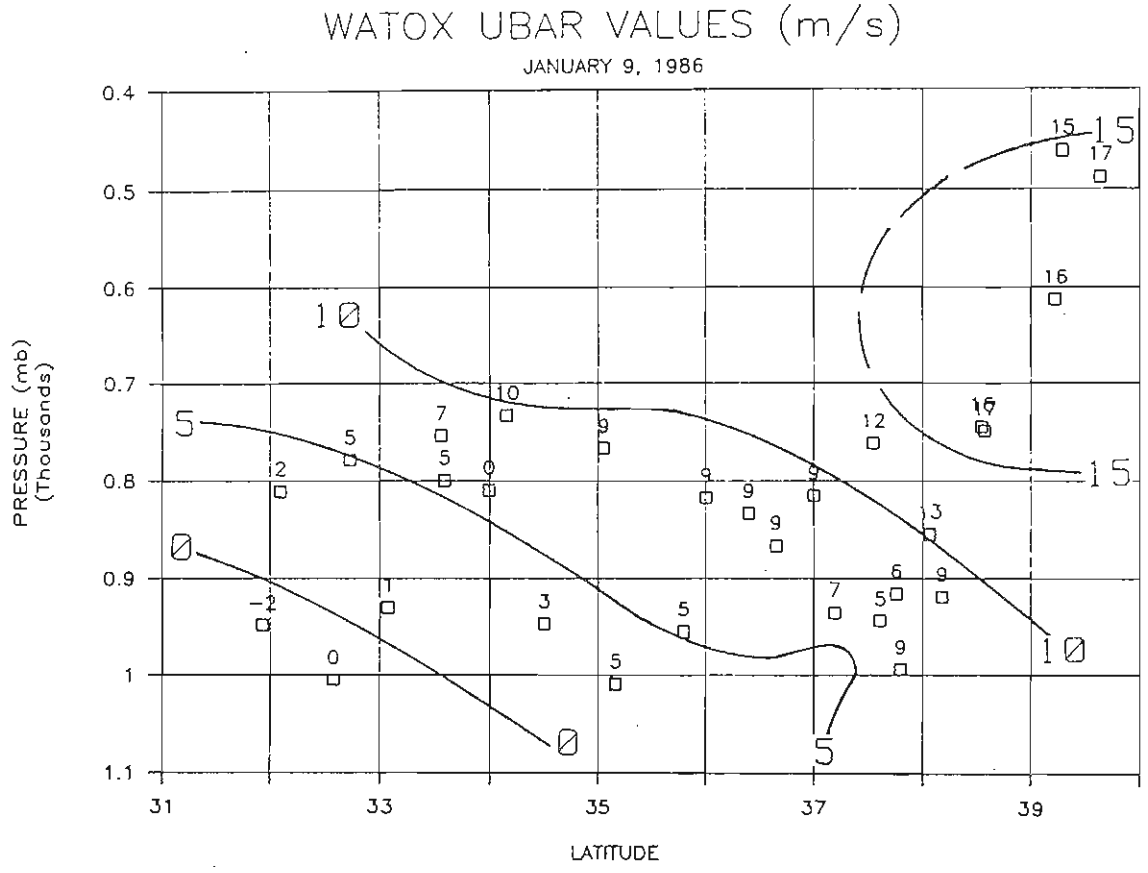
WATOX UBAR VALUES (m/s)
JANUARY 9, 1986
PRESSURE (mb)
(Thousands)
0.4
0.5
0.6
0.7
0.8
0.9
1
1.1
31
33
35
37
39
LATITUDE

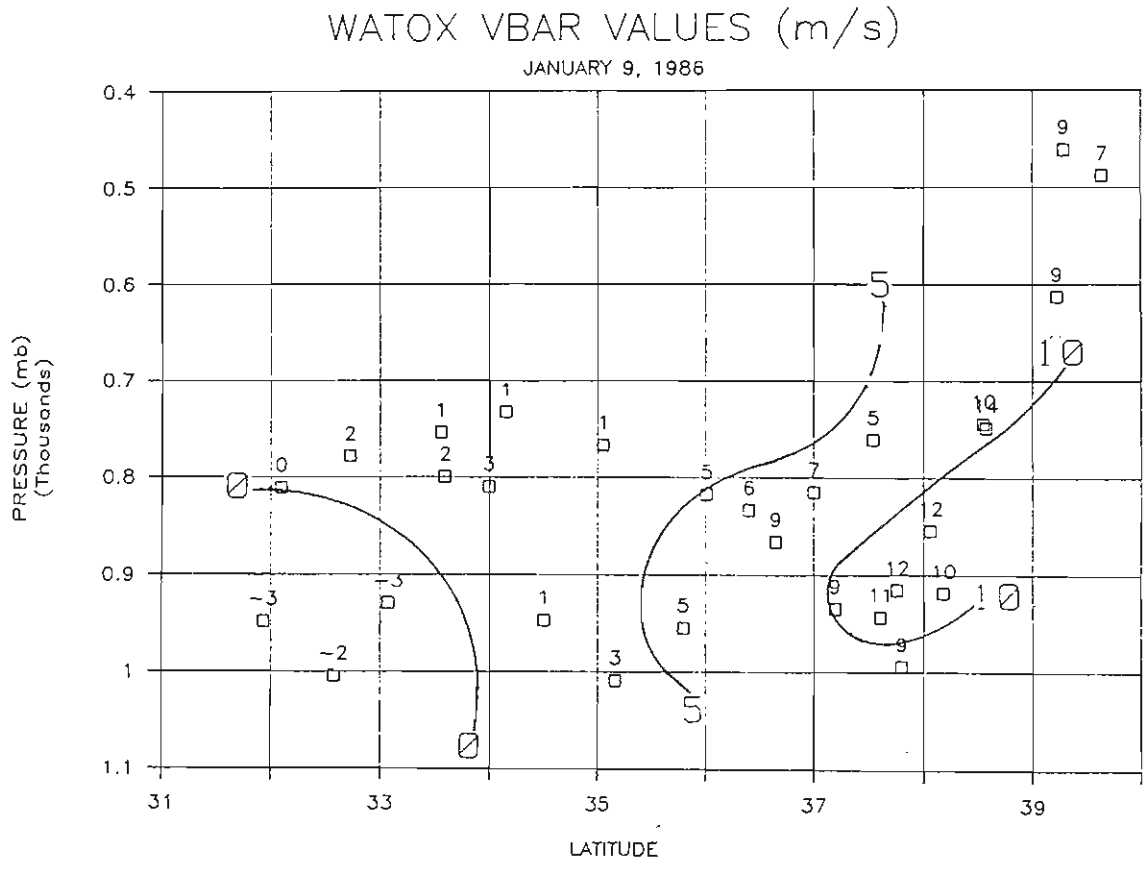
WATOX VBAR VALUES (m/s)
JANUARY 9, 1986
PRESSURE (mb)
(Thousands)
0.4
0.5
0.6
0.7
0.8
0.9
1
1.1
31
33
35
37
39
LATITUDE